NORSAR

NORSAR Scientific Report No. 2-2004

Semiannual Technical Summary

1 January - 30 June 2004

Frode Ringdal (ed.)

Kjeller, August 2004

SECURITY CLASSIFICATION OF THIS PAGE

REPORT DOCUMENTATION PAGE

Form Approved OMB No. 0704-0188

1a. REPORT SECURITY CLASSIFICATION Unclassified	1b. RESTRICTIVE MARKINGS Not applicable
2a. SECURITY CLASSIFICATION AUTHORITY Not Applicable	3. DISTRIBUTION/AVAILABILITY OF REPORT Approved for public release; distribution unlimited
2b. DECLASSIFICATION/DOWNGRADING SCHEDULE	
4. PERFORMING ORGANIZATION REPORT NUMBER(S) Scientific Rep. 2-2004	5. MONITORING ORGANIZATION REPORT NUMBER(S) Scientific Rep. 2-2004
6a. NAME OF PERFORMING ORGANIZATION NORSAR 6b. OFFICE SYMBOL *(If applicable)*	7a. NAME OF MONITORING ORGANIZATION HQ/AFTAC/TTS
6c. ADDRESS *(City, State, and ZIP Code)* Post Box 53 NO-2027 Kjeller, Norway	7b. ADDRESS *(City, State, and ZIP Code)* Patrick AFB, FL 32925-6001
8a. NAME OF FUNDING/SPONSORING ORGANIZATION Army Space and Missile Defense Command/ 8b. OFFICE SYMBOL *(If applicable)* ASMDC	9. PROCUREMENT INSTRUMENT IDENTIFICATION NUMBER Contract No. F08650-01-C-0055
8c. ADDRESS *(City, State, and ZIP Code)* 1515 Wilson Blvd., Suite 720 Arlington, VA 22209	10. SOURCE OF FUNDING NUMBERS PROGRAM ELEMENT NO. R&D; PROJECT NO. NORSAR Phase 3; TASK NO. SOW Task 5.0; WORK UNIT ACCESSION NO. Sequence No. 004A2
11. TITLE *(Include Security Classification)* Semiannual Technical Summary, 1 January - 30 June 2004 (Unclassified)	
12. PERSONAL AUTHOR(S)	
13a. TYPE OF REPORT Scientific Summary 13b. TIME COVERED FROM 1 Jan 04 TO 30 Jun 04	14. DATE OF REPORT *(Year, Month, Day)* 2004 August 15. PAGE COUNT 79
16. SUPPLEMENTARY NOTATION	

17. COSATI CODES			18. SUBJECT TERMS *(Continue on reverse if necessary and identify by block number)*
FIELD	GROUP	SUB-GROUP	NORSAR, Norwegian Seismic Array
8	11		

19. ABSTRACT *(Continue on reverse if necessary and identify by block number)*

This report describes the research activities carried out at NORSAR under Contract No. F08650-01-C-0055 for the period 1 January - 30 June 2004. In addition, it provides summary information on operation and maintenance (O&M) activities at the Norwegian National Data Center (NDC) during the same period. Research activities described in this report, as well as transmission of selected data to the United States NDC, are funded by the United States Government. The O&M activities, including operation of transmission links within Norway and to Vienna, Austria, are being funded jointly by the CTBTO/PTS and the Norwegian Government, with the understanding that the funding of O&M activities for primary IMS will gradually be transferred to the CTBTO/PTS. The O&M statistics presented in this report are included for the purpose of completeness, and in order to maintain consistency with earlier reporting practice.

(cont.)

20. DISTRIBUTION/AVAILABILITY OF ABSTRACT ☐ UNCLASSIFIED/UNLIMITED ☐ SAME AS RPT. ☐ DTIC USERS	21. ABSTRACT SECURITY CLASSIFICATION
22a. NAME OF RESPONSIBLE INDIVIDUAL TSgt Mark C. Gerick	22b. TELEPHONE *(Include Area Code)* (321) 494-3582 22c. OFFICE SYMBOL AFTAC/TTD

DD Form 1473, JUN 86 *Previous editions are obsolete.* SECURITY CLASSIFICATION OF THIS PAGE

Abstract

The NOA Detection Processing system has been operated throughout the period with an uptime of 100%. A total of 2114 seismic events have been reported in the NOA monthly seismic bulletin from January through June 2004. On-line detection processing and data recording at the NDC of ARCES and FINES data have been conducted throughout the period. Data from the two small-aperture arrays at sites in Spitsbergen and Apatity, Kola Peninsula, as well as the Hagfors array in Sweden, have also been recorded and processed. Processing statistics for the arrays for the reporting period are given.

A summary of the activities at the Norwegian NDC and relating to field installations during the reporting period is provided in Section 4. Norway is now contributing primary station data from two seismic arrays: NOA (PS27) and ARCES (PS28) one auxiliary seismic array SPITS (AS72) and one auxiliary three-component station (JMIC). These data are being provided to the IDC via the global communications infrastructure (GCI). Continuous data from the three arrays are in addition being transmitted to the US NDC. The performance of the data transmission to the US NDC has been satisfactory during the reporting period.

A status report on the ongoing Spitsbergen array refurbishment are presented in Section 4.4. Installation of the equipment at the array site will commence on 9 August 2004.

Summaries of five scientific and technical contributions are presented in Chapter 6 of this report.

Section 6.1 is entitled "Research in Regional Seismic Monitoring" and contains a paper presented at the 26th Annual Seismic Research Review. The paper summarizes some of the research efforts at NORSAR during the past year. It contains a description of ground truth data obtained from Kola Regional Seismological Center for mining explosions in the Kola Peninsula. The paper also discusses some aspects and potential improvements of the regional processing currently carried out at NORSAR for the European Arctic. In particular, the study addresses the question of automatic detection and association of phases for small seismic events in the Novaya Zemlya region, using the on-line Generalized Beamforming (GBF) process. It is noted that the number of false associations can be reduced by 90 per cent through relatively simple selection criteria. Furthermore, some possibilities for additional future improvements are discussed, including the development of a systematic automatic post-processing algorithm to be applied to event candidates produced by the GBF process currently in operation. Finally, the paper summarizes results from a study of location accuracy for seismic events near the Spitsbergen archipelago.

Section 6.2 is entitled "A waveform correlation procedure for detecting decoupled chemical explosions". Between 1986 and 1989, a total of 11 decoupled chemical explosions were carried out in two underground chambers at a site in Älvdalen, central Sweden. Explosions with yields 10, 1000, and 5000 kg were performed in each of the two chambers, one with size 300 m^3 and one with size 200 m^3. The origin times of these explosions were not known, and we were interested in analyzing the corresponding waveforms in order to supplement the previously reported analysis of such explosions during 2000-2002.

A procedure was developed using a novel array correlation technique, and proved to be highly successful. All of the decoupled explosions of 1000 kg and more were detected by this procedure, using NORES and NORSAR array data. Furthermore, we succeeded in detecting a decoupled explosion in December 2000 with a yield of only 500 kg. This explosion was known to have been carried out during the first part of December, but we were unable to detect the signals with conventional processing techniques. An important feature of the correlation detector is its extremely low false alarm rate. As a test, we ran the detector on NORSAR large array data for selected time segments totalling more than one year, and the process triggered 5 times, all corresponding to verified explosions. No Älvdalen explosion which the authors know of has failed to be detected by this test, and on no occasion did the test produce a detection without there having been a confirmed explosion at Älvdalen.

Section 6.3 is entitled "Observed and predicted travel times of Pn and P phases recorded at NORSAR from regional events". The principal objective of this study is to estimate the absolute travel-time path anomalies of regional seismic phases observed at the Norwegian Seismic Array (NORSAR) with respect to the Earth model AK135 and to determine their relationship to the Earth's three-dimensional (3D) structure.

At least with respect to the large-scale features of the correction surfaces, the agreement between the empirical path anomalies and the model-predicted travel times is quite good. The observed and predicted regional anomalies show strong differences in the P and Pn anomalies observed between explosion source areas in northern and southern Novaya Zemlya, apparently produced by a sharp structural boundary that strongly affects ray paths to NORSAR from these sources. The separation distance between these source areas is on the order of only 300 km, yet the P and Pn median travel time anomalies observed at NORSAR at a distance of about 20 degrees differ by more than 5s. These differences between the two Novaya Zemlya sources are also reflected in typical waveforms observed at NORSAR from these test areas.

Section 6.4 is a study of regional discriminants using data from the ARCES and HFS arrays. The discriminants considered here are the following:

- Maximum peak in the cepstrum
- P/S ratio
- Complexity
- Third moment of frequency (TMF)
- Spectral misfit to earthquake (mean square error of the best fit)

A database of regional events has been assembled, and the events are presumed to be one of the following four classes:

- Underwater explosions
- Mining explosions
- Other types of explosions
- Earthquakes

By using a combination of the cepstral peak and the spectral misfit to an earthquake, the earthquakes are well separated from underwater explosions and mining explosions. The other types of explosions are generally not separated from the earthquake population.

The *P/S* relation seems to perform well when it comes to separating explosions from earthquakes. However, the ratio has only been calculated for events where body-wave S-phases exist in the bulletin.

The third moment of frequency does not separate different classes of events satisfactorily, the earthquakes are also spread out in the feature space. The same holds for the complexity discriminants, although these are slightly better. These methods might require tuning and adjustments.

Generally the presented discriminants do not separate explosions from earthquakes, but ripple fired explosions and underwater explosions seem to separate from the other types of events reasonably well.

Section 6.5 is entitled: "Comparison of the Love-Rayleigh discrepancy in central Europe (GRSN) and southern Scandinavia (NORSAR)". The study presents examples of the investigation of the Love-Rayleigh discrepancy in two tectonically different continental regions: for the Phanerozoic asthenosphere and lithosphere in central Europe and at the border of the Precambrian Baltic Shield. Data from the German Regional Seismic Network (GRSN) and the NORSAR array were used.

Dispersion curves of the fundamental modes were measured by a two-station method. One event is recorded at two stations. The cross correlation of the seismograms leads to phase differences and with the known distance between the stations the phase velocities can be calculated. This procedure is repeated for many events. Then, the inversion of averaged phase velocity curves of fundamental surface wave modes yields one-dimensional models of the S-wave velocity structure. These are interpreted as a average models describing the structure beneath the paths.

In *central Europe* the asthenosphere is found between 80 km and 250 km depth. The Love-Rayleigh discrepancy in the asthenosphere amounts to about 5%. This is comparable to the amount of the Love-Rayleigh discrepancy in the Pacific. Azimuthal variations of the Rayleigh phase velocity point to azimuthal anisotropy in the lower crust. The orientation of the fast axis is about NE-SW. In contrast to the Rayleigh wave phase velocities, Love waves do not show dependence on azimuth. Further studies should reveal if this discrepancy is caused by finite-frequency effects, or contamination of the Love-wave phase velocities by higher modes, or if this discrepancy might yield constraints on models of the anisotropy in the lower crust.

In *southern Scandinavia*, the S-wave velocity in the mantle lithosphere is lower than expected for stable cratonic regions. However, the NORSAR array is located at the border of the Precambrian Baltic Shield and this region was influenced by several tectonic processes. The depth of the Moho is about 35 km. Variations in the phase velocity between the paths point to lateral heterogeneities with S velocity variations of up to +/- 3.5%. The strike of the observed velocity anomaly in the crust is NW-SE. It is similar to the strike of the Precambrian structures at the surface. The amount of the Love-Rayleigh discrepancy in the lower crust is not significant, which might be partly due to the large standard deviation of the phase velocities.

AFTAC Project Authorization	:	T/0155/PKO
ARPA Order No.	:	4138 AMD # 53
Program Code No.	:	0F10
Name of Contractor	:	Stiftelsen NORSAR
Effective Date of Contract	:	1 Feb 2001 (T/0155/PKO)
Contract Expiration Date	:	31 December 2005
Project Manager	:	Frode Ringdal +47 63 80 59 00
Title of Work	:	The Norwegian Seismic Array (NORSAR) Phase 3
Amount of Contract	:	$ 3,383,445
Period Covered by Report	:	1 January - 30 June 2004

The views and conclusions contained in this document are those of the authors and should not be interpreted as necessarily representing the official policies, either expressed or implied, of the U.S. Government.

The research presented in this report was supported by the Army Space and Missile Defense Command and was monitored by AFTAC, Patrick AFB, FL32925, under contract no. F08650-01-C-0055.

The operational activities of the seismic field systems and the Norwegian National Data Center (NDC) are currently jointly funded by the Norwegian Government and the CTBTO/PTS, with the understanding that the funding of IMS-related activities will gradually be transferred to the CTBTO/PTS.

NORSAR Contribution No. 904

Table of Contents

1 Summary

This report describes the research activities carried out at NORSAR under Contract No. F08650-01-C-0055 for the period 1 January - 30 June 2004. In addition, it provides summary information on operation and maintenance (O&M) activities at the Norwegian National Data Center (NDC) during the same period. Research activities described in this report, as well as transmission of selected data to the United States NDC, are funded by the United States Government. The O&M activities, including operation of transmission links within Norway and to Vienna, Austria are being funded jointly by the CTBTO/PTS and the Norwegian Government, with the understanding that the funding of O&M activities for primary IMS stations will gradually be transferred to the CTBTO/PTS. The O&M statistics presented in this report are included for the purpose of completeness, and in order to maintain consistency with earlier reporting practice.

The seismic arrays operated by the Norwegian NDC comprise the Norwegian Seismic Array (NOA), the Arctic Regional Seismic Array (ARCES) and the Spitsbergen Regional Array (SPITS). This report also presents statistics for additional seismic stations which through cooperative agreements with institutions in the host countries provide continuous data to the NORSAR Data Processing Center (NDPC). These stations comprise the Finnish Regional Seismic Array (FINES), the Hagfors array in Sweden (HFS) and the regional seismic array in Apatity, Russia.

The NOA Detection Processing system has been operated throughout the period with an uptime of 100%. A total of 2114 seismic events have been reported in the NOA monthly seismic bulletin from January through June 2004. On-line detection processing and data recording at the NDC of ARCES and FINES data have been conducted throughout the period. Data from the two small-aperture arrays at sites in Spitsbergen and Apatity, Kola Peninsula, as well as the Hagfors array in Sweden, have also been recorded and processed. Processing statistics for the arrays for the reporting period are given.

A summary of the activities at the Norwegian NDC and relating to field installations during the reporting period is provided in Section 4. Norway is now contributing primary station data from two seismic arrays: NOA (PS27) and ARCES (PS28) one auxiliary seismic array SPITS (AS72) and one auxiliary three-component station (JMIC). These data are being provided to the IDC via the global communications infrastructure (GCI). Continuous data from the three arrays are in addition being transmitted to the US NDC. The performance of the data transmission to the US NDC has been satisfactory during the reporting period.

So far among the Norwegian stations, the NOA and the ARCES array (PS27 and PS28 respectively) and the radionuclide station at Spitsbergen (RN49) have been certified. Provided that adequate funding continues to be made available (from the PTS and the Norwegian Ministry of Foreign Affairs), we envisage continuing the provision of data from these and other Norwegian IMS-designated stations in accordance with current procedures.

A status report on the ongoing Spitsbergen array refurbishment are presented in Section 4.4. Installation of the equipment at the array site will commence on 9 August 2004.

Summaries of five scientific and technical contributions are presented in Chapter 6 of this report.

Section 6.1 is entitled "Research in Regional Seismic Monitoring" and contains a paper presented at the 26th Annual Seismic Research Review. The paper summarizes some of the

research efforts at NORSAR during the past year. It contains a description of ground truth data obtained from Kola Regional Seismological Center for mining explosions in the Kola Peninsula. The paper also discusses some aspects and potential improvements of the regional processing currently carried out at NORSAR for the European Arctic. In particular, the study addresses the question of automatic detection and association of phases for small seismic events in the Novaya Zemlya region, using the on-line Generalized Beamforming (GBF) process. It is noted that the number of false associations can be reduced by 90 per cent through relatively simple selection criteria. Furthermore, some possibilities for additional future improvements are discussed, including the development of a systematic automatic post-processing algorithm to be applied to event candidates produced by the GBF process currently in operation. Finally, the paper summarizes results from a study of location accuracy for seismic events near the Spitsbergen archipelago.

Section 6.2 is entitled "A waveform correlation procedure for detecting decoupled chemical explosions". Between 1986 and 1989, a total of 11 decoupled chemical explosions were carried out in two underground chambers at a site in Älvdalen, central Sweden. Explosions with yields 10, 1000, and 5000 kg were performed in each of the two chambers, one with size 300 m^3 and one with size 200 m^3. The origin times of these explosions were not known, and we were interested in analyzing the corresponding waveforms in order to supplement the previously reported analysis of such explosions during 2000-2002.

A procedure was developed using a novel array correlation technique, and proved to be highly successful. All of the decoupled explosions of 1000 kg and more were detected by this procedure, using NORES and NORSAR array data. Furthermore, we succeeded in detecting a decoupled explosion in December 2000 with a yield of only 500 kg. This explosion was known to have been carried out during the first part of December, but we were unable to detect the signals with conventional processing techniques. An important feature of the correlation detector is its extremely low false alarm rate. As a test, we ran the detector on NORSAR large array data for selected time segments totalling more than one year, and the process triggered 5 times, all corresponding to verified explosions. No Älvdalen explosion which the authors know of has failed to be detected by this test, and on no occasion did the test produce a detection without there having been a confirmed explosion at Älvdalen.

Section 6.3 is entitled "Observed and predicted travel times of Pn and P phases recorded at NORSAR from regional events". The principal objective of this study is to estimate the absolute travel-time path anomalies of regional seismic phases observed at the Norwegian Seismic Array (NORSAR) with respect to the Earth model AK135 and to determine their relationship to the Earth's three-dimensional (3D) structure.

At least with respect to the large-scale features of the correction surfaces, the agreement between the empirical path anomalies and the model-predicted travel times is quite good. The observed and predicted regional anomalies show strong differences in the P and Pn anomalies observed between explosion source areas in northern and southern Novaya Zemlya, apparently produced by a sharp structural boundary that strongly affects ray paths to NORSAR from these sources. The separation distance between these source areas is on the order of only 300 km, yet the P and Pn median travel time anomalies observed at NORSAR at a distance of about 20 degrees differ by more than 5s. These differences between the two Novaya Zemlya sources are also reflected in typical waveforms observed at NORSAR from these test areas.

Section 6.4 is a study of regional discriminants using data from the ARCES and HFS arrays. The discriminants considered here are the following:

- Maximum peak in the cepstrum
- P/S ratio
- Complexity
- Third moment of frequency (TMF)
- Spectral misfit to earthquake (mean square error of the best fit)

A database of regional events has been assembled, and the events are presumed to be one of the following four classes:

- Underwater explosions
- Mining explosions
- Other types of explosions
- Earthquakes

By using a combination of the cepstral peak and the spectral misfit to an earthquake, the earthquakes are well separated from underwater explosions and mining explosions. The other types of explosions are generally not separated from the earthquake population.

The *P/S* relation seems to perform well when it comes to separating explosions from earthquakes. However, the ratio has only been calculated for events where body-wave S-phases exist in the bulletin.

The third moment of frequency does not separate different classes of events satisfactorily, the earthquakes are also spread out in the feature space. The same holds for the complexity discriminants, although these are slightly better. These methods might require tuning and adjustments.

Generally the presented discriminants do not separate explosions from earthquakes, but ripple fired explosions and underwater explosions seem to separate from the other types of events reasonably well.

Section 6.5 is entitled: "Comparison of the Love-Rayleigh discrepancy in central Europe (GRSN) and southern Scandinavia (NORSAR)". The study presents examples of the investigation of the Love-Rayleigh discrepancy in two tectonically different continental regions: for the Phanerozoic asthenosphere and lithosphere in central Europe and at the border of the Precambrian Baltic Shield. Data from the German Regional Seismic Network (GRSN) and the NORSAR array were used.

Dispersion curves of the fundamental modes were measured by a two-station method. One event is recorded at two stations. The cross correlation of the seismograms leads to phase differences and with the known distance between the stations the phase velocities can be calculated. This procedure is repeated for many events. Then, the inversion of averaged phase velocity curves of fundamental surface wave modes yields one-dimensional models of the S-wave velocity structure. These are interpreted as a average models describing the structure beneath the paths.

In *central Europe* the asthenosphere is found between 80 km and 250 km depth. The Love-Rayleigh discrepancy in the asthenosphere amounts to about 5%. This is comparable to the amount of the Love-Rayleigh discrepancy in the Pacific. Azimuthal variations of the Rayleigh phase velocity point to azimuthal anisotropy in the lower crust. The orientation of the fast axis is about NE-SW. In contrast to the Rayleigh wave phase velocities, Love waves do not show dependence on azimuth. Further studies should reveal if this discrepancy is caused by finite-frequency effects, or contamination of the Love-wave phase velocities by higher modes, or if this discrepancy might yield constraints on models of the anisotropy in the lower crust.

In *southern Scandinavia*, the S-wave velocity in the mantle lithosphere is lower than expected for stable cratonic regions. However, the NORSAR array is located at the border of the Precambrian Baltic Shield and this region was influenced by several tectonic processes. The depth of the Moho is about 35 km. Variations in the phase velocity between the paths point to lateral heterogeneities with S velocity variations of up to +/- 3.5%. The strike of the observed velocity anomaly in the crust is NW-SE. It is similar to the strike of the Precambrian structures at the surface. The amount of the Love-Rayleigh discrepancy in the lower crust is not significant, which might be partly due to the large standard deviation of the phase velocities.

Frode Ringdal

2 Operation of International Monitoring System (IMS) Stations in Norway

2.1 PS27 — Primary Seismic Station NOA

The average recording time was 100%, the same as for the previous reporting period.

There were no outages of all subarrays at the same time.

Monthly uptimes for the NORSAR on-line data recording task, taking into account all factors (field installations, transmissions line, data center operation) affecting this task were as follows:

January	:	100%
February	:	100%
March	:	100%
April	:	100%
May	:	100%
June	:	100%

J. Torstveit

NOA Event Detection Operation

In Table 2.1.1 some monthly statistics of the Detection and Event Processor operation are given. The table lists the total number of detections (DPX) triggered by the on-line detector, the total number of detections processed by the automatic event processor (EPX) and the total number of events accepted after analyst review (teleseismic phases, core phases and total).

	Total DPX	Total EPX	Accepted Events		Sum	Daily
			P-phases	Core Phases		
Jan	12,242	961	256	48	304	9.8
Feb	10,483	843	222	55	277	9.6
Mar	11,103	1,014	264	120	384	12.4
Apr	8,283	933	296	109	405	13.5
May	7,684	924	289	83	372	12.0
Jun	8,068	959	300	72	372	12.4
	57,863	5,634	1,627	487	2,114	11.6

Table 2.1.1. *Detection and Event Processor statistics, 1 January - 30 June 2004.*

NOA detections

The number of detections (phases) reported by the NORSAR detector during day 001, 2004, through day 182, 2004, was 57,863, giving an average of 318 detections per processed day (182 days processed).

B. Paulsen

U. Baadshaug

2.2 PS28 — Primary Seismic Station ARCES

The average recording time was 100%, as compared to 99.65% for the previous reporting period.

There were no outages in the reporting period.

Monthly uptimes for the ARCES on-line data recording task, taking into account all factors (field installations, transmission lines, data center operation) affecting this task were as follows:

January	:	100%
February	:	100%
March	:	100%
April	:	100%
May	:	100%
June	:	100%

J. Torstveit

Event Detection Operation

ARCES detections

The number of detections (phases) reported during day 001, 2004, through day 182, 2004, was 178,370, giving an average of 980 detections per processed day (182 days processed).

Events automatically located by ARCES

During days 001, 2004, through 182, 2004, 9,552 local and regional events were located by ARCES, based on automatic association of P- and S-type arrivals. This gives an average of 46.6 events per processed day (182 days processed). 56% of these events are within 300 km, and 82% of these events are within 1000 km.

U. Baadshaug

2.3 AS72 — Auxiliary Seismic Station Spitsbergen

The average recording time was 95.76% as compared to 98.84% for the previous reporting period.

Table 2.3.1 lists the time periods of the main downtimes in the reporting period.

Day	Period
05/01	08.39.08 - 08.43.09
28/01	22.02.55 - 22.06.56
18/02	02.33.16 - 02.37.17
04/03	01.30.16 - 01.37.50
11/03	12.24.13 - 12.28.14
01/04	09.07.51 - 09.08.35
12/04	06.32.27 -
19/04	- 19.29.00
22/04	10.06.48 - 10.36.58
03/05	21.23.21 - 21.27.20
26/05	17.53.43 - 17.57.44
29/05	17.37.24 - 17.44.58
30/05	17.31.15 - 17.38.49
02/06	17.25.10 - 17.32.44
08/06	16.52.22 - 16.59.57
10/06	16.46.16 - 16.53.49
11/06	16.40.10 - 16.47.43
12/06	16.40.42 - 16.48.16
20/06	16.08.01 - 16.12.01

Table 2.3.1. *The main interruptions in recording of Spitsbergen data at NDPC, 1 January - 30 June 2004.*

Monthly uptimes for the Spitsbergen on-line data recording task, taking into account all factors (field installations, transmissions line, data center operation) affecting this task were as follows:

January	:	99.98%
February	:	99.99%
March	:	99.97%
April	:	74.80%
May	:	99.95%
June	:	99.89%

J. Torstveit

Event Detection Operation

Spitsbergen array detections

The number of detections (phases) reported from day 001, 2004, through day 182, 2004, was 255,655, giving an average of 1453 detections per processed day (176 days processed).

Events automatically located by the Spitsbergen array

During days 001, 2004, through 182, 2004, 27,259 local and regional events were located by the Spitsbergen array, based on automatic association of P- and S-type arrivals. This gives an average of 154.9 events per processed day (176 days processed). 70% of these events are within 300 km, and 85% of these events are within 1000 km.

U. Baadshaug

2.4 AS73 — Auxiliary Seismic Station at Jan Mayen

The IMS auxiliary seismic network includes a three-component station on the Norwegian island of Jan Mayen. The station location given in the protocol to the Comprehensive Nuclear-Test-Ban Treaty is 70.9°N, 8.7°W.

The University of Bergen has operated a seismic station at this location since 1970. A so-called Parent Network Station Assessment for AS73 was completed in April 2002. A vault at a new location (71.0°N, 8.5°W) was prepared in early 2003, after its location had been approved by the PrepCom. New equipment was installed in this vault in October 2003, as a cooperative effort bertween NORSAR and the CTBTO/PTS. Continuous data from this station are being transmitted to the NDC at Kjeller via a satellite link installed in April 2000. Data are also made available to the University of Bergen.

J. Fyen

2.5 IS37 — Infrasound Station at Karasjok

The IMS infrasound network will include a station at Karasjok in northern Norway. The coordinates given for this station are 69.5°N, 25.5°E. These coordinates coincide with those of the primary seismic station PS28.

A site survey for this station was carried out during June/July 1998 as a cooperative effort between the Provisional Technical Secretariat of the CTBTO and NORSAR. The site survey led to a recommendation on the exact location of the infrasound station. This location needs to be surveyed in detail. The next step will be to approach the local authorities to obtain the permission necessary to establish the station. Station installation is expected to take place in the year 2005, provided that adequate resources for project planning and execution are made available.

S. Mykkeltveit

2.6 RN49 — Radionuclide Station on Spitsbergen

The IMS radionuclide network includes a station on the island of Spitsbergen. This station is also among those IMS radionuclide stations that will have a capability of monitoring for the presence of relevant noble gases upon entry into force of the CTBT.

A site survey for this station was carried out in August of 1999 by NORSAR, in cooperation with the Norwegian Radiation Protection Authority. The site survey report to the PTS contained a recommendation to establish this station at Platåberget, near Longyearbyen. The infrastructure for housing the station equipment was established in early 2001, and a noble gas detection system, based on the Swedish "SAUNA" design, was installed at this site in May 2001, as part of PrepCom's noble gas experiment. A particulate station ("ARAME" design) was installed at the same location in September 2001. A certification visit to the station took place in October 2002, and the particulate station was certified on 10 June 2003. The equipment at RN49 is being maintained and operated in accordance with a contract with the CTBTO/PTS.

S. Mykkeltveit

3 Contributing Regional Seismic Arrays

3.1 NORES

NORES has been out of operation since a thunderstorm destroyed the station electronics on 11 June 2002.

J. Torstveit

3.2 Hagfors (IMS Station AS101)

Data from the Hagfors array are made available continuously to NORSAR through a cooperative agreement with Swedish authorities.

The average recording time was 100% as compared to 96.89% for the previous reporting period.

There were no outages in the reporting period.

Monthly uptimes for the Hagfors on-line data recording task, taking into account all factors (field installations, transmissions line, data center operation) affecting this task were as follows:

January	:	100%
February	:	100%
March	:	100%
April	:	100%
May	:	100%
June	:	100%

J. Torstveit

Hagfors Event Detection Operation

Hagfors array detections

The number of detections (phases) reported from day 001, 2004, through day 182, 2004, was 168,012, giving an average of 923 detections per processed day (182 days processed).

Events automatically located by the Hagfors array

During days 001, 2004, through 182, 2004, 4004 local and regional events were located by the Hagfors array, based on automatic association of P- and S-type arrivals. This gives an average of 22.0 events per processed day (182 days processed). 64% of these events are within 300 km, and 88% of these events are within 1000 km.

U. Baadshaug

3.3 FINES (IMS station PS17)

Data from the FINES array are made available continuously to NORSAR through a cooperative agreement with Finnish authorities.

The average recording time was 100% as it was for the previous reporting period.

There were 51 outages that lasted from 1 to 10 seconds in the period.

Monthly uptimes for the FINES on-line data recording task, taking into account all factors (field installations, transmissions line, data center operation) affecting this task were as follows:

January	:	100%
February	:	100%
March	:	100%
April	:	100%
May	:	100%
June	:	100%

J. Torstveit

FINES Event Detection Operation

FINES detections

The number of detections (phases) reported during day 001, 2004, through day 182, 2004, was 74,686, giving an average of 410 detections per processed day (182 days processed).

Events automatically located by FINES

During days 001, 2004, through 182, 2004, 2734 local and regional events were located by FINES, based on automatic association of P- and S-type arrivals. This gives an average of 15.0 events per processed day (183 days processed). 76% of these events are within 300 km, and 84% of these events are within 1000 km.

U. Baadshaug

3.4 Apatity

The average recording time was 99.94% in the reporting period compared to 97.71% during the previous period.

The main outages in the period are given in Table 3.4.1.

Day	Time
12/02	05.55.00 - 06.00.00
28/02	00.25.00 - 00.30.00
16/03	16.30.00 - 16.35.00
03/05	08.22.14 - 10.55.33
29/05	12.21.37 - 12.21.48
05/06	20.25.00 - 20.30.00
11/06	15.10.00 - 15.15.00
14/06	01.20.00 - 01.25.00

Table 3.4.1. *The main interruptions in recording of Apatity data at NDPC, 1 January - 30 June 2004.*

Monthly uptimes for the Apatity on-line data recording task, taking into account all factors (field installations, transmissions line, data center operation) affecting this task were as follows:

January	:	100%
February	:	99.98%
March	:	99.99%
April	:	100%
May	:	99.66%
June	:	99.97%

J. Torstveit

Apatity Event Detection Operation

Apatity array detections

The number of detections (phases) reported from day 001, 2004, through day 182, 2004, was 176,703, giving an average of 971 detections per processed day (182 days processed).

As described in earlier reports, the data from the Apatity array is transferred by one-way (simplex) radio links to Apatity city. The transmission suffers from radio disturbances that occasionally result in a large number of small data gaps and spikes in the data. In order for the communication protocol to correct such errors by requesting retransmission of data, a two-way

radio link would be needed (duplex radio). However, it should be noted that noise from cultural activities and from the nearby lakes cause most of the unwanted detections. These unwanted detections are "filtered" in the signal processing, as they give seismic velocities that are outside accepted limits for regional and teleseismic phase velocities.

Events automatically located by the Apatity array

During days 001, 2004, through 182, 2004, 2224 local and regional events were located by the Apatity array, based on automatic association of P- and S-type arrivals. This gives an average of 12.2 events per processed day (182 days processed). 42% of these events are within 300 km, and 74% of these events are within 1000 km.

U. Baadshaug

3.5 Regional Monitoring System Operation and Analysis

The Regional Monitoring System (RMS) was installed at NORSAR in December 1989 and has been operated at NORSAR from 1 January 1990 for automatic processing of data from ARCES and NORES. A second version of RMS that accepts data from an arbitrary number of arrays and single 3-component stations was installed at NORSAR in October 1991, and regular operation of the system comprising analysis of data from the 4 arrays ARCES, NORES, FINES and GERES started on 15 October 1991. As opposed to the first version of RMS, the one in current operation also has the capability of locating events at teleseismic distances.

Data from the Apatity array was included on 14 December 1992, and from the Spitsbergen array on 12 January 1994. Detections from the Hagfors array were available to the analysts and could be added manually during analysis from 6 December 1994. After 2 February 1995, Hagfors detections were also used in the automatic phase association.

Since 24 April 1999, RMS has processed data from all the seven regional arrays ARCES, NORES, FINES, GERES (until January 2000), Apatity, Spitsbergen, and Hagfors. Starting 19 September 1999, waveforms and detections from the NORSAR array have also been available to the analyst.

Phase and event statistics

Table 3.5.1 gives a summary of phase detections and events declared by RMS. From top to bottom the table gives the total number of detections by the RMS, the number of detections that are associated with events automatically declared by the RMS, the number of detections that are not associated with any events, the number of events automatically declared by the RMS, and finally the total number of events worked on interactively (in accordance with criteria that vary over time; see below) and defined by the analyst.

New criteria for interactive event analysis were introduced from 1 January 1994. Since that date, only regional events in areas of special interest (e.g, Spitsbergen, since it is necessary to acquire new knowledge in this region) or other significant events (e.g, felt earthquakes and large industrial explosions) were thoroughly analyzed. Teleseismic events of special interest are also analyzed.

To further reduce the workload on the analysts and to focus on regional events in preparation for Gamma-data submission during GSETT-3, a new processing scheme was introduced on 2 February 1995. The GBF (Generalized Beamforming) program is used as a pre-processor to

RMS, and only phases associated with selected events in northern Europe are considered in the automatic RMS phase association. All detections, however, are still available to the analysts and can be added manually during analysis.

	Jan 04	Feb 04	Mar 04	Apr 04	May 04	Jun 04	Total
Phase detections	184,518	135,278	162,094	109,859	119,458	137,942	849,149
- Associated phases	6,593	4,691	5,379	4,556	6,094	5,837	33,150
- Unassociated phases	177,925	130,587	156,715	105,303	113,364	132,105	815,999
Events automatically declared by RMS	1,477	1,012	1,072	836	949	1,109	6,455
No. of events defined by the analyst	89	71	108	119	179	115	681

Table 3.5.1. RMS phase detections and event summary 1 January - 30 June 2004.

U. Baadshaug
B. Paulsen

4 NDC and Field Activities

4.1 NDC Activitities

NORSAR functions as the Norwegian National Data Center (NDC) for CTBT verification. Six monitoring stations, comprising altogether 119 field instruments, will be located on Norwegian territory as part of the future IMS as described elsewhere in this report. The four seismic IMS stations are all in operation today, and three of them are currently providing data to the IDC on a regular basis. The radionuclide station at Spitsbergen was certified on 10 June 2003, whereas the infrasound station in northern Norway will need to be established within the next few years. Data recorded by the Norwegian stations is being transmitted in real time to the Norwegian NDC, and provided to the IDC through the Global Communications Infrastructure (GCI). Norway is connected to the GCI with a frame relay link to Vienna.

Operating the Norwegian IMS stations continues to require increased resources and additional personnel both at the NDC and in the field. The PTS has established new and strictly defined procedures as well as increased emphasis on regularity of data recording and timely data transmission to the IDC in Vienna. This has led to increased reporting activities and implementation of new procedures for the NDC operators. The NDC carries out all the technical tasks required in support of Norway's treaty obligations. NORSAR will also carry out assessments of events of special interest, and advise the Norwegian authorities in technical matters relating to treaty compliance.

Verification functions; information received from the IDC

After the CTBT enters into force, the IDC will provide data for a large number of events each day, but will not assess whether any of them are likely to be nuclear explosions. Such assessments will be the task of the States Parties, and it is important to develop the necessary national expertise in the participating countries. An important task for the Norwegian NDC will thus be to make independent assessments of events of particular interest to Norway, and to communicate the results of these analyses to the Norwegian Ministry of Foreign Affairs.

Monitoring the Arctic region

Norway will have monitoring stations of key importance for covering the Arctic, including Novaya Zemlya, and Norwegian experts have a unique competence in assessing events in this region. On several occasions in the past, seismic events near Novaya Zemlya have caused political concern, and NORSAR specialists have contributed to clarifying these issues.

International cooperation

After entry into force of the treaty, a number of countries are expected to establish national expertise to contribute to the treaty verification on a global basis. Norwegian experts have been in contact with experts from several countries with the aim of establishing bilateral or multilateral cooperation in this field. One interesting possibility for the future is to establish NORSAR as a regional center for European cooperation in the CTBT verification activities.

NORSAR event processing

The automatic routine processing of NORSAR events as described in NORSAR Sci. Rep. No. 2-93/94, has been running satisfactorily. The analyst tools for reviewing and updating the solutions have been continually modified to simplify operations and improve results. NORSAR is currently applying teleseismic detection and event processing using the large-aperture NORSAR array as well as regional monitoring using the network of small-aperture arrays in Fennoscandia and adjacent areas.

Communication topology

Norway has implemented an independent subnetwork, which connects the IMS stations AS72, AS73, PS28, and RN49 operated by NORSAR to the GCI at NOR_NDC. A contract has been concluded and VSAT antennas have been installed at each station in the network. Under the same contract, VSAT antennas for 6 of the PS27 subarrays have been installed for intra-array communication. The seventh subarray is connected to the central recording facility via a leased land line. The central recording facility for PS27 is connected directly to the GCI (Basic Topology). All the VSAT communication is functioning satisfactorily.

Jan Fyen

4.2 Status Report: Provision of data from Norwegian seismic IMS stations to the IDC

Introduction

This contribution is a report for the period January - June 2004 on activities associated with provision of data from Norwegian seismic IMS stations to the International Data Centre (IDC) in Vienna. This report represents an update of contributions that can be found in previous editions of NORSAR's Semiannual Technical Summary. It is noted that as of 30 June 2004, two out of the three Norwegian seismic stations providing data to the IDC have been formally certified.

Norwegian IMS stations and communications arrangements

During the reporting interval 1 January - 30 June 2004, Norway has provided data to the IDC from the three seismic stations shown in Fig. 4.2.1. The NORSAR array (PS27, station code NOA) is a 60 km aperture teleseismic array, comprised of 7 subarrays, each containing six vertical short period sensors and a three-component broadband instrument. ARCES is a 25-element regional array with an aperture of 3 km, whereas the Spitsbergen array (station code SPITS) has 9 elements within a 1-km aperture.

The intra-array communication for NOA utilizes a land line for subarray NC6 and VSAT links based on TDMA technology for the other 6 subarrays. The central recording facility for NOA is located at the Norwegian National Data Center (NOR_NDC).

Continuous ARCES data has been transmitted from the ARCES site to NOR_NDC using a 64 kbits/s VSAT satellite link, based on BOD technology.

Continuous SPITS data has been transmitted to NOR_NDC via a VSAT terminal located at Platåberget in Longyearbyen (which is the site of the IMS radionuclide monitoring station RN49 installed during 2001).

Seven-day station buffers have been established at the ARCES and SPITS sites and at all NOA subarray sites, as well as at NOR_NDC for ARCES, SPITS and NOA.

The NOA and ARCES arrays are primary stations in the IMS network, which implies that data from these stations is transmitted continuously to the receiving international data center. Since October 1999, this data has been transmitted (from NOR_NDC) via the Global Communications Infrastructure (GCI) to the IDC in Vienna. The SPITS array is an auxiliary station in the IMS, and the SPITS data have been available to the IDC throughout the reporting period on a request basis via use of the AutoDRM protocol (Kradolfer, 1993; Kradolfer, 1996). In addition, continuous data from all three arrays is transmitted to the US NDC.

Uptimes and data availability

Figs. 4.2.2 and 4.2.3 show the monthly uptimes for the Norwegian IMS primary stations ARCES and NOA, respectively, for the period 1 January - 30 June 2004, given as the hatched (taller) bars in these figures. These barplots reflect the percentage of the waveform data that is available in the NOR_NDC tape archives for these two arrays. The downtimes inferred from these figures thus represent the cumulative effect of field equipment outages, station site to NOR_NDC communication outage, and NOR_NDC data acquisition outages.

Figs. 4.2.2 and 4.2.3 also give the data availability for these two stations as reported by the IDC in the IDC Station Status reports. The main reason for the discrepancies between the NOR_NDC and IDC data availabilities as observed from these figures is the difference in the ways the two data centers report data availability for arrays: Whereas NOR_NDC reports an array station to be up and available if at least one channel produces useful data, the IDC uses weights where the reported availability (capability) is based on the number of actually operating channels.

Use of the AutoDRM protocol

NOR_NDC's AutoDRM has been operational since November 1995 (Mykkeltveit & Baadshaug, 1996). The monthly number of requests by the IDC for SPITS data for the period January - June 2004 is shown in Fig. 4.2.4.

NDC automatic processing and data analysis

These tasks have proceeded in accordance with the descriptions given in Mykkeltveit and Baadshaug (1996). For the period January - June 2004, NOR_NDC derived information on 733 supplementary events in northern Europe and submitted this information to the Finnish NDC as the NOR_NDC contribution to the joint Nordic Supplementary (Gamma) Bulletin, which in turn is forwarded to the IDC. These events are plotted in Fig. 4.2.5.

Data access for the station NIL at Nilore, Pakistan

NOR_NDC continued to provide access to the seismic station NIL at Nilore, Pakistan, through a VSAT satellite link between NOR_NDC and Pakistan's NDC in Nilore.

Current developments and future plans

NOR_NDC is continuing the efforts towards improving and hardening all critical data acquisition and data forwarding hardware and software components, so as to meet the requirements related to operation of IMS stations.

The NOA array was formally certified by the PTS on 28 July 2000, and a contract with the PTS in Vienna currently provides partial funding for operation and maintenance of this station. The ARCES array was formally certified by the PTS on 8 November 2001, and a contract with the PTS is in place which also provides for partial funding of the operation and maintenance of this station. Provided that adequate funding continues to be made available (from the PTS and the Norwegian Ministry of Foreign Affairs), we envisage continuing the provision of data from all Norwegian seismic IMS stations without interruption to the IDC in Vienna.

U. Baadshaug
S. Mykkeltveit
J. Fyen

References

Kradolfer, U. (1993): Automating the exchange of earthquake information. *EOS, Trans., AGU*, 74, 442.

Kradolfer, U. (1996): AutoDRM — The first five years, *Seism. Res. Lett.*, 67, 4, 30-33.

Mykkeltveit, S. & U. Baadshaug (1996): Norway's NDC: Experience from the first eighteen months of the full-scale phase of GSETT-3. *Semiann. Tech. Summ., 1 October 1995 - 31 March 1996*, NORSAR Sci. Rep. No. 2-95/96, Kjeller, Norway.

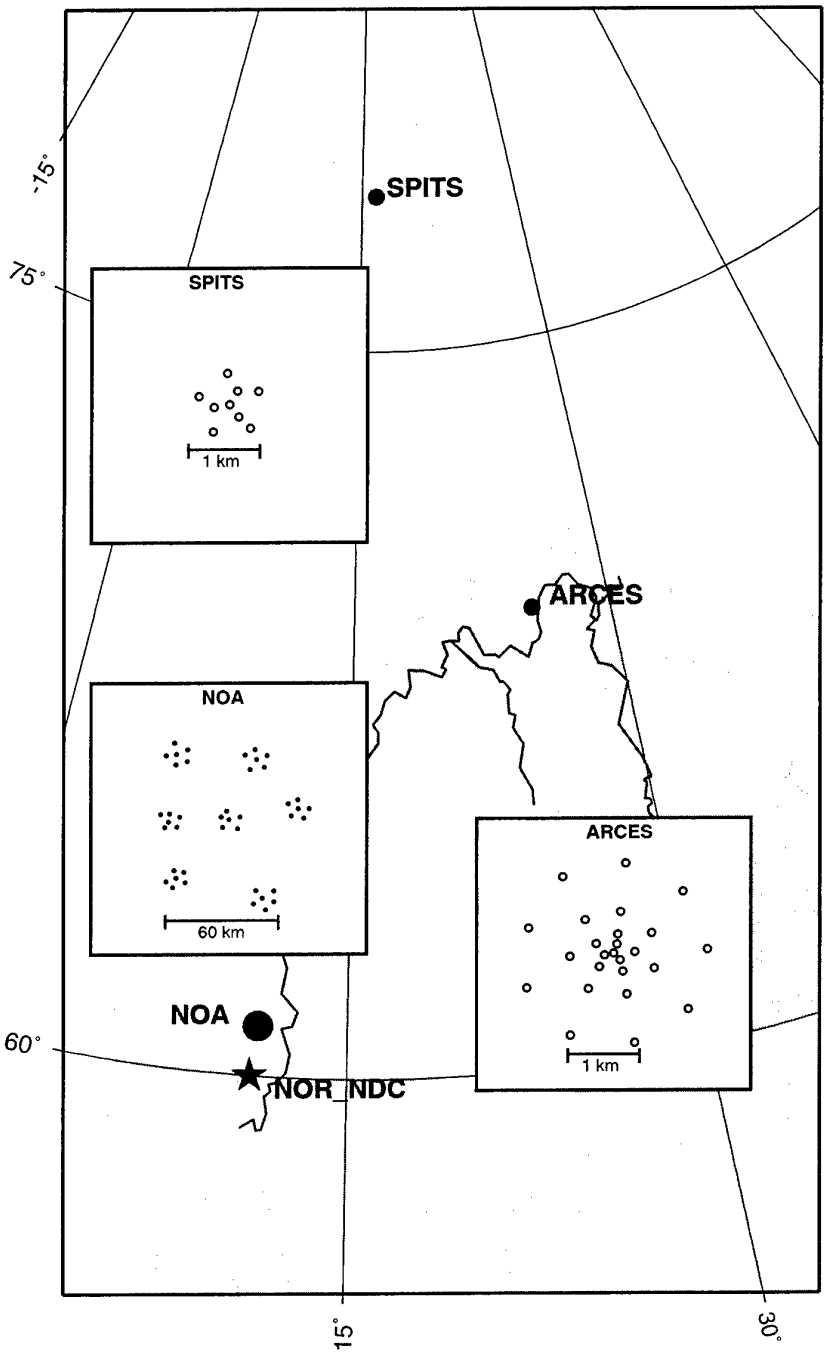

Fig. 4.2.1. The figure shows the locations and configurations of the three Norwegian seismic IMS array stations that provided data to the IDC during the period January - June 2004. The data from these stations are transmitted continuously and in real time to the Norwegian NDC (NOR_NDC). The stations NOA and ARCES are primary IMS stations, whereas SPITS is an auxiliary IMS station.

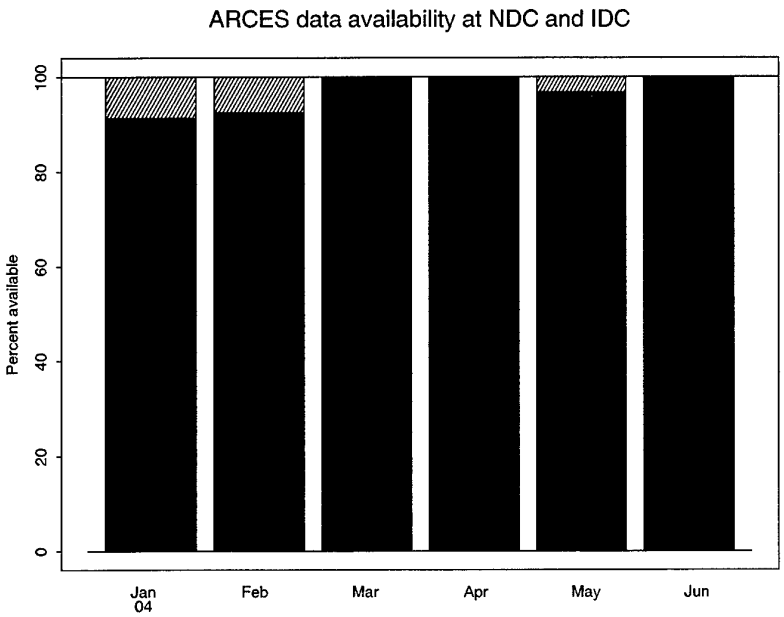

Fig. 4.2.2. The figure shows the monthly availability of ARCES array data for the period January - June 2004 at NOR_NDC and the IDC. See the text for explanation of differences in definition of the term "data availability" between the two centers. The higher values (hatched bars) represent the NOR_NDC data availability.

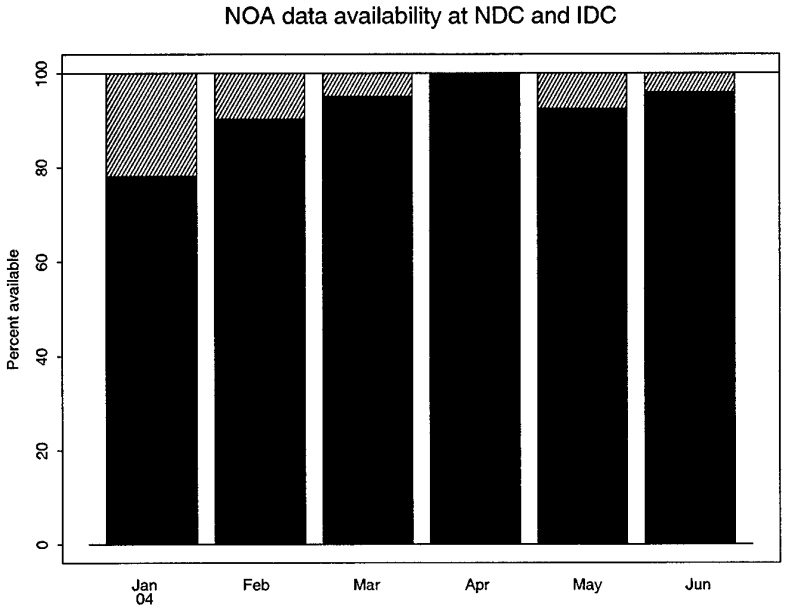

Fig. 4.2.3. The figure shows the monthly availability of NORSAR array data for the period January - June 2004 at NOR_NDC and the IDC. See the text for explanation of differences in definition of the term "data availability" between the two centers. The higher values (hatched bars) represent the NOR_NDC data availability.

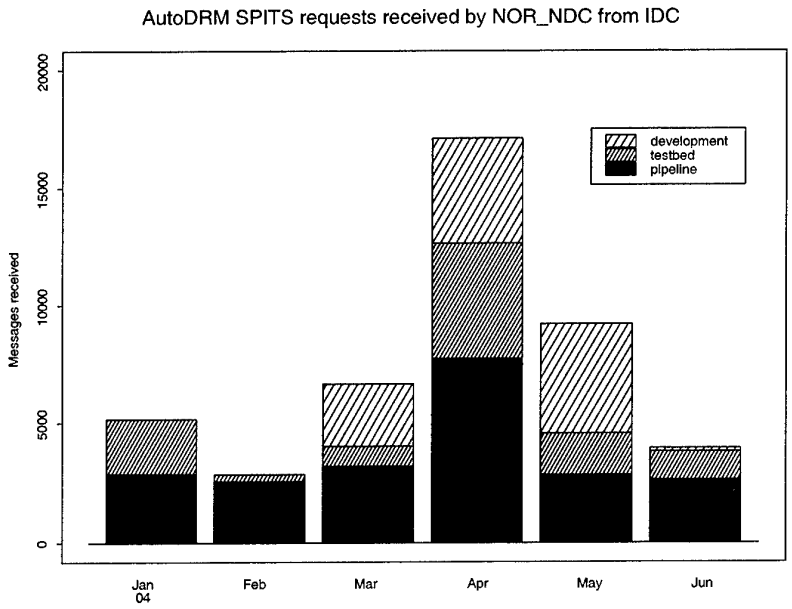

Fig. 4.2.4. The figure shows the monthly number of requests received by NOR_NDC from the IDC for SPITS waveform segments during January - June 2004.

Reviewed Supplementary events

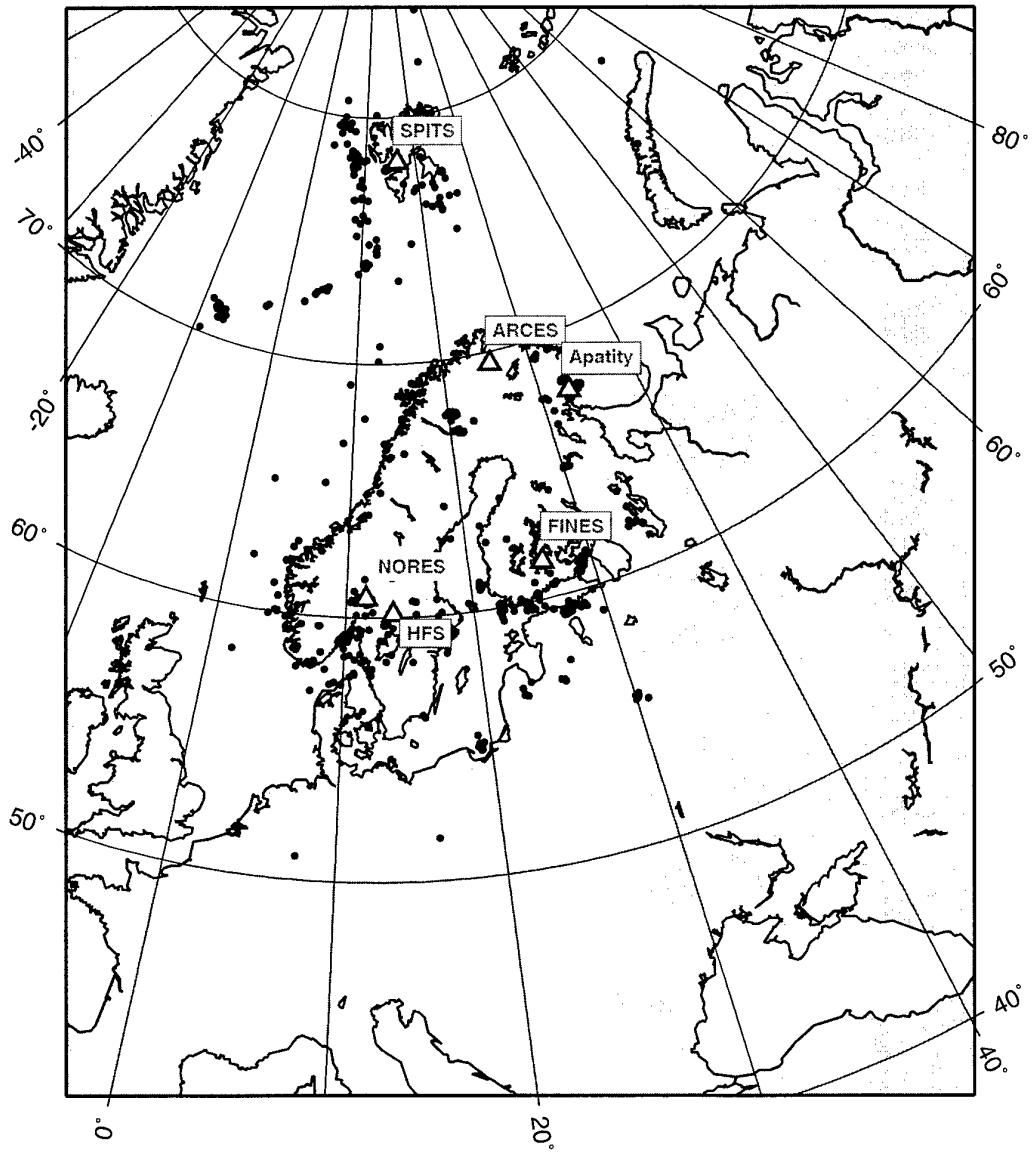

Fig. 4.2.5. The map shows the 733 events in and around Norway contributed by NOR_NDC during January - June 2004 as supplementary (Gamma) events to the IDC, as part of the Nordic supplementary data compiled by the Finnish NDC. The map also shows the seismic stations used in the data analysis to define these events.

4.3 Field Activities

The activities at the NORSAR Maintenance Center (NMC) at Hamar currently include work related to operation and maintenance of the following IMS seismic stations: the NOA teleseismic array (PS27), the ARCES array (PS28) and the Spitsbergen array (AS72). Some work has also been carried out in connection with the seismic station on Jan Mayen (AS73), the infrasound station at Karasjok (IS37) and the radionuclide station at Spitsbergen (RN49). NORSAR also acts as a consultant for the operation and maintenance of the Hagfors array in Sweden (AS101).

NORSAR carries out the field activities relating to IMS stations in a manner generally consistent with the requirements specified in the appropriate IMS Operational Manuals, which are currently being developed by Working Group B of the Preparatory Commission. For seismic stations these specifications are contained in the Operational Manual for Seismological Monitoring and the International Exchange of Seismological Data (CTBT/WGB/TL-11/2), currently available in a draft version.

All regular maintenance on the NORSAR field systems is conducted on a one-shift-per-day, five-day-per-week basis. The maintenance tasks include:

- Operating and maintaining the seismic sensors and the associated digitizers, authentication devices and other electronics components.
- Maintaining the power supply to the field sites as well as backup power supplies.
- Operating and maintaining the VSATs, the data acquisition systems and the intra-array data transmission systems.
- Assisting the NDC in evaluating the data quality and making the necessary changes in gain settings, frequency response and other operating characteristics as required.
- Carrying out preventive, routine and emergency maintenance to ensure that all field systems operate properly.
- Maintaining a computerized record of the utilization, status, and maintenance history of all site equipment.
- Providing appropriate security measures to protect against incidents such as intrusion, theft and vandalism at the field installations.

Details of the daily maintenance activities are kept locally. As part of its contract with CTBTO/PTS NORSAR submits, when applicable, problem reports, outage notification reports and equipment status reports. The contents of these reports and the circumstances under which they will be submitted are specified in the draft Operational Manual.

P.W. Larsen
K.A. Løken

4.4 Spitsbergen array refurbishment

As part of this contract, NORSAR is refurbishing the Spitsbergen array to satisfy the IMS technical specifications. The refurbishment includes upgrading 5 of the array sites to comprise three-component seismometers instead of the current vertical sensors. Both before and after this refurbishment, the Spitsbergen array configuration conforms to the minimum IMS requirement for a new seismic array, having 9 short-period vertical seismometers and one three-component broadband sensor.

In NORSAR Sci. Rep. No. 1-2004 we reported on work done to compare different versions of Guralp seismometers, and it was here concluded that all the seismometers of the upgraded Spitsbergen array should have acceleration responses.

The production of the equipment at the factory has taken much longer time than anticipated. The main reason for this delay is that the array system that has been produced is the first delivery of this type of processing system from the manufacturer (Guralp systems).

During May 5 - 7, 2004, NORSAR staff visited Guralp Systems for a final check of all equipment before shipment. It became, however, clear that Guralp Systems were far from having a system ready for shipment at that time.

We requested continuous data transmission to monitor further developments and testing at the factory. This testing was concluded on July 8, at which time we accepted the equipment to be ready for shipment to Norway.

During the May - July testing at the factory, we could only verify that the system could deliver a continuous CD1.1 data stream from 36 channels. The sensors were situated in a very noisy environment (inside the factory), so all sensors were mounted on a *granite plate* to obtain equal conditions. With this set-up, we could verify that amplitudes (and phase) were within 2 percent. For periods above 50 seconds, we saw larger differences which were explained to be an effect of the loose cables hanging down from the sensors. See Figure 4.4.1for a picture of the sensors.

During the final testing at the facory, the CD1.1 format and protocol, including status bits, was verified by Gonzalo Perez at PTS.

All equipment has been through testing in a temperature chamber for operation at low temperatures. The chamber could cool the GPS down to -31 degrees Celsius, whereas for the digitizer and authenticator that produce heat, the temperature came down to -20 degrees Celsius.

During these final tests, two authenticator units failed in cold temperature testing at -15 degrees Celsius. The fault was identified to come from a mechanical connection with an interface board for the PCMCIA interface. Additionally, Guralp found an issue with soldering on some of the flash chips for the authenticator. These faults have been reported to be fixed, and all the units have been tested again to -20 degrees Celsius.

The cooperation with the vendor has been very good throughout the development and production phase.

Installation of the equipment at the array site will commence on 9 August 2004.

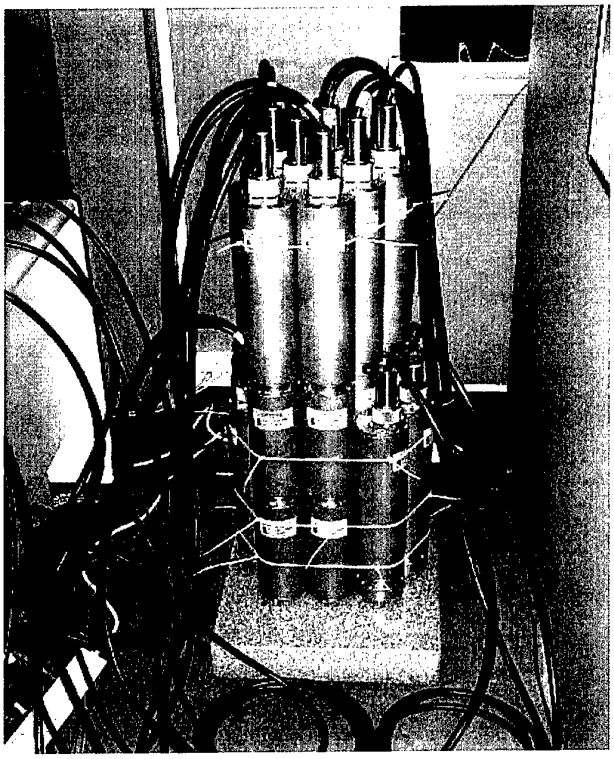

Fig. 4.4.1. The picture is from the factory testing of CMG-3T and CMG-3TV sensors. The sensors are coupled together to obtain as closely as possible the same output.

J. Fyen

5 Documentation Developed

Bischoff, M., J. Schweitzer & T. Meier (2004): Comparison of the Love-Rayleigh discrepancy in central Europe (GRSN) and southern Scandinavia (NORSAR). **In**: NORSAR Sci. Rep. 2-2004, 1 January - 30 June 2004, Kjeller, Norway.

Bommer, J.J., N.A. Abrahamson, F.O. Strasser, A. Pecker, P.-Y. Bard, H. Bungum, F. Cotton, D. Fäh, F. Sabetta, F. Scherbaum & J. Studer (2004): The challenge of defining upper bounds on earthquake ground motions. Seism. Res. Lett., 75, 1, 82-95.

Bommer, J.J., F. Sabetta, F. Scherbaum, H. Bungum, F. Cotton & N.A. Abrahamson (2004): On the use of logic trees for ground-motion prediction equations in PSHA. Bull. Seis. Soc. Am., submitted.

Bungum, H., C. Lindholm & J.I. Faleide (Revised 2004): Postglacial seismicity offshore mid-Norway with emphasis on spatio-temporal magnitudal variations. Marine and Petroleum Geology.

Douglas, J., H. Bungum & F. Scherbaum (2004): Ground-motion prediction equations for southern Spain and southern Norway obtained using the composite hybrid method. J. Earthq. Eng., submitted.

Engdahl, E.R. & J. Schweitzer (2004): Observed and predicted travel times of Pn and P phases recorded at NORSAR from regional events. **In**: NORSAR Sci. Rep. 2-2004, 1 January - 30 June 2004, Kjeller, Norway.

Gibbons, S.J. & F. Ringdal (2004): A waveform correlation procedure for detecting decoupled chemical explosions. **In**: NORSAR Sci. Rep. 2-2004, 1 January - 30 June 2004, Kjeller, Norway.

Ringdal, F., T. Kværna, E. Kremenetskaya, V. Asming, S. Kozyrev, S. Mykkeltveit, S.J. Gibbons & J. Schweitzer (2004): Research in regional seismic monitoring, **In**: NORSAR Sci. Rep. 2-2004, 1 January - 30 June 2004, Kjeller, Norway.

Sabetta, F., A. Lucantoni, H. Bungum & J.J. Bommer (2004): Sensitivity of PSHA results to ground-motion prediction relations and logic-tree weights. Soil Dyn. Earthq. Eng., submitted.

Öberg, D., T. Kværna & F. Ringdal (2004): Discriminants for seismic monitoring. **In**: NORSAR Sci. Rep. 2-2004, 1 January - 30 June 2004, Kjeller, Norway.

6 Summary of Technical Reports / Papers Published

6.1 Research in regional seismic monitoring

(Paper presented at the 26th Annual Seismic Research Review)

Abstract

This project represents a continuing research effort aimed at improving seismic monitoring tools at regional distances, with emphasis on the Barents/Kara Sea region, which includes the former Novaya Zemlya test site. The tasks comprise development and improvement of detection, location and discrimination algorithms as well as experimental on-line monitoring using tools such as regional Generalized Beamforming (GBF) and Threshold Monitoring (TM). It also includes special studies of mining events, for which detailed ground truth information is being provided by the Kola Regional Seismological Centre (KRSC).

We have used data from the regional networks operated by NORSAR and KRSC to assess the seismicity and characteristics of regional phases of the European Arctic. KRSC has for the past 10 years provided to NORSAR ground truth information for selected mining explosions in the Kola Peninsula. Since 2001, the project has been expanded in scope, and is currently carried out jointly with Lawrence Livermore National Laboratory, in a DOE-funded project. This ground truth information comprises accurate locations, charges and explosion characteristics, relating to large underground and surface ripple-fired explosions as well as smaller "compact" underground explosions. The Mining Institute of the Kola Science Centre has made a video recording of two large explosions (one surface and one underground) on 16 November 2002. This video has been made available to us, and the paper presents selected snapshots of the explosions.

We have made some significant progress in automating the detection and location of seismic events from selected areas. In particular, we have continued to improve the regional processing currently carried out at NORSAR for the European Arctic. The emphasis has been on automatic detection and association of phases for small seismic events in the Novaya Zemlya region, using the on-line Generalized Beamforming (GBF) process. We have shown that the number of false associations can be reduced by 90 per cent through relatively simple selection criteria, while still retaining the "real" seismic events. Furthermore, some possibilities for additional future improvements are discussed, including the development of a systematic automatic post-processing algorithm to be applied to event candidates produced by the GBF process currently in operation. Examples of recent small seismic events at Novaya Zemlya detected by the regional network are presented.

We have carried out a study of location accuracy for seismic events near the Spitsbergen archipelago. In cooperation with Kola Regional Seismological Centre (KRSC), we have relocated more than 200 earthquakes occurring during the first half of 2003 with epicenters in Spitsbergen and adjacent areas. We have compared our location results with those published in the Reviewed NORSAR Regional Bulletin, which makes use of the same station network. Additionally, we compared both of these interactive location results to the automatic location provided by the on-line GBF procedure at NORSAR. The Spitsbergen region is geologically far more complex than Fennoscandia, and multiple arrivals of P and S phases are quite common. Consequently, different phase interpretation by different analysts result in occasionally large deviations in location estimates, sometimes as much as 100 km for events located by the SPITS

array alone. Some possibilities for future enhancements of the event location procedures are discussed.

6.1.1 Objective

This work represents a continued effort in seismic monitoring, with emphasis on studying earthquakes and explosions in the Barents/Kara Sea region, which includes the former Russian nuclear test site at Novaya Zemlya. The overall objective is to characterize the seismicity of this region, to investigate the detection and location capability of regional seismic networks and to study various methods for screening and identifying seismic events in order to improve monitoring of the Comprehensive Nuclear-Test-Ban Treaty. Another objective is to carry out special studies of mining events, for which detailed ground truth information is being provided by the Kola Regional Seismological Centre (KRSC).

6.1.2 Research Accomplished

NORSAR and Kola Regional Seismological Centre (KRSC) of the Russian Academy of Sciences have for many years cooperated in the continuous monitoring of seismic events in North-West Russia and adjacent sea areas. The research has been based on data from a network of sensitive regional arrays which has been installed in northern Europe during the last decade in preparation for the CTBT monitoring network. This regional network, which comprises stations in Fennoscandia, Spitsbergen and NW Russia provides a detection capability for the Barents/Kara Sea region that is close to $m_b = 2.5$ (Ringdal, 1997).

The research carried out during this effort is documented in detail in several contributions contained in the NORSAR Semiannual Technical Summaries. In the present paper we will limit the discussions to some recent results of interest in the general context of regional monitoring of seismic events in the European Arctic. In particular our studies have focused on mining explosions in the Kola Peninsula, using data from stations shown in Figure 6.1.1. This figure also shows some of the most active mining areas.

Khibiny mine explosions

We have used data from the regional networks operated by NORSAR and KRSC to assess the seismicity and characteristics of regional phases of the European Arctic. KRSC has for the past 10 years provided to NORSAR ground truth information for selected mining explosions in the Kola Peninsula. Since 2001, the project has been expanded in scope, and is currently carried out jointly with Lawrence Livermore National Laboratory, in a DOE-funded project (Harris et. al., 2003). This ground truth information comprises accurate locations, charges and explosion characteristics, relating to large underground and surface ripple-fired explosions as well as smaller "compact" underground explosions.

Of particular interest are two explosions, one underground and one at the surface carried out in the Rasvumchorr mine in Khibiny on 16 November 2002. These explosions were briefly discussed in Ringdal et. al. (2003), and here we present some additional information. As illustrated in Figures 6.1.2 and 6.1.3, the underground explosion was a ripple-fired explosion of 257 tons, whereas the open-pit explosion comprised four separate ripple-fired explosions, set off with about 1 second intervals, from south to north. The surface and underground explosions were only 300 m apart, so that differences in path effects at the more distant stations can be

ignored. Nevertheless, the recorded signals, e.g. at the temporary station in Ivalo, Finland at 300 km distance, were remarkably different: The vertical component of these recordings is shown in Figure 6.1.4 in different filter bands. At lower frequencies (2-4 Hz), the underground explosion was stronger by a factor of 10 in amplitude, whereas above 10 Hz, the surface explosion had by far the stronger signals. The Mining Institute of the Kola Science Centre has made a video recording of these explosions. This video has been made available to us, and Figure 6.1.5 presents selected snapshots of the explosions.

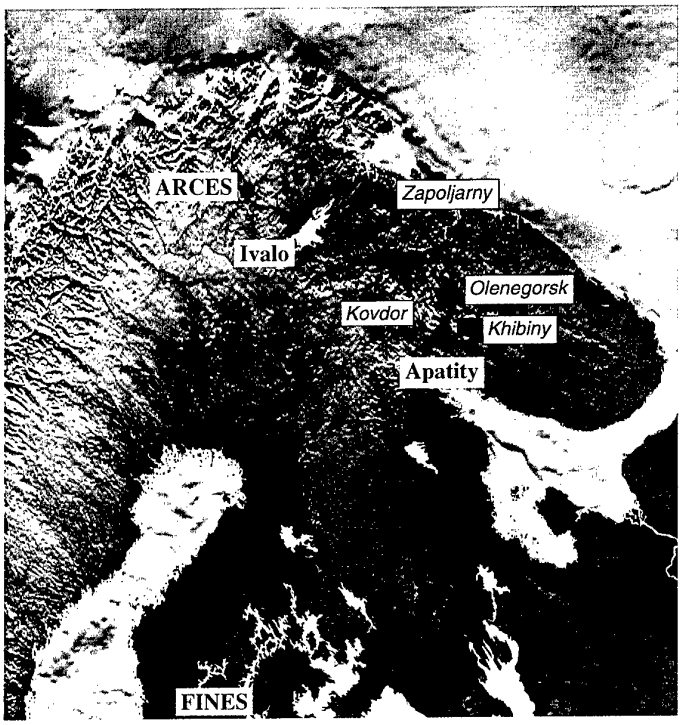

Fig. 6.1.1. Seismic stations (circles) used in our studies of mine explosions in Kola Peninsula. The main mining sites are marked as squares. The station Ivalo is one of six temporary stations established in cooperation with LLNL.

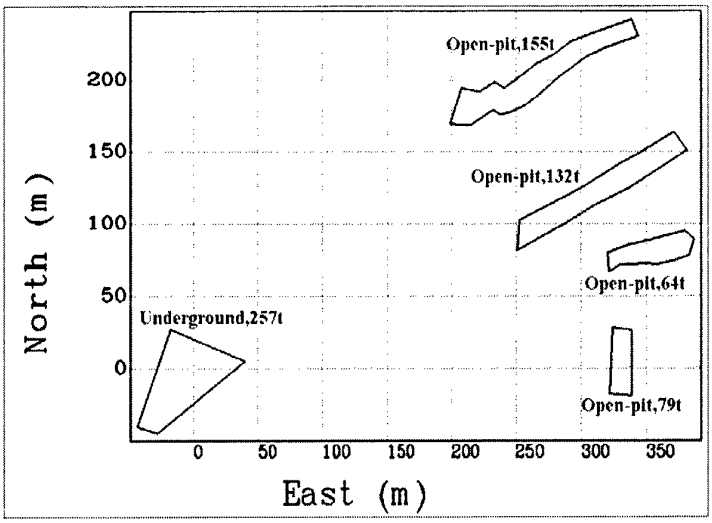

Fig. 6.1.2. Schematic view of the shot configuration for the two explosions in Khibiny on 16 November 2002. Geographical coordinates of the point (0,0) are 67.6322N 33.8565E. See text for details.

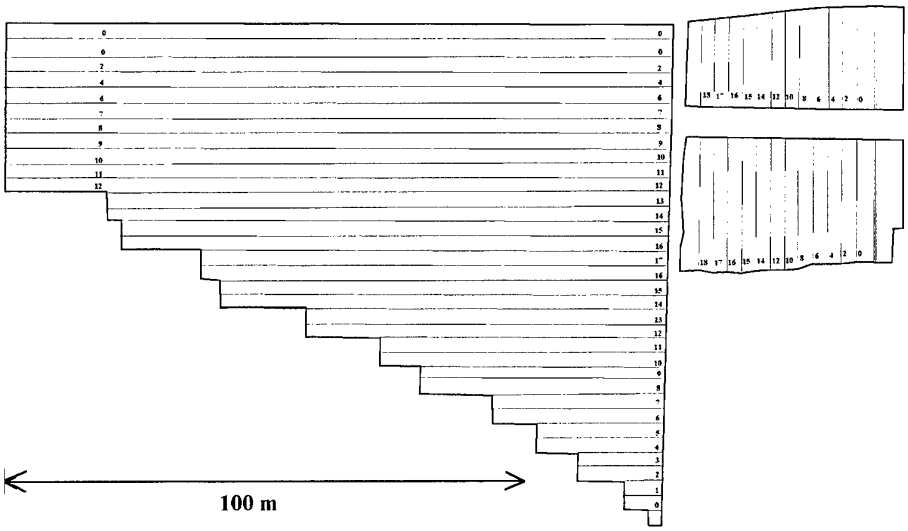

Fig. 6.1.3. Geometry of the underground mining explosion in Khibiny 16 November 2002. The charges were detonated in 19 groups (delay 23 ms between each group). The sequence is indicated by the numbers, and individual charge sizes have been made available.

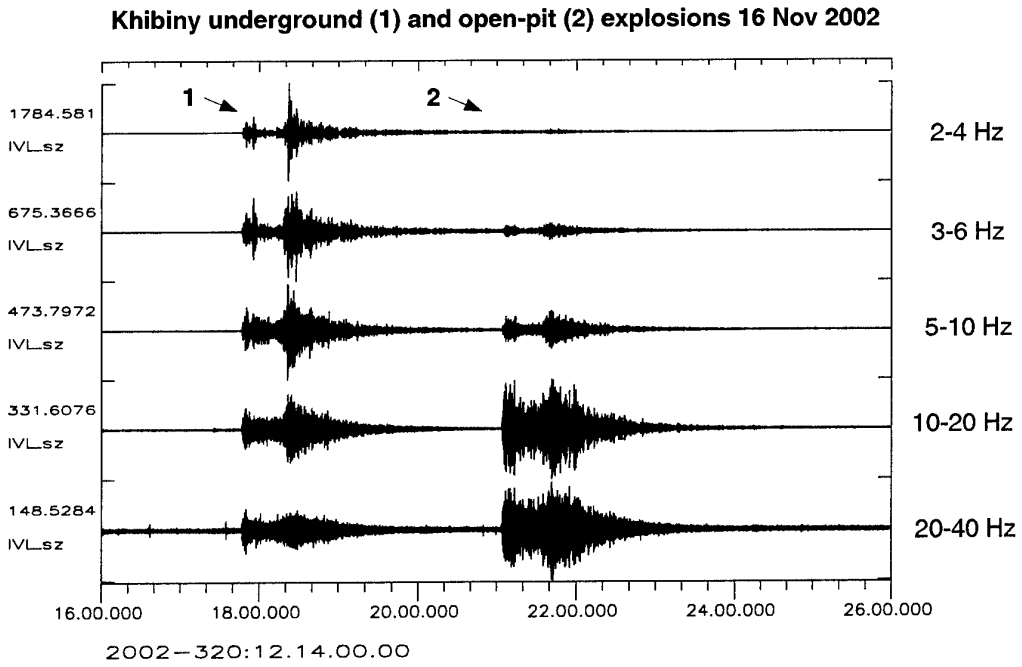

Fig. 6.1.4. Recorded SPZ waveforms at station Ivalo (northern Finland) for the two explosions in Khibiny on 16 November 2002. The data have been filtered in five different frequency bands. Note the significant difference in relative size of the two events as a function of frequency.

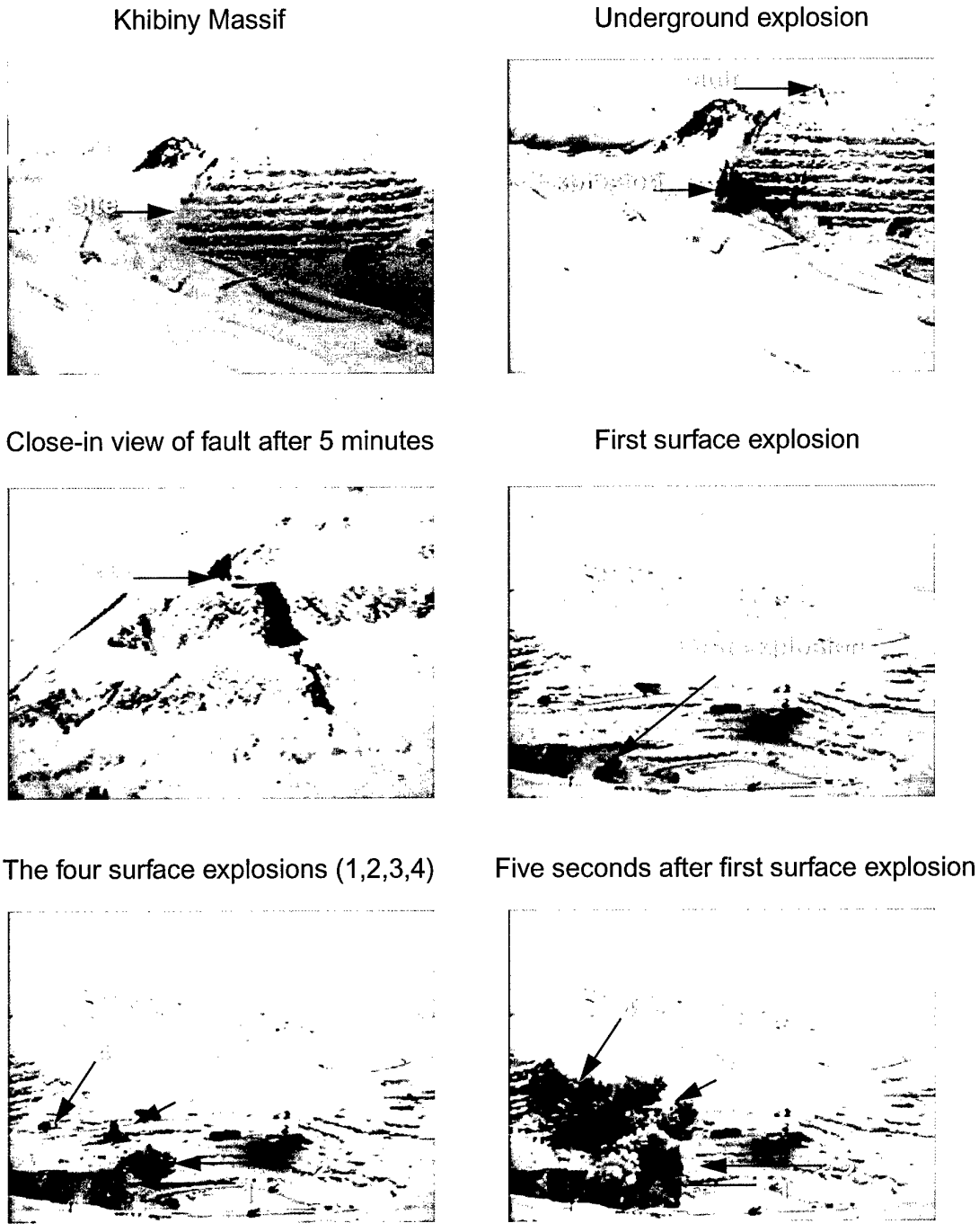

Fig. 6.1.5. Snapshots of video from the sequence of Khibiny explosions on 16 November 2002 Note in particular the large crack ("fault") opening up in the mountainside at the time of the first (underground) explosion.

Developing NORSARs regional processing system

NORSAR has for a number of years carried out processing and analysis of seismic events in the European Arctic, using the regional array network in Fennoscandia and NW Russia. The regional processing system at the NORSAR Data Center comprises the following steps:

- Automatic single array processing, using a suite of bandpass filters in parallel and a beam deployment that covers both P and S type phases for the region of interest.
- An STA/LTA detector applied independently to each beam, with broadband f-k analysis for each detected phase in order to estimate azimuth and phase velocity.
- Single-array phase association for initial location of seismic events, and also for the purpose of chaining together phases belonging to the same event, so as to prepare for the subsequent multiarray processing.
- Multi-array event detection, using the Generalized Beamforming (GBF) approach (Ringdal and Kværna, 1989) to associate phases from all stations in the regional network and thereby provide automatic network locations for events in all of northern Europe. The resulting automatic event list is made available on the Internet (www.norsar.no).
- Interactive analysis of selected events, resulting in a reviewed regional seismic bulletin, which includes hypocentral information, magnitudes and selected waveform plots. This reviewed bulletin is also available on the Internet.

Monitoring the Novaya Zemlya region

The philosophy behind the automatic process at NORSAR is to ensure, as far as possible, that no real detectable event is lost. The penalty is that a number of false associations are generated. This problem is most significant for regions at large distances from the arrays, such as the Novaya Zemlya region. We describe below some initial steps undertaken to eliminate many of these false associations.

It is well known that the most sensitive arrays for seismic events in the Novaya Zemlya region are ARCES and SPITS. Our initial step to reduce the number of false associations is therefore to require detection by one or both of these two arrays, using a combination of the following criteria:

1. Pn and Sn detections by SPITS
2. Pn and Sn detections by ARCES
3. Pn detections by both SPITS and ARCES

In addition, we have experimented with additional constraints on Pn phase velocities for the two arrays, in order to eliminate obvious teleseismic or near-regional phases. Reasonable constraints, based on observational evidence, are:

- For ARCES: Pn velocity between 8-12 km/s
- For SPITS: Pn velocity between 7-10 km/s

Furthermore, we have considered the effects of constraining the acceptable difference in estimated azimuth for the P and S phase, by removing single-station events that have an azimuth difference (P-S) exceeding 15 degrees.

Table 6.1.1 gives an overview of the number of GBF event candidates located in the region surrounding Novaya Zemlya for the years 2002 and 2003. The geographical limits are 70-78 degrees North, 50-70 degrees East. The counts using the current on-line GBF algorithm as well as the counts requiring detection by ARCES and SPITS, and counts imposing additional constraints are given.

Table 6.1.1. GBF event candidates 70-78 deg N, 50-70 deg E

Detection criterion	ARCES Pn velocity	SPITS Pn velocity	Az. diff.	Total 2002	Total 2003	Sum
All GBF	All	All	All	683	950	1733
1 or 2 or 3	All	All	All	294	382	676
1 or 2 or 3	8-12 km/s	7-10 km/s	All	177	211	388
1 or 2 or 3	8-12 km/s	7-10 km/s	<15 deg	66	81	147

The criteria specified in the table are conservative in the sense that they should not eliminate any potential real seismic events occurring in this region. Nevertheless, we see from the table that the number of event candidates is reduced by about 90 per cent when applying the final (strongest) test.

We note that the significant reduction in false detections when imposing the azimuth constraint is due to a too wide azimuth window currently applied in the GBF processing. The GBF algorithm allows phases to be associated to the same event if they deviate less than 30 degrees from the grid point toward which the generalized beam is steered. This implies that P and S phases associated to a given event could (in extreme cases) differ by up to 60 degrees, which is clearly excessive. There is therefore a good argument for adding a more restrictive azimuth test in the second step of the on-line GBF process.

Table 6.1.2. List of seismic events in or near Novaya Zemlya (1980-2003) located outside the test site.

Date/time	Location	m_b	Comment
01.08.86/ 13.56.38	72.945 N, 56.549 E	4.3	Located by Blacknest, UK
31.12.92/ 09.29.24	73.600 N 55.200 E	2.7	Located by NORSAR
23.02.95/ 21.50.00	71.856 N, 55.685 E	2.5	Located by NORSAR
13.06.95/ 19.22.38	75.170 N, 56.740 E	3.5	Located by NORSAR
13.01.96/ 17.17.23	75.240 N, 56.660 E	2.4	Approximately co-located with preceding event
16.08.97/ 02.11.00	72.510 N, 57.550 E	3.5	Located by NORSAR
16.08.97/ 06.19.10	72.510 N, 57.550 E	2.6	Co-located with preceding event
23.02.02/ 01.21.14	74.047 N, 57.671 E	3.0	Located by NORSAR
08.10.03/ 23.07.10	75.645N, 63.345E	2.5	Located by NORSAR

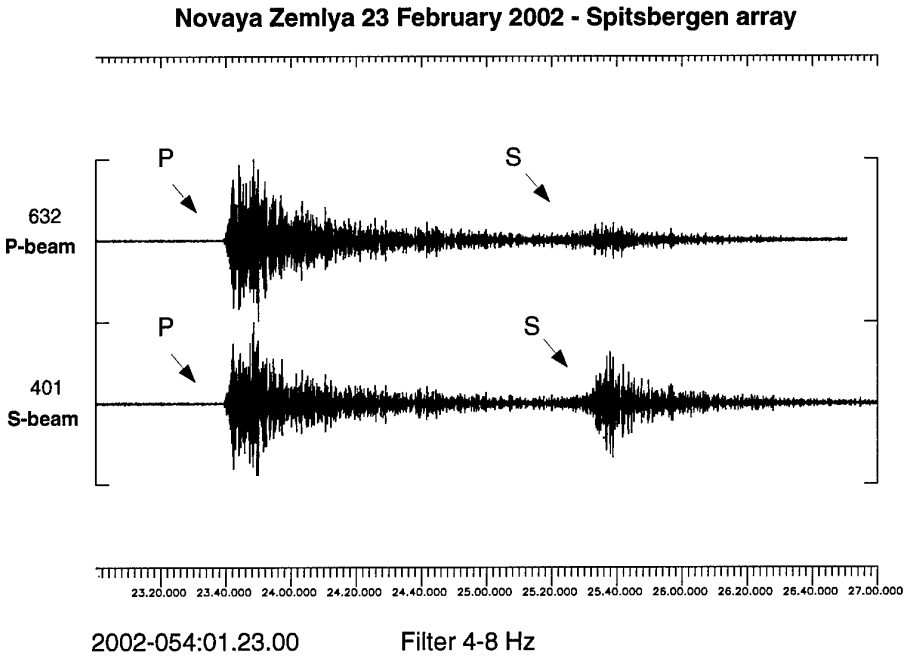

Fig. 6.1.6. Spitsbergen P and S beams for the Novaya Zemlya event on 23 February 2002.

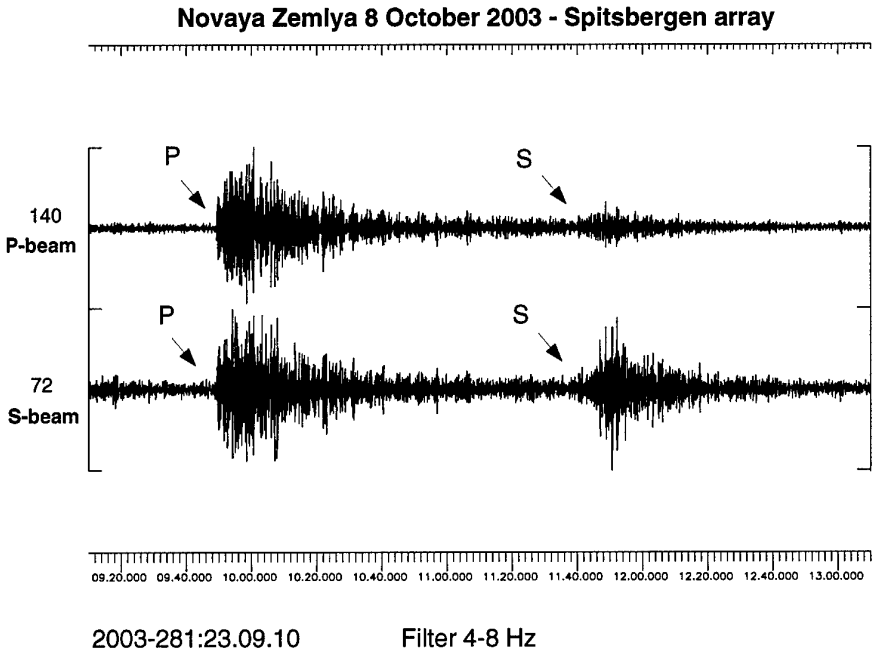

Fig. 6.1.7. Spitsbergen P and S beams for the Novaya Zemlya event on 8 October 2003.

Examples of recent low-magnitude events

Table 6.1.2 lists small events in the Novaya Zemlya region, located outside the test site and detected over the years by the NORSAR regional processing. Recordings of the two most recent events are illustrated in Figures 6.1.6 and 6.1.7. The first figure shows a magnitude 3.0 event on 23 February 2002, as recorded by the SPITS array. Two filtered (4-8 Hz) array beams are displayed, corresponding to Pn and Sn velocities and directed towards the epicenter. We note the high SNR for the P-phase, and also note that the S-phase is clearly detected on the S-beam. The second event (magnitude 2.5) occurred on 8 October 2003, and Figure 6.1.7 shows the SPITS Pn and Sn beams for this event. The waveforms have similar characteristics to those observed for the 23 February 2002 event. This event illustrates the importance of including in the detection criteria single-station detections (P and S phases detected at the same array) as well as events detected at both arrays. In fact, there was no automatic detection of this event at ARCES. However, by inspecting the ARCES waveforms visually, P and S onsets could be found, and were included in the reviewed event location in Table 6.1.2.

Locating small events near Spitsbergen

The geology of the Spitsbergen archipelago and surrounding regions is complex, and results in very complex seismograms from some areas. Multiple onsets of P and S waves are not uncommon, and can strongly increase location errors. We have relocated more than 200 small earthquakes (mostly of magnitude around 2.0) occurring during the first half of 2003 with epicenters in Spitsbergen and adjacent areas. All of these events were detected by at least two stations (usually KBS and SPITS, sometimes with addition of ARCES and other distant stations). We compared our location results with those published in the Reviewed NORSAR Regional Bulletin, which makes use of the same station network. Additionally, we compared both of these interactive location results to the automatic location provided by the on-line GBF procedure at NORSAR. Detailed results are presented in Asming et. al. (2004).

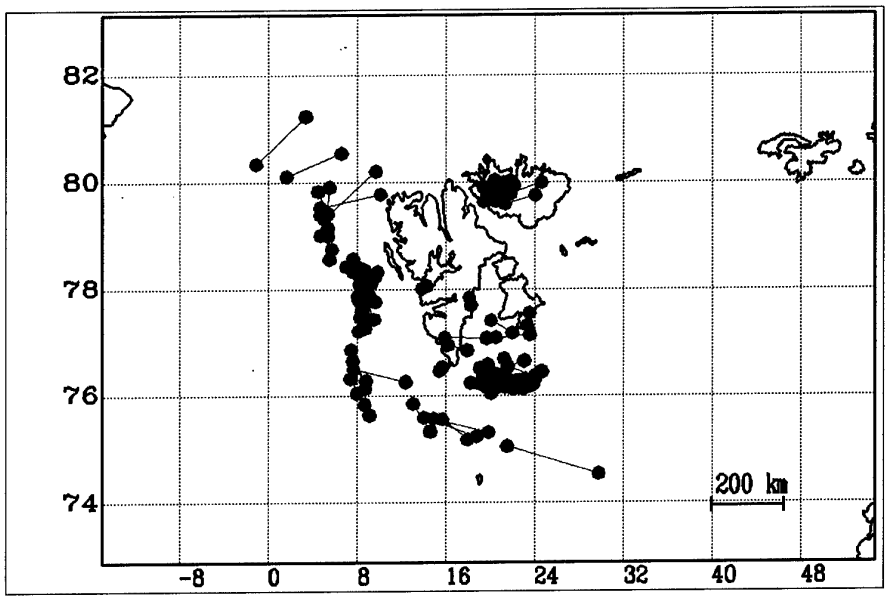

Fig. 6.1.8. Location comparison: Relocated events (red) vs. NORSAR reviewed bulletin (blue).

In Figure 6.1.8 we compare the two sets of analyst reviewed locations (marked NORSAR for the results in the NORSAR Regional Bulletin and KRSC for the relocated solutions). In general, they are quite consistent, but we note a systematic shift in the locations of groups of events, with the KRSC locations generally being shifted in westernly directions compared to those of the NORSAR analyst. Mostly, the location differences are small (a few tens of kilometers), but for a few events the difference exceeds 100 km, and in one case it is more than 200 km. The smaller differences can be attributed, at least in part, to the different velocity models used at KRSC and NORSAR (KRSC uses the SPITS0 model, whereas NORSAR uses a general Fennoscandian model). The cases with large differences are a direct consequence of the difficulties in phase interpretations, and demonstrate that locations of small earthquakes in this region can be associated with significant uncertainties.

6.1.3 Conclusions and recommendations

The accumulation of detailed ground truth for mining explosions in the Kola Peninsula is a significant step towards improved understanding of the waveform characteristics of various types of mining explosions. Our analysis shows significant spectral differences between surface and open-pit explosions. We recommend to pursue this work as more ground truth data of mining events is accumulated, and a larger database of recordings from near-field stations becomes available.

We have demonstrated that a set of relatively simple post-processing criteria can significantly reduce the number of false associations in the automatic GBF process. Nevertheless, there is still room for considerable improvement. A promising approach is to use fixed-frequency filter bands for the broad-band f-k estimation. In this way, one can obtain more stable azimuth estimates, thereby enabling a much lower tolerance than the currently used threshold of 15 degrees for the difference in P and S azimuths. We will continue our work on reducing the false alarm rate in the automatic GBF lists, while retaining as many as possible of the real seismic events. Furthermore, the automatic detector algorithms could be further improved, and work towards this end is continuing.

By studying a set of more than 200 earthquakes in the Spitsbergen region, we have shown that analyst reviewed locations (as processed by different analysts) can have occasional large deviations, in several cases exceeding 100 km. This is due to the complexity of the seismograms, which sometimes results in ambiguous phase identification. Detection of S-phases using the SPITS array is often problematic, and improvements here is a topic of current research. With the planned refurbishment of SPITS, several 3-component sites will be included in the array, and this should improve the detection potential for S-phases in the future. In particular, attention should be given to high-frequency processing of data for phase identification and velocity/azimuth estimation purposes.

F. Ringdal
T. Kværna
E. Kremenetskaya
V. Asming
S. Kozyrev
S. Mykkeltveit
S. J. Gibbons
J. Schweitzer

References

Asming, V. E., E. O. Kremenetskaya and F. Ringdal (2004): Locating seismic events near the Spitsbergen Archipelago. *Semiannual Technical Summary 1 July - 31 December 2003*, NORSAR Sci. Rep. 1-2004, Kjeller, Norway.

Harris, D. B., F. Ringdal, E. O. Kremenetskaya, S. Mykkeltveit, J. Schweitzer, T. F. Hauk, V. E. Asming, D. W. Rock and J. P. Lewis (2003). Ground-truth Collection for Mining Explosions in Northern Fennoscandia and Russia. "*Proceedings of the 25th Seismic Research Review - Nuclear Explosion Monitoring: Building the Knowledge Base*, Los Alamos National Laboratory, *LA-UR-03-6029*, Tucson, AZ, Sept. 23-25, 2003.

Ringdal, F. (1997): Study of low-magnitude seismic events near the Novaya Zemlya nuclear test site, *Bull. Seism. Soc. Am. 87 No. 6,* 1563-1575.

Ringdal, F. and T. Kværna (1989). A multichannel processing approach to real time network detection, phase association and threshold monitoring, *Bull. Seism. Soc. Am.*, **79**, 1927-1940.

Ringdal, F., T. Kværna, E. O. Kremenetskaya, V. E. Asming, S. Mykkeltveit, S. J. Gibbons and J. Schweitzer (2003). Research in Regional Seismic Monitoring. "*Proceedings of the 25th Seismic Research Review - Nuclear Explosion Monitoring: Building the Knowledge Base*, Los Alamos National Laboratory, *LA-UR-03-6029*, Tucson, AZ, Sept. 23-25, 2003.

6.2 A waveform correlation procedure for detecting decoupled chemical explosions

6.2.1 Introduction

Between 1986 and 1989, a total of 11 decoupled chemical explosions were carried out in two underground chambers at a site in Älvdalen, central Sweden, by the Klotz Group of ammunition safety experts. Explosions with yields 10, 1000, and 5000 kg were performed in each of the two chambers, one with size 300 m^3 and one with size 200 m^3.

A complete list of these experiments is provided in Table 6.2.1 after Vretblad (1991), the date of each explosion being provided but without origin time. Both the NORES regional seismic array, central element a distance of 143 km from the test site, and the large aperture NORSAR teleseismic array, with instruments at distances between 123 and 175 km, were operational at the time. It should be noted, however, that the explosions were carried out prior to the NORSAR upgrade of 1995 and so this array only recorded data with a 20 Hz sampling rate. All NORES data is recorded with a 40 Hz sampling rate.

Our primary goal is to investigate the effects of seismic decoupling on the characteristics of seismograms recorded at regional distances. If we are to include these tests into the very small available database of such explosions, we need first to determine which part of the recorded data corresponds to the signals resulting from these experiments, or, equivalently, to determine the unknown origin times. An initial inspection of the NORES detection lists for the days in question does not produce any obvious candidates for the hitherto unidentified Klotz tests with the possible exception of shot number 4[1]. Gibbons et al. (2002) demonstrate that the Älvdalen signals are dominated by higher frequencies at which coherence between instruments is very poor, even over the small aperture NORES array; this makes it more difficult to determine the slowness and azimuth of detected phases using traditional array processing techniques.

We have at our disposal waveform data from four subsequent explosions from a third chamber at the same site which took place between December 2000 and June 2002 (see Gibbons et al., 2002, Stevens et al., 2003). In addition, the three largest of the experiments listed in Table 6.2.1 (shots 8, 9, and 11) have already been identified since they resulted in signals which are clearly visible in NORES and NORSAR data without filtering (Figure 6.2.1). These three shots are labelled 1987C146, 1987C259, and 1989C263 respectively in Stevens et al. (2003).

We aim to identify the data which corresponds to the unknown events by matching waveform data with signals resulting from the known events. We assess first the degree of correlation between waveforms from the events already identified and subsequently apply this to continuous data for the days on which the events in Table 6.2.1 are known to have taken place.

1. See http://www.norsar.no/NDC/bulletins/dpep/1986/177/NRS/NRS86177.html - automatic location ID number 135320 is ascribed an origin time of 1986-177:09.14.06.2, latitude 61.422°, longitude 13.901° a distance of 148 km from NORES at a backazimuth of 57.9°.

Table 6.2.1. The 11 Klotz group explosions at the Älvdalen site between 1986 and 1989. Information obtained from Vretblad (1991). Chambers A and B have volumes of 300m^3 and 200m^3 respectively.

Shot number	Date (yym-mdd)	Yield/ kg	Ammu-nition type	Site	Purpose of test
1	860611	10	TNT	A	Calibration
2	860610	10	TNT	B	Calibration
3	860617	1000	TNT	A	Study of large ejecta pieces
4	860626	1000	TNT	B	As (3) with debris trap
5	860917	1000	Shells	A	Comparison of pressures with and without casing. Study of fragment throw
6	860903	1000	Shells	B	As (5) but with debris trap
7	870521	1000	ANFO	A	Study of the effectiveness of ANFO for this type of simulation
8	870916	5000	ANFO	A	As (5) but with higher loading density and artificial debris
9	870916	5000	ANFO	B	As (6) but with higher loading density and with artificial debris.
10	890830	1000	Shells	A	As (5) but with a berm in front of the tunnel
11	890920	5000	ANFO	A	As (8) but with a berm in front of the tunnel.

We note that waveform correlation methods have been applied in the past e.g. for detecting routine blasting operations at known industrial sites (Harris, 1991). These studies have shown considerable promise, but a major problem has been that seismograms from similar industrial explosions can differ significantly in waveform characteristics, both as a function of variations in blasting practice (see, for example, Stump et al., 2001) and because of differences in locations even within the same mine (Bonner et al., 2003). In our study, the explosion sources are very simple and of similar nature, and the shot points are closely spaced (the shots are detonated in a total of three chambers, separated by less than 200 meters). As will be shown in the following, this results in a significant improvement in the detection capability of such events by using waveform cross-correlation as compared with using conventional detectors. Furthermore, we will show that applying array processing to the correlation traces gives a considerable improvement over single-station correlation procedures.

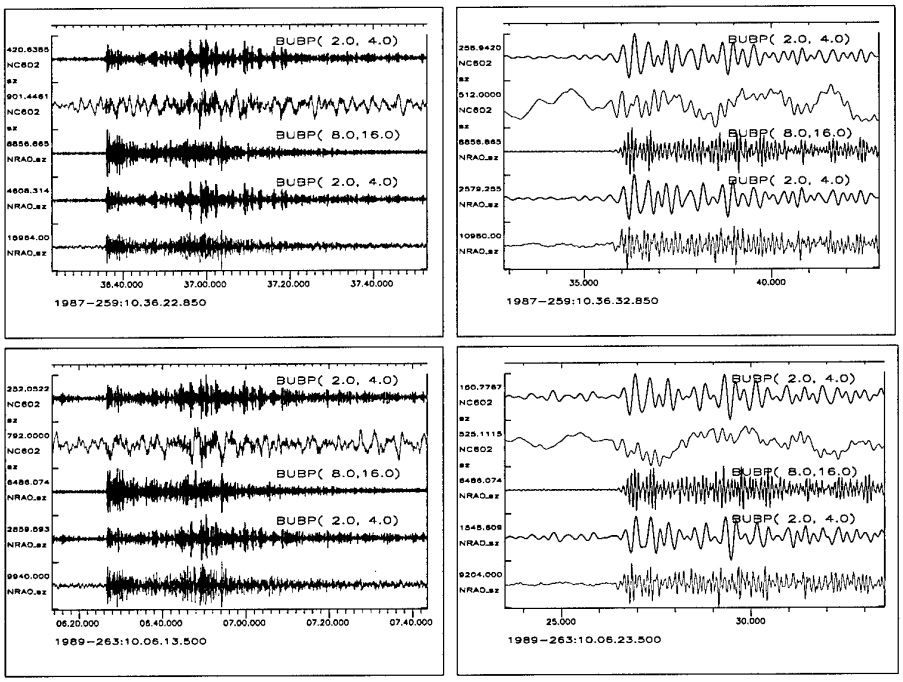

Fig. 6.2.1. Waveforms from two of the 5000 kg yield explosions recorded at the NORES central element NRA0 and the co-located NC602 element of the NORSAR array. The blue waveforms are unfiltered data and the black waveforms are bandpass filtered in the ranges indicated. The events are shots (9) and (11) in Table 6.2.1 respectively. Note the similarity between the waveforms from the events in the two different chambers.

6.2.2 Single-station correlation coefficients for the known events

Table 6.2.2 shows the fully normalized correlation coefficients for NRA0 data for explosions already known to have taken place in the various chambers at the Älvdalen site. Note that the final event from June 13th 2002 is not included as there is no NORES data for this explosion. When the broad frequency band (2.0-18.0 Hz) is used, the correlation coefficient is high for all of the event combinations except for those that include the 2001C150 event which was by far the weakest signal. However, when a higher frequency band (14.0-18.0 Hz) is used, even this event results in very high correlation coefficients since the signal to noise ratio is far better for these frequencies. All the data used here was resampled to 200 Hz in order to perform the cross-correlation.

Given that the signals that we are searching for are likely to be very weak, we proceed to use data filtered in a high frequency band for the correlation tests.

Table 6.2.2. Correlation coefficients of waveforms recorded at the instrument NRA0_sz for events as labelled in Gibbons et al. (2002). All values are calculated for a five second time window beginning shortly after the P-onset time; values below the diagonal are for waveforms filtered in the frequency band (2.0-18.0 Hz) and those above the diagonal are for the frequency band (14.0-18.0 Hz). Values in red indicate that the two events took place within the same chamber.

Correlation coefficients (NRA0_sz)	1987C146	1987C259	1989C263	2000C348	2001C150	2001C186
1987C146	-	0.984	0.977	0.855	0.805	0.845
1987C259	0.919	-	0.987	0.877	0.821	0.871
1989C263	0.981	0.914	-	0.862	0.796	0.853
2000C348	0.852	0.862	0.851	-	0.902	0.997
2001C150	0.310	0.293	0.318	0.423	-	0.900
2001C186	0.846	0.846	0.843	0.971	0.448	-

6.2.3 Multiple channel waveform correlation for the detection of the unknown events

The correlation coefficients provided in Table 6.2.2 refer only to a single channel. Each of these coefficients is in fact the maximum value of a trace produced by correlating a short, fixed time window from a 'master event' with consecutive sections of a much longer time series. This trace would reach a maximum value of 1.0 should the master event time window be an exact (positive) multiple of the corresponding segment of the longer seismogram. Otherwise the waveform correlation trace will vary between 1.0 and -1.0, fluctuating about a zero mean depending upon whether the contribution from the in-phase parts of the waveform exceeds the contribution from the out-of-phase parts or not.

Given that we have array data available, we ought to be able identify correlation maxima more easily by an appropriate stacking of the individual correlation traces. Deterministic correlation will occur simultaneously for all channels used (subject to any time-shift imposed when defining the master event time-windows) whereas other local maxima and minima of the individual waveform correlation (WFC) traces are assumed to occur randomly.

An 8 second long time-window was selected from the signal from event 1987C259 (the event with best SNR) for each sz channel of the NORES array. For simplicity these windows started simultaneously, removing the need to apply time-shifts when stacking the WFC traces. The master event traces were subsequently filtered in the frequency band 14.0-18.0 Hz and resampled to 200 Hz. The resulting waveforms were correlated against the corresponding filtered data for the days of the unknown events.

Figure 6.2.2 indicates the results of this procedure for an hour of data beginning at 1986-177:09.00.00.0. A clear and unique peak is observed for all of the WFC traces at a time 1986-177:09.14.28.61 and therefore also on the summation channel. Note (a) the degree of noise suppression which results from the stacking of the WFC traces and (b) the fact that several

other regional signals are observed in this one hour long data segment and that none of them have a noticeable effect upon the fully normalized correlation coefficient traces.

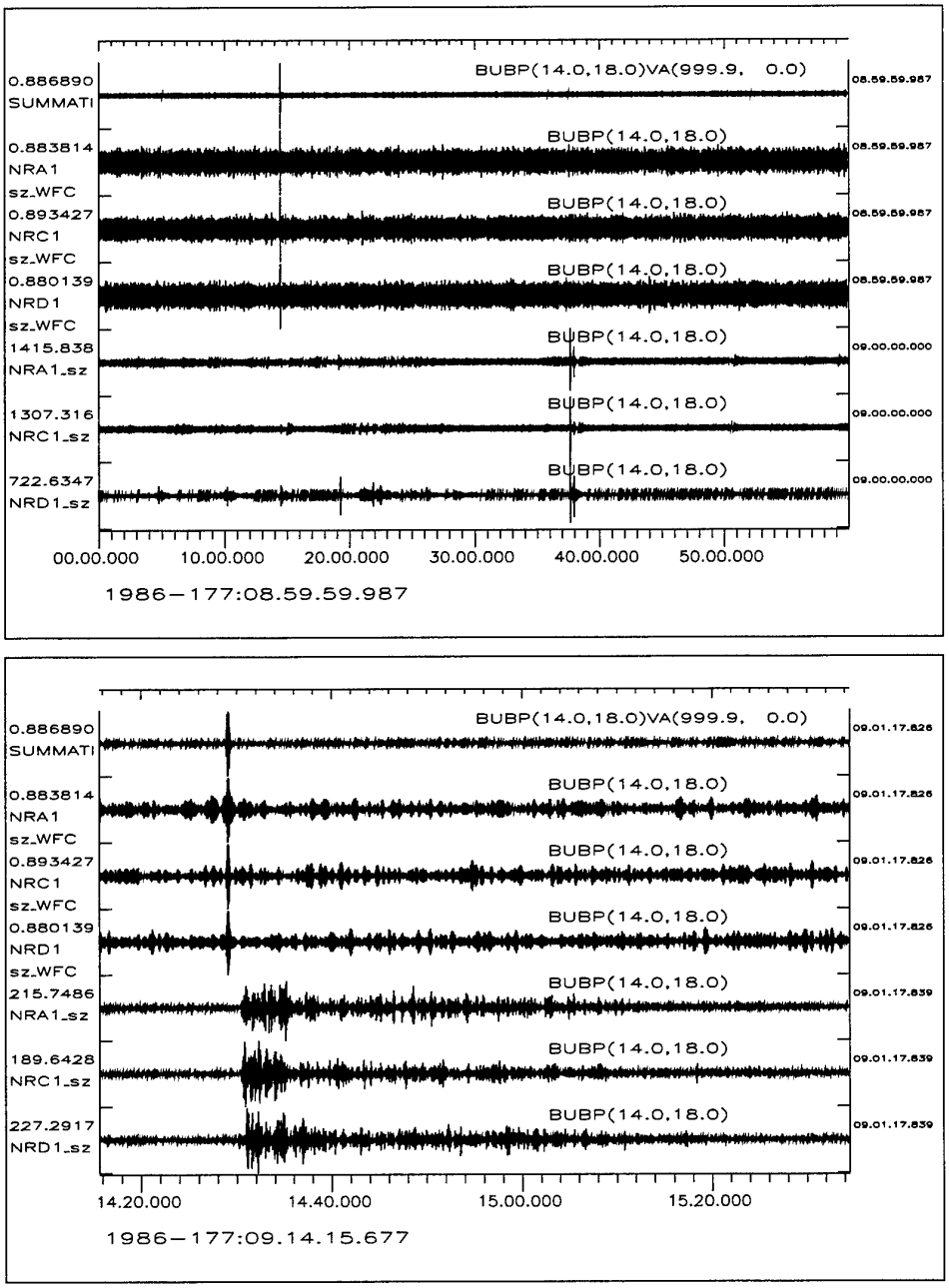

Fig. 6.2.2. Results of a waveform correlation between the filtered master event waveforms and an hour of NORES data on the day on which shot 4 in Table 6.2.1 is reported to have taken place. The upper frame shows a full hour of data and the lower frame a zoom in. The lowermost three traces indicate the filtered data, the traces labelled WFC, the corresponding correlation coefficient traces and the upper trace gives the summation of all NORES waveform correlation traces.

The process was also applied to the days 1986-168, 1986-177, 1986-260, 1986-246, 1987-141, and 1989-242. For all but one of these days, a single correlation peak was observed and corresponding event origin times (deduced from the times of these peaks, the definitions of the master event time windows, and the source to receiver travel times) are tabulated in Table 6.2.3. It is worthy of note that, with the exception of shot 4, no NORES detection was made using the standard on-line processing (shot 4 resulted in the strongest signals given the higher charge density due to the smaller size of chamber B).

Table 6.2.3. Estimated origin times for the 1000 kg Klotz explosions determined from NORES data.

Shot number	Estimated origin time from NORES data
3	1986-168:10.06.15.9
4	1986-177:09.14.07.1
5	1986-260:11.34.17.4
6	No correspondance found in existing NORES data
7	1987-141:10.16.08.3
10	1989-242:10.12.21.0

On day 1986-246, the day of shot number 6 in Table 6.2.1, there is no NORES data until approximately 12.50 GMT and there are no clear correlations following this time. NORSAR data does exist for the whole of this period although it is not clear that this data would allow us to identify this event given; the Nyquist frequency of this data is 10 Hz and the anti-aliasing filter cutoff frequency is 4.5 Hz, well below the frequencies where these signals achieve their optimal SNR. Nevertheless, the slope of the anti-aliasing filter is such that useful energy is recorded up to the Nyquist frequency for high-frequency signals.

In order to increase the likelihood that a positive correlation could be achieved using the 1987C259 event, a full minute of NORSAR data was taken from the master event thus including secondary phases (especially Lg) which are likely to feature better at low frequencies. The data was filtered in the frequency band 6.0-9.5 Hz.

As indicated by Figure 6.2.3, a positive correlation was indeed observed indicating an origin time for this last remaining event of 1986-246:11.50.45.1. This positive identification is remarkable in that the waveforms themselves do not (in the available frequency band) display a signal which can be identified by an analyst or, consequently, detected by a standard STA/LTA detector. Figure 6.2.3 purposefully displays the closest station to the origin (NC301) and the most distant (NAO03). The WFC trace for NAO03 does not even achieve a global maximum at this time, the corresponding correlation coefficient being 0.232. The other stations of the NORSAR array generally give higher correlation coefficients the closer they are to the source and, indeed, the WFC trace for NC301 does give a higher correlation coefficient at this time than at any other during this one hour period. When creating the summation trace, all WFC traces are included since even those which do not have a global maximum at this time do interfere constructively to produce the summation maximum at the point indicated (see the lowermost panel).

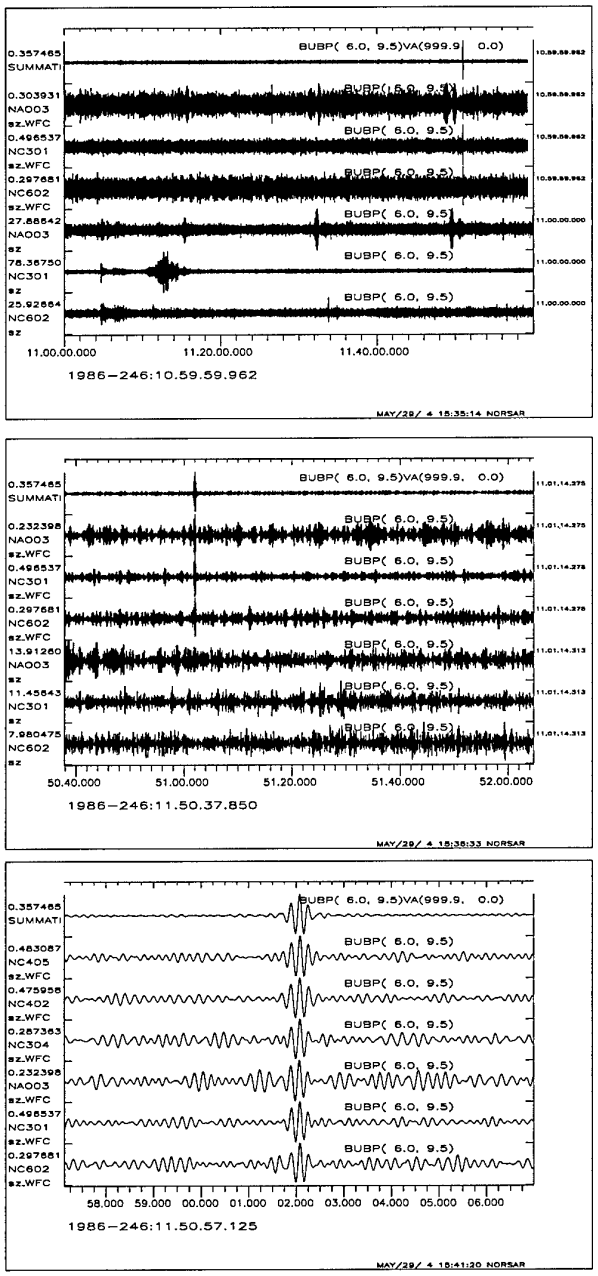

Fig. 6.2.3. Illustration of how we were able to detect shot number 6 in Table 6.2.1 using data from the large aperture NORSAR array (no NORES data exists for this time period). Waveforms, WFC traces, and summation trace for an hour long segment (top), a close up view (centre), and a zoom of the stacking of the WFC traces (lowermost) are shown.

6.2.4 Identification of a 500 kg explosion in the 1000 m^3 chamber at Älvdalen.

Five days prior to the December 13th 2000 Älvdalen explosion, in which 10000 kg of pure TNT was detonated within a chamber of size 1000 m^3, a detonation of 500 kg TNT took place

in the same chamber (Wu et al., 2003). No signals from this events were detected at the nearby seismic arrays. In addition to NORES and NOA (now with data at 40 Hz sampling rate), there is also data from the Hagfors array in Sweden. Segments of signal were extracted from each of the short period instruments for the 2000-348 event and filtered in the frequency band 14.0-18.0 Hz. The cross-correlation procedure was applied to data from each of the three arrays separately.

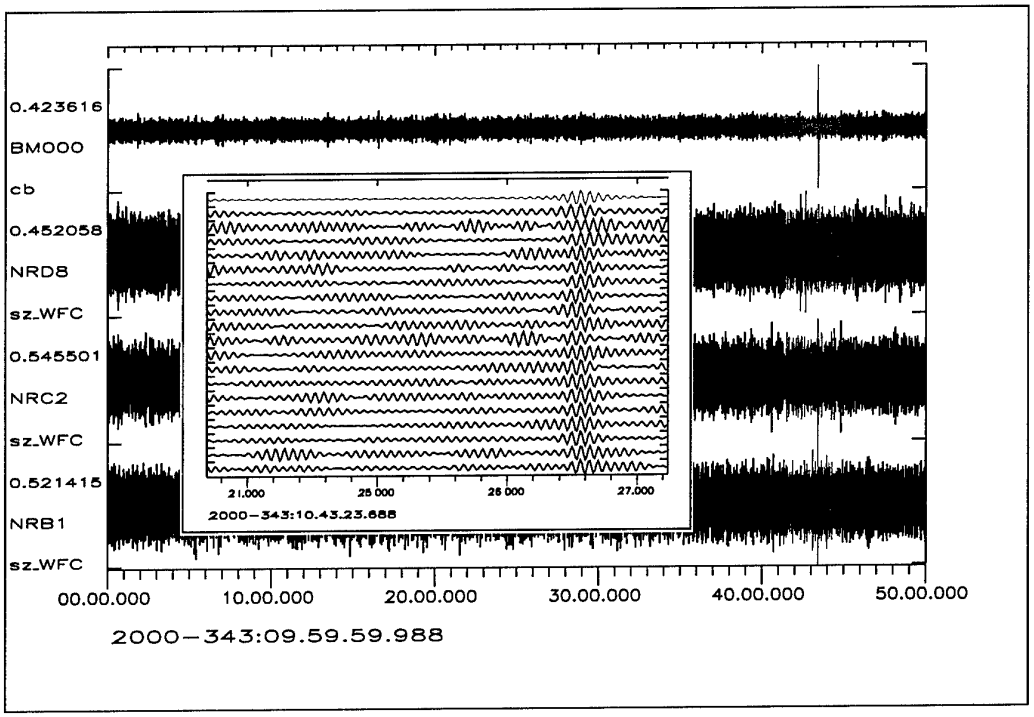

Fig. 6.2.4. Results of waveform correlation for the 8th December 2000 explosion using NORES data. The inset panel indicates how the constructive interference from the individual WFC traces leads to the significant global maximum despite the fact that this time is a global maximum for very few of the single station WFC traces.

Each of the arrays NRS, NOA, and HFS produced a unique WFC summation peak at a time consistent with an origin time of 2000-343:10.43.04.5. On none of the waveforms is it possible for an analyst to identify the direct signal from this small explosion, even filtered in this high frequency band. There are very few stations which produced a global maximum correlation coefficient at this time; a stacking of the WFC traces from each of the full arrays did however lead to clear peaks corresponding to this time.

It is important to emphasize that the three different arrays all resulted in times of maximum cross-correlation which were consistent with one single source at the Älvdalen test site.

6.2.5 Conclusions

- The waveforms resulting from subsequent explosions in the various chambers at the Älvdalen site correlate very well, even at very high frequencies. Unlike many mining explosions where source characteristics can vary greatly between events, these decoupled chemical explosions have a simple source function which has been almost identical for each of the tests.
- A further seven events from this site have been identified by finding the data which best matches waveforms from larger events confirmed to have taken place at Älvdalen.
- Only one of these events had been detected by the standard on-line processing. The 1000 kg Klotz explosions from 1986 to 1989 could probably have all been detected and processed in this way given sufficient modifications to the detection and processing recipes. Any such modifications would, however, lead to far more false alarms with limited returns in detectability given the poor coherence of the weakest signals from these events.
- A 500 kg explosion in the 10000 m^3 chamber was detected by applying the same process to data from the NRS, HFS, and NOA arrays. The signal is only observable in the sense that the waveform correlation traces stack to maximum values for all three arrays, independently implying the same origin time for a hypothetical event at the Älvdalen site.
- The noise suppression obtained by stacking the waveform correlation traces over the arrays was significant. The teleseismic NORSAR array is as effective as the NORES and Hagfors regional seismic arrays for these detections by cross-correlation since the interstation coherency of the waveforms themselves is of no consequence. A similar result could be achieved using a network of many stations.

An online process was set up to test continuous NOA data, correlating with the master event 2002C164 (see Stevens et al., 2003). Waveform correlation channels were calculated and stacked as described here and an optimal STA/LTA detector run on the WFC summation channel. The SNR threshold for this detector was set to 3.5 (following extensive tests whereby it was shown that, within any given hour, the maximum SNR value would probably be between 2.0 and 2.8 and would very rarely exceed 3.2). The process was performed for selected days from 2000, 2001, and 2002, and run on continuous data from July 1st 2003 to the present.

For all the data processed so far, the STA/LTA detector has only triggered 5 times: each time for a confirmed event from the Älvdalen site. The smallest event from December 8th, 2000, produced a stacked correlation coefficient of 0.31 and a corresponding signal to noise ratio of 6.91. For the 10000 kg explosion in the same chamber 5 days later, a correlation coefficient of 0.98 was achieved with a corresponding SNR of 24.55. The May 30th, 2001, test (2001C150, which was the weakest of the events detected by normal processing) resulted in a mean correlation coefficient of 0.76 and a corresponding SNR of 15.39. No Älvdalen explosion which the authors know of has failed to be detected by this test, and on no occasion did the test produce a detection without there having been a confirmed explosion at Älvdalen.

References

Bonner, J. L., Pearson, D. C. and Blomberg, S. (2003). Azimuthal variation of short-period Rayleigh waves from cast blasts in northern Arizona. Bull. seism. Soc. Am., **93**, 724-736.

Gibbons, S. J., Lindholm, C., Kværna, T., and Ringdal, F. (2002): Analysis of cavity-decoupled chemical explosions, Semiannual Technical Summary, 1 January - 30 June 2002, NORSAR Sci. Rep. 2-2002, Norway.

Harris, D. (1991). A waveform correlation method for identifying quarry explosions. Bull. seism. Soc. Am., **81**, 2395-2418.

Stevens, J. L., Rimer, N., Xu, H., Baker, G. E., Murphy, J. R., Barker, B. W., Lindholm, C., Ringdal, F., Gibbons, S., Kværna, T., and Kitov, I. (2003). Analysis and Simulation of Cavity-Decoupled Chemical Explosions. *Nuclear Explosion Monitoring: Building the Knowledge Base. Proceedings of the 25th Seismic Research Review*, September 23-25, 2003, Tucson, Arizona.

Stump, B. W., Hayward, C. T., Hetzer, C. and Zhou, R. M. (2001). Utilization of seismic and infrasound signals for characterizing mining explosions, *Proc. 23rd Seismic Research Review on Worldwide Monitoring of Nuclear Explosions*, 2-5 October 2001, Jackson, Wyoming.

Vretblad, B. (1991). Klotz Club Tests 1986-1989. Report C1:91. Fortifikationsförvaltningen, Forskningsbyrån, Eskilstuna, Sweden.

Wu, C., Lu, W., Hao, H., Lim, W. K., Zhou, Y., and Seah, C. C. (2003). Characterisation of underground blast-induced ground motions from large-scale field tests. Shock Waves, **13**, 237-252.

S. J. Gibbons
F. Ringdal

6.3 Observed and predicted travel times of Pn and P phases recorded at NORSAR from regional events

6.3.1 Objective

The principal objective of this study is to estimate the absolute travel-time path anomalies of regional seismic phases observed at the Norwegian Seismic Array (NORSAR) with respect to the Earth model AK135 (Kennett et al., 1995) and to determine their relationship to the Earth's three-dimensional (3D) structure.

6.3.2 Reference event phase data

Over the operational period of the NORSAR array (1971-present), phase arrival times for earthquakes and explosions worldwide have been routinely reported to international agencies by NORSAR. These onset time readings were made at different reference sites and sometimes different station codes due to array geometry changes over time, temporary outages of array components, and the installation of the regional array NORES at one of NORSAR's subarray sites. However, since NORSAR first began reporting phase data in 1971, these reports were made primarily from only three reference points (NAO, NOA and NRA0) and most of these phase data are available in a computer accessible form. We associate these NORSAR archived phase reports with a reference event database comprised of explosions and well-constrained earthquakes with global coverage that has been independently assembled by Engdahl (cf., Bondar et al., 2004) and with events at regional distances from NORSAR that are well located by local and regional stations (Hicks et al., 2004). The events in this combined reference event database are usually well recorded at regional and teleseismic distances and the absolute locations and origin times are known to higher accuracy than is typical of even the best global earthquake catalogue. There are currently 1905 events in the global data set, including 1234 explosions with locations known to 2 km or better and 671 earthquakes believed to be accurate to 5 km or better. In this report we will focus on events in the combined database that are within the regional distance range from NORSAR. The process of associating phase arrival times reported by NORSAR with this database required several data preparation tasks:

(1) a phase association script was tested and implemented with the combined regional reference event database (nearly all the events had one or more NORSAR phase reports);

(2) a program was developed to convert the output of the phase association program to a format that could be used as input to the EHB location program (Engdahl et al., 1998), and

(3) the EHB location program was used to convert phase data from each of the NORSAR reference points to residual data (with respect to the model AK135) for the corresponding events in the reference event database.

6.3.3 Event and array clusters

The reference event database contains a number of events globally that are clustered within areas of radius no larger than 100 km. These clustered events in the global database have been validated using the method of Hypocentroidal Decomposition (HDC, Jordan & Sverdrup, 1981) for multiple event relocation. The basic premise of this method is that path anomalies from each station to all observed events in a given cluster are correlated. Thus, multiple event

location analysis can produce robust estimates of source-station path anomalies that are far more difficult to extract from single event location catalogs. The set of residuals for Pn and P phases observed at NORSAR relative to absolute hypocenter estimates derived by HDC cluster analysis is used to calculate phase path anomalies at all distance ranges. These anomalies are estimated relative to the 1D reference model AK135. Medians and spreads of groomed residuals for each cluster are calculated for the phases of interest (here primarily P and Pn) at each of the NORSAR reference stations reporting phase arrivals for that cluster. The resulting source-station "empirical phase path anomalies" (the median) are accepted with a minimum requirement of five observations and a spread of <1.40 s for P-type phases (the spread is a robust analog to the standard deviation). The correlation of median phase residuals observed at the NORSAR reference points NAO and NRA0 with respect to NOA for the same event cluster is plotted in Fig. 6.3.1. In spite of some scatter, largely produced by the effect of differences in local structure beneath the array reference points, the correlation is quite good. Hence, for the purposes of this study, cluster medians or single event residual data could be treated as coming from a single NORSAR cluster of reference points, nominally centered at the reference point with the most observations (NOA).

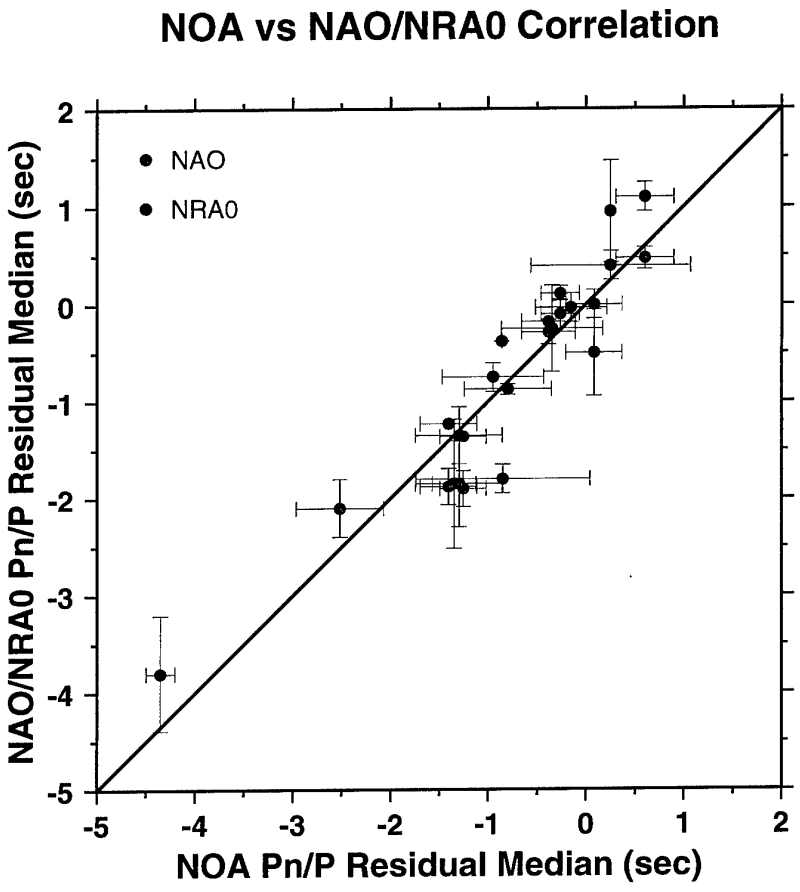

Fig. 6.3.1. Median residual and spread for the phases Pn and P observed from common clusters at the reference points NAO and NRA0 plotted with respect to the corresponding median residual at reference point NOA.

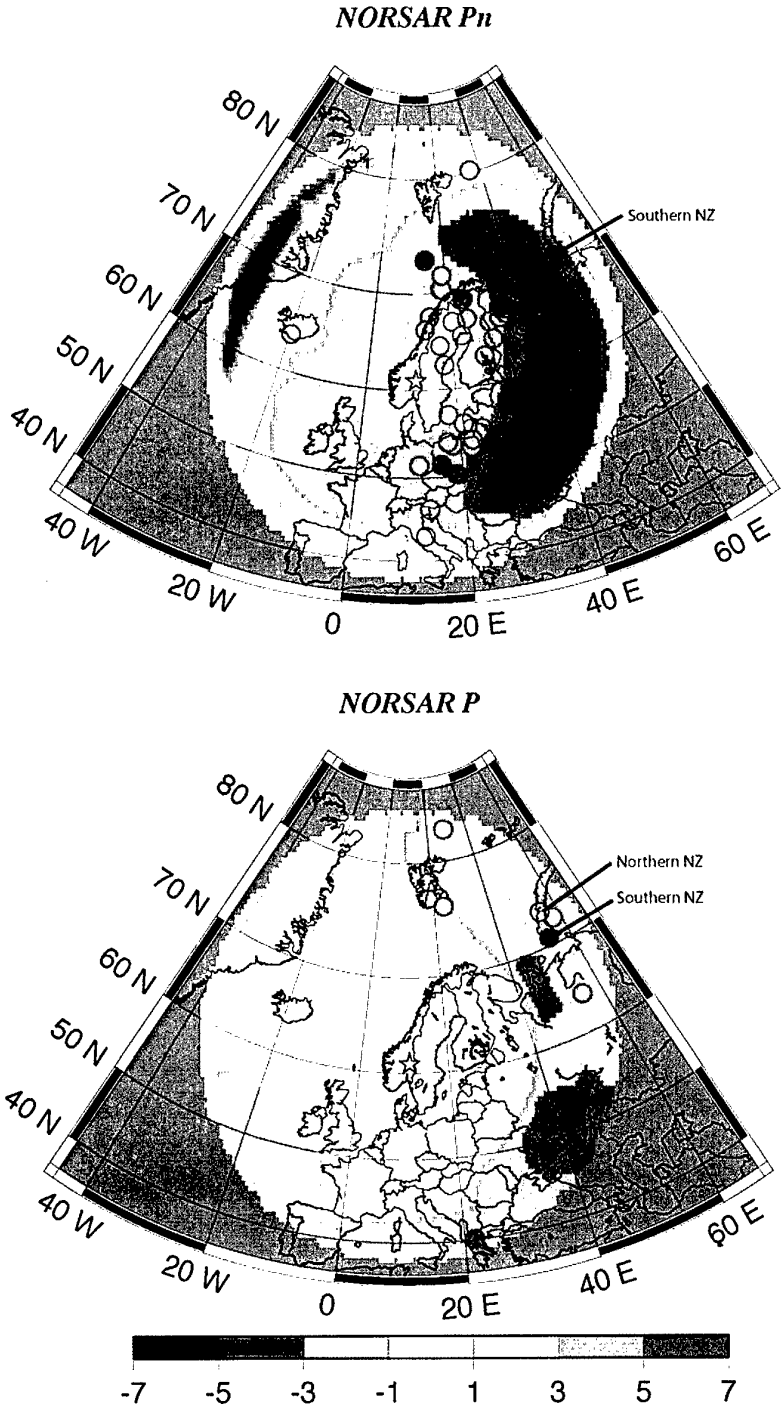

Fig. 6.3.2. Predicted travel time anomalies with respect to AK135 for (a) Pn and (b) P phases centered on the NORSAR reference point NOA and computed for event sources at a depth of 10 km. Bar at the bottom is color coded by the size of predicted anomalies. Observed Pn and P empirical path anomalies are shown as filled circles on the same color scale for qualitative comparison. Path anomalies at the northern and southern Novaya Zemlya test sites are also indicated.

6.3.4 3-D model predictions

Fig. 6.3.2 presents travel time correction surfaces for Pn and P (with respect to the 1D model AK135) for events centered on the NORSAR reference point NOA that was produced using a three-dimensional crust and upper mantle Earth model (CUB) developed by the University of Colorado (Ritzwoller, et al., 2003). This 3D model, based on broadband surface wave group and phase speed measurements, is a Vs model that has been converted to Vp using the thermoelastic properties of an assumed mantle composition. These travel time surfaces depict the predicted travel times from events at a depth of 10 km on a grid of epicentral locations observed at NORSAR and are presented relative to the travel time predicted from the 1D model AK135. For qualitative comparison observed empirical path anomalies for shallow crustal events at regional distances are also plotted. A quantitative comparison is shown in Fig. 6.3.3 where predicted time anomalies for events that could be successfully traced through the CUB model are plotted against observed anomalies. The bounding lines (+/- 2 sec) define the normal range of data based on uncertainties in the 3D model. Later observed P anomalies (near 2 sec) are from shallow focus events near Svalbard where there exists a thick, slower velocity, upper crust not included in the CUB model. The northern and southern Novaya Zemlya (NZ) data points are discussed below.

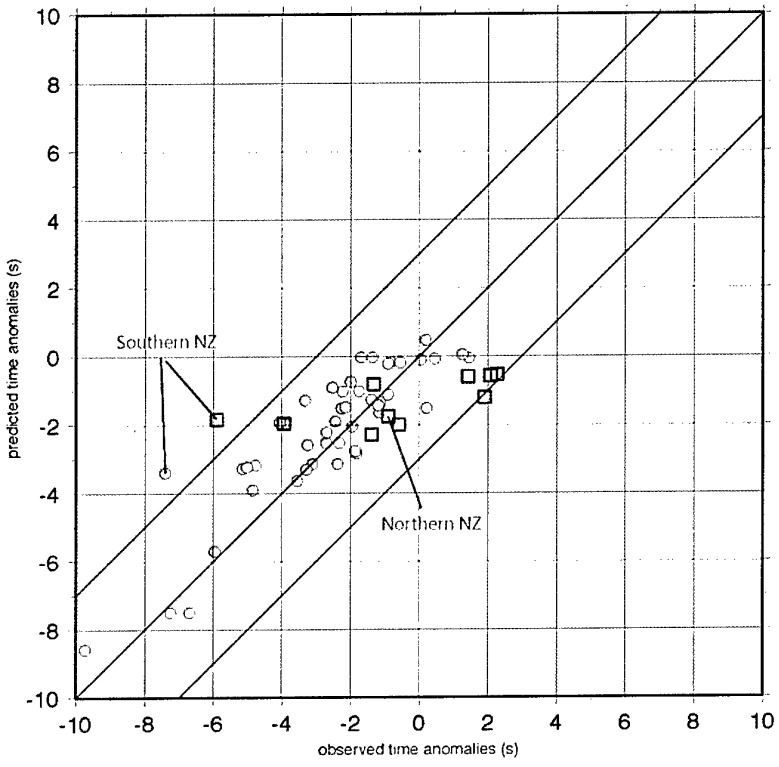

Fig. 6.3.3. Time anomalies for Pn (solid circles) and P (open squares) phases observed at NORSAR plotted with respect to time anomalies predicted by ray tracing through the CUB 3D model. Bounding lines indicate the range (+/- 2 sec) in anomalies that can be a result of uncertainties in the model. P anomaly data for northern Novaya Zemlya test site and Pn and P data for southern test site are also shown.

6.3.5 Discussion

At least with respect to the large-scale features of the correction surfaces, the agreement between the empirical path anomalies and the model-predicted travel times is quite good.

The observed and predicted regional anomalies show strong differences in the P and Pn anomalies observed between explosion source areas in northern and southern Novaya Zemlya, apparently produced by a sharp structural boundary that strongly affects ray paths to NORSAR from these sources. The separation distance between these source areas is on the order of only 300 km, yet the P and Pn median travel time anomalies observed at NORSAR at a distance of about 20 degrees differ by more than 5 seconds (see Fig. 6.3.3). A Pn arrival from the northern Novaya Zemlya source is not predicted by the 3D model while on the other hand the southern source could be interpreted as either a Pn or P phase arrival as shown in Fig. 6.3.3.

These differences between the two Novaya Zemlya sources are also reflected in typical waveforms observed at NORSAR from these test areas (Fig. 6.3.4). The top figure shows a simple Pn waveform observed at NORSAR from the northern test site. The bottom figure, observed at NORSAR from the southern test site, shows a more complex waveform. Ray tracing suggests that for the southern source the first arrival is a Pn wave that has penetrated deeper into the fast lithosphere (a diving ray path) whereas the second arrival is most likely the P wave. The 3D model resolution is only on the order of 400-500 km, so that it is difficult to model these anomalous arrivals without the rays from these source regions encountering a sharper boundary than that presently shown by travel time predictions of the CUB model (see Fig. 6.3.2).

6.3.6 Conclusions

1. For the purposes of this study, residual data from NORSAR reference points can be treated as a single median station cluster residual centered on NOA for single events or event clusters.
2. In the regional distance range P and Pn single event or median cluster residuals generally agree quite well with travel time residuals predicted by the CUB 3D model.
3. There is more than a 5 sec difference in the P median residual observed at NORSAR from the northern Novaya Zemlya test site with respect to the Pn (or P) residual observed from the southern test site, although the separation distance of these test sites is only about 300 km. Residuals predicted by the CUB 3D model, which displays a structural boundary between ray paths from the two test sites to NORSAR partially explains these observations, but a sharper boundary is called for.

Acknowledgements

The research presented was supported partly by the Norwegian Research Council, which supported the visit of E.R. Engdahl to NORSAR through a Senior Scientist Fellowship.

E. Robert Engdahl (University of Colorado)
Johannes Schweitzer

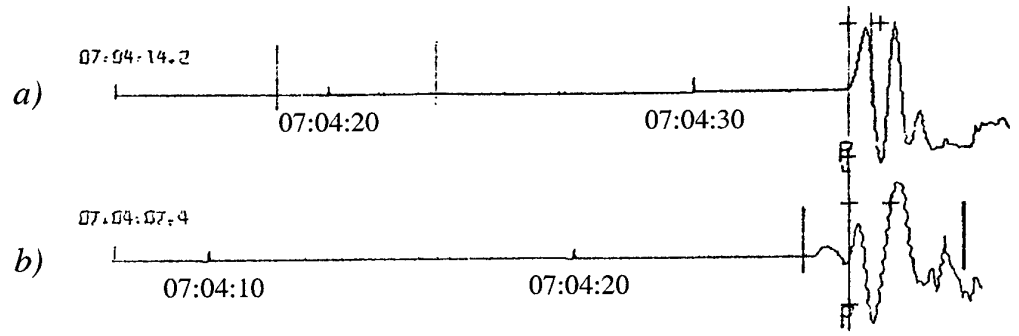

Fig. 6.3.4. NORSAR (NOA) waveforms from events in the (a) northern and (b) southern Novaya Zemlya test sites. Shown are the whole NORSAR array beams as analyzed and plotted on 12 September 1973 (a) and 27 October 1973 (b) in original size. The data were filtered with 3rd order Butterworth band pass filters between 1.4 and 3.4 Hz (a) and between 1.2 and 3.2 Hz (b). Time scale is indicated.

References

Bondár, I., S.C. Myers, E.R. Engdahl and E.A. Bergman (2004). Epicenter accuracy based on seismic network criteria. Geophys. J. Int. **156**, 483-496.

Engdahl, E.R., R.D. Van der Hilst and R.P. Buland (1998). Global teleseismic earthquake relocation with improved travel times and procedures for depth determination. Bull. Seism. Soc. Amer. **88**, 722-743.

Hicks, E.C., T. Kværna, S. Mykkeltveit, J. Schweitzer and F. Ringdal (2004). Travel-times and attenuation relations for regional phases in the Barents Sea region. Pure and Appl. Geophys. **161**, 1-19.

Jordan, T.H. and K.A. Sverdrup (1981). Teleseismic location techniques and their application to earthquake clusters in the South-central Pacific. Bull. Seism. Soc. Am. **71**, 1105-1130.

Kennett, B.L.N., E.R. Engdahl and R.P. Buland (1995). Constraints on seismic velocities in the Earth from traveltimes. Geophys. J. Int. **122**, 108-124.

Ritzwoller, M.H., N.M. Shapiro, A.L. Levshin, E.A. Bergman and E.R. Engdahl (2003). Assessment of global 3D models based on regional ground truth locations and travel times. J. Geophys. Res. **108**, no. B7, pp. ESE 9-1 - ESE9-24.

6.4 Discriminants for seismic monitoring

6.4.1 Introduction

In this study a number of different discriminants are calculated for a set of seismic events. The data consists of recordings of events presumed to be mining explosions, underwater explosions, other types of explosions, and earthquakes. Recordings from the seismic arrays HFS and ARCES are used, and the events are located at distances up to 700 km from these arrays. Fig. 6.4.1 shows a map where events and seismic stations are marked with different symbols.

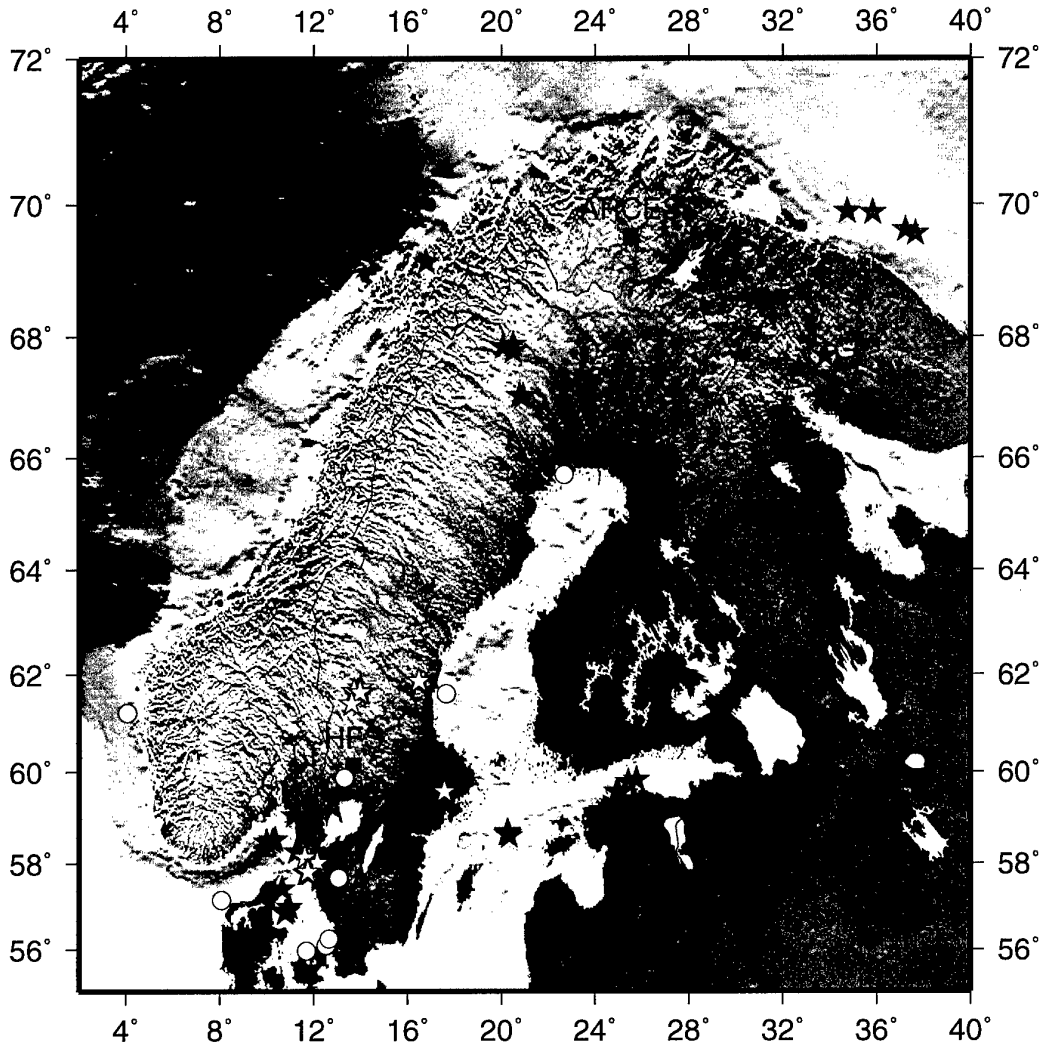

Fig. 6.4.1. Seismic events and array stations used in this study. The stars and circles indicate the presumed types of events, where black stars are mining explosions, red stars are underwater explosions, cyan stars are other types of explosions, and circles are earthquakes. The squares mark the seismic array stations HFS and ARCES.

The main objective is to discriminate recordings with spectral modulation from other recordings. It is known that spectral modulation appears for recordings originating from ripple fired explosions (common in mining, see Hedlin et al., 1998), and underwater explosions. A second objective is to discriminate between other types of seismic events, using classical discriminants.

The discriminants considered here are the following:

- Maximum peak in the cepstrum
- P/S ratio
- Complexity
- Third moment of frequency (TMF)
- Spectral misfit to earthquake (mean square error of the best fit)

It should be stressed that the discriminants most certainly can be optimized by tuning the processing parameters, compensating for the effects of epicentral distance and prefiltering of the data.

6.4.2 The discriminants

The cepstrum definition used here is $C(\tau) = P(\log\{P(f)\})$, where $P(f)$ is the ordinary power spectrum (see Kanasewich, 1981). When estimating the cepstrum, the power spectrum is first estimated with Welch's method. The spectrum calculation uses the first 40 seconds after the first P-phase, and is calculated for $4f_s$ frequency bins, a Hamming window with $3f_s$ samples and 25% overlap (here f_s is the sampling frequency). The power spectrum is also estimated for noise prior to the first P-phase. For the largest possible frequency interval, where the signal to noise ratio is greater than or equal to 3 dB, the cepstrum is calculated, again with Welch's method. The cepstrum estimator used here is not optimized for time-lag resolution, but rather chosen to simplify interpretation of the cepstrum (usually one main peak appears in the estimate). The value of the maximum cepstrum peak is used as a discriminant. A high peak indicates strong modulation in the spectrum.

The *P/S* ratio used is fairly primitive, not taking the distance to the source into account. The energy for the first 2.5 seconds of the first P-phase (in the frequency interval 2 - 12 Hz) and the energy for the first 2.5 seconds of the first S-phase (in the frequency interval 2 - 8 Hz) are used. The ratio of these two energies is the *P/S* discriminant. Explosions are expected to generate relatively strong P-phases as compared with S-phases.

A definition of complexity is given in Dahlman and Israelsson (1977). The basic idea is to compare the energy around the first onset with energies in time intervals later in the coda. Here the two complexity measures S_1 and S_2 are defined as

$$S_1 = I_{0,2}/I_{0,7} \text{ and } S_2 = I_{2,5}/I_{0,7}, \text{ where } I_{a,b} = \int_a^b s^2(t)dt \text{ and } s(t)$$

is the time domain signal with the first onset at $t=0$. Generally earthquakes are believed to produce more complex codas than explosions, which can be detected in these measurements.

One discriminant that measures how dominant the higher frequencies are in relation to the lower frequencies in the spectrum is the third moment of frequency, which is here defined as

$$TMF = \left(\frac{\int_{f_0}^{f_1} f^3 A(f) df}{\int_{f_0}^{f_1} A(f) df} \right)^{1/3}$$

where $A(f)$ is the amplitude spectrum of the first P-phase. Here $f_0 = 0$, and $f_1 = 5$ is used, which is equivalent to the definition given in Dahlman and Israealsson (1977). Like the *P/S* ratio the spectrum is not corrected for the distance.

In theory, the displacement close to the source of an earthquake should be the convolution of two boxcar pulses (Lay and Wallace, 1995). This generates a displacement spectrum $A(f)$, which consists basically of a constant level for low frequencies, and above a certain cut-off frequency the spectrum decays proportionally to f^{-k} (i.e. linearly for $\log(A(f))$ as a function of $\log(f)$). Depending on which phase is analyzed k can be 1, 2 or 3 (for a P-phase $k=1$). With correction for the source sensor distance the spectrum is basically just tilted and translated to a lower level (the constant level gets a negative slope, and the linear function above the cut-off frequency gets a steeper slope). A fit to a piecewise linear function (two straight lines intersecting at the cut-off frequency) is therefore performed for $\log(A)$ as a function of $\log(f)$. The mean squared error for this fit is then used as a discriminant, and is called the spectral misfit to earthquake. Therefore a low value should indicate an earthquake, and high value some other type of event. This discriminant can be extended to a vector by including the slopes of the two linear functions, and the cut-off frequency. This has not been done, but doing so might improve the separation between the different events.

6.4.3 Data

The list of analyzed events is given in Table 6.4.1, and are mainly chosen from NORSAR's regional reviewed bulletin. Some events have also been chosen from NORSAR's automatic GBF-bulletin (bulletins at NORSAR are available at *http://www.norsar.no/*). The events are presumed to be one of the following four classes:

- Underwater explosions
- Mining explosions
- Other types of explosions
- Earthquakes

Some of the presumed earthquakes are confirmed as felt close to the epicenters in Denmark and Finland (see *http://www.kms.dk/* and *http://www.seismo.helsinki.fi/bul/*, respectively). However most of the presumed earthquakes have not been confirmed in any other way than by interactive analysis and expert assessments.

The category underwater explosions comprises the Kursk accident in the Barents Sea (Ringdal et al., 2000; Savage and Helmberger, 2001; Schweitzer, 2002), and also one of the following explosions for cleaning up the area. Not too far away from the Kursk events two other explo-

sions are included. These are believed to be the Russian missile tests in February 2004 which were reported in the news. Some other underwater explosions are from the Baltic Sea and from Skagerrak.

Mining explosions in the study are taken from three mining areas: Kiruna (Sweden), Malmberget (Sweden) and the Khibiny Massif on the Kola Peninsula, Russia (mine KH4).

Other types of explosions which are included in the study are an explosion from a road construction outside Stockholm and explosions from ammunition destruction sites in Sweden situated at Mossibränden and Älvdalen. The events in Mossibränden and Älvdalen are confirmed; 8 of these explosions took place on the surface, one took place underground and was decoupled. General information about similar explosions in Mossibränden and Älvdalen are given by Gibbons et al. (2002). Also some unknown explosions near the West Coast of Sweden are included (some of these are possibly underwater explosions).

The seismic arrays which have been used are HFS situated near Hagfors in Sweden, and ARCES situated near Karasjok in northern Norway. The used seismometers at are all vertical component and of type GS-13, at HFS sampled at 80 Hz, and at ARCES sampled at 40 Hz.

For HFS, all sensors are used, covering an aperture of about 1.5 km, whereas only the 8 innermost sensors of the ARCES array are used, covering an aperture of about 600 m. For spectral estimates, the mean of the estimates from individual sensors have been calculated. Similarly, the mean is used for energy estimates of the signals.

Table 6.4.1. Information about the events used. Origin time is given in year, day number and time. In the column 'Array' the array used is specified. Class specifies the type of event (EQ=Earthquake, MX=mining explosion, UWX=underwater explosion, X=other explosion). Countries are abbreviated according to Sweden (Se), Norway (No), Denmark (Dk), Finland (Sf) and Russia (Ru).

Origin time	Lat	Lon	Mag	Array	Class	Comments
2000-225:07.30.41.76	69.573	37.643	3.50	ARC	UWX	Barents Sea, Kursk accident
2001-294:00.31.29.71	57.172	8.082	3.28	HFS	EQ	E. North Sea. Felt in Dk
2001-310:18.05.30.71	55.975	11.705	2.69	HFS	EQ	Sjaelland,Dk. Felt in Dk
2002-164:08.59.25.75	61.410	13.629	1.43	HFS	X	Älvdalen, Se
2002-176:10.04.52.64	61.559	13.879	1.87	HFS	X	Mossibränden, Se
2002-176:14.00.14.00	61.600	13.850	1.77	HFS	X	Mossibränden, Se
2002-251:17.16.28.51	69.628	37.221	2.75	ARC	UWX	Barents Sea, Kursk cleaning up.
2003-004:17.47.58.31	61.868	16.483	2.69	HFS	X	Gävleborg, Se
2003-022:10.41.42.87	58.068	11.715	2.08	HFS	X	Värmland, Se
2003-022:21.05.08.83	58.125	11.617	1.92	HFS	X	Värmland, Se
2003-023:16.13.55.50	58.011	12.166	2.27	HFS	X	Värmland, Se
2003-056:09.09.40.49	57.670	13.071	2.33	HFS	EQ	S.W. Götaland, Se
2003-071:11.01.51.72	56.883	10.792	2.18	HFS	UWX	Jylland, Dk
2003-071:20.15.42.77	57.422	10.670	2.24	HFS	UWX	Jylland, Dk
2003-071:23.28.08.43	56.913	10.865	1.96	HFS	UWX	Jylland, Dk
2003-072:01.19.39.57	56.996	10.980	2.50	HFS	UWX	Jylland, Dk

Origin time	Lat	Lon	Mag	Array	Class	Comments
2003-133:06.49.36.07	57.777	11.864	2.01	HFS	X	S.W. Götaland, Se
2003-135:08.23.48.88	57.778	11.688	2.36	HFS	X	S.W. Götaland, Se
2003-139:07.18.21.06	57.780	11.742	2.35	HFS	X	S.W. Götaland, Se
2003-144:20.19.07.25	57.812	11.753	2.11	HFS	X	S.W. Götaland, Se
2003-182:07.21.12.32	61.734	14.018	1.78	HFS	X	Mossibränden, Se
2003-182:12.17.02.09	61.656	13.890	1.93	HFS	X	Mossibränden, Se
2003-183:09.47.01.00	61.633	13.918	1.74	HFS	X	Mossibränden, Se
2003-183:14.06.41.13	61.627	14.044	1.88	HFS	X	Mossibränden, Se
2003-184:09.17.01.78	61.662	13.725	1.80	HFS	X	Mossibränden, Se
2003-184:13.31.44.92	61.644	13.989	1.79	HFS	X	Mossibränden, Se
2003-234:03.49.32.38	56.256	12.668	3.07	HFS	EQ	Malmöhus, Se
2003-236:03.42.29.03	61.612	17.649	2.11	HFS	EQ	S. Gulf of Bothnia
2003-245:12.20.58.33	59.875	13.313	2.25	HFS	EQ	Värmland, Se
2003-255:07.23.56.57	59.830	25.759	2.61	HFS	UWX	Gulf of Finland
2003-255:07.44.32.93	59.784	25.420	2.61	HFS	UWX	Gulf of Finland
2003-255:08.44.07.65	59.541	24.995	2.72	HFS	UWX	Gulf of Finland
2003-255:09.16.44.44	59.575	24.931	2.37	HFS	UWX	Gulf of Finland
2003-259:21.37.48.40	58.662	20.246	2.52	HFS	UWX	Baltic Sea
2003-260:00.37.14.53	58.697	20.265	2.28	HFS	UWX	Baltic Sea
2003-260:06.16.24.44	58.607	20.330	2.46	HFS	UWX	Baltic Sea
2003-260:14.47.40.77	58.669	20.286	2.45	HFS	UWX	Baltic Sea
2003-273:14.54.26.00	60.580	15.220	1.28	HFS	X	Gävleborg, Se
2003-273:14.56.50.30	59.054	11.182	2.50	HFS	UWX	Värmland, Se
2003-295:01.55.00.74	65.709	22.679	3.08	HFS ARC	EQ	Bothnian region, Se. Felt in Sf
2003-308:12.48.35.78	67.686	33.790	1.99	ARC	MX	KH4,Kola Peninsula, Ru
2003-338:20.04.18.39	58.490	10.250	2.66	HFS	UWX	Skagerrak
2003-339:12.32.20.14	67.502	32.690	2.50	ARC	MX	KH4,Kola Peninsula, Ru
2004-007:00.19.56.39	67.874	20.501	2.01	ARC	MX	Kiruna, Se
2004-008:00.16.38.20	67.839	20.062	2.13	ARC	MX	Kiruna, Se
2004-013:18.00.48.41	67.051	20.763	1.97	ARC	MX	Malmberget, Se
2004-016:18.12.12.08	67.033	20.925	2.24	ARC	MX	Malmberget, Se
2004-030:00.16.08.19	67.769	20.504	1.95	ARC	MX	Kiruna, Se
2004-034:03.26.17.73	58.524	10.361	2.18	HFS	UWX	Skagerrak
2004-034:03.37.29.05	58.477	10.011	1.67	HFS	UWX	Skagerrak
2004-043:13.04.09.98	58.264	11.265	2.51	HFS	UWX	Skagerrak
2004-048:09.22.49.95	69.820	34.336	1.19	ARC	UWX	Barents Sea, Missile test
2004-048:09.26.34.36	69.942	34.310	1.17	ARC	UWX	Barents Sea, Missile test
2004-054:08.38.30.90	56.111	12.534	2.77	HFS	EQ	Malmöhus, Se. Felt in Dk
2004-058:18.11.59.76	61.107	4.113	3.16	HFS	EQ	N. North Sea
2004-062:14.06.57.03	59.578	17.572	1.96	HFS	X	Road work, Stockholm, Se
2004-074:12.30.50.90	69.155	16.797	2.31	ARC	UWX	Troms, No

Based on the onset times for the first P-phase, waveform segments have been collected, starting 20 seconds before the onset and with a total length of 320 seconds. Some bulletin information such as arrival times for different phases have been used in order to calculate the discriminants, but most of the calculations rely on the waveforms directly.

6.4.4 Results

The performance of the discriminants using the data is presented in Figs 6.4.2-6.4.5. The discriminants for all the events are presented in pairs. Different symbols or colors are used for different types of events.

We see from Fig. 6.4.2 that by using a combination of the cepstral peak and the spectral misfit to an earthquake, the earthquakes are well separated from underwater explosions and mining explosions. The other types of explosions are generally not separated from the earthquake population.

The *P/S* relation seems to perform well when it comes to separating explosions from earthquakes (see Fig. 6.4.3). However, the ratio has only been calculated for events where body-wave S-phases exist in the bulletin.

The third moment of frequency does not separate different classes of events satisfactorily (see Fig. 6.4.4), the earthquakes are also spread out in the feature space. The same holds for the complexity discriminants (Fig. 6.4.5), although these are slightly better. These methods might require tuning and adjustments.

One of the earthquakes seems to stand out from the rest (this is the presumed earthquake in E. North Sea in 2001-294). It has high spectral misfit, a high *P/S* ratio, and a high S_1- complexity, however, it has a normal cepstral peak. This event should probably be considered as an outlier, but because of the quite limited number of events, there is too little data to obtain a reliable assessment of the statistical properties of the discriminants.

Generally the presented discriminants do not separate explosions from earthquakes, but ripple fired explosions and underwater explosions seem to separate from the other types of events reasonably well.

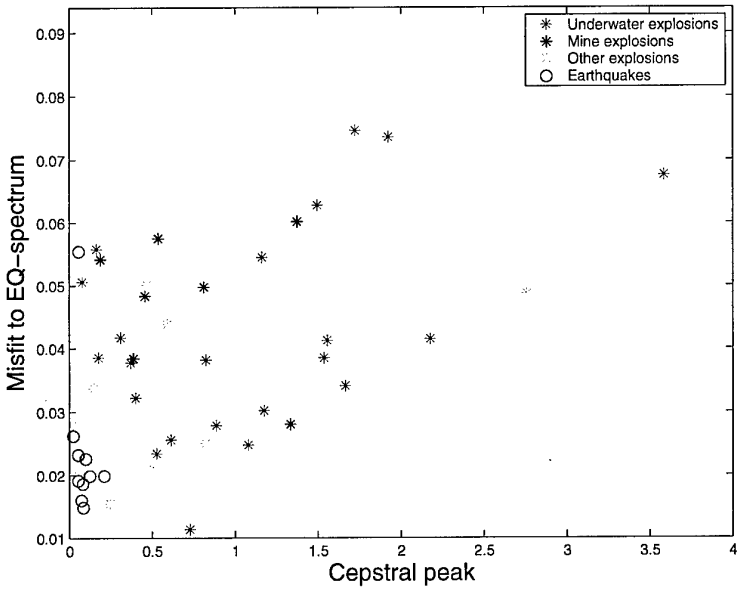

Fig. 6.4.2. Distribution of the maximum cepstral peaks and the spectral misfit to earthquake for the dataset given in Table 6.4.1.

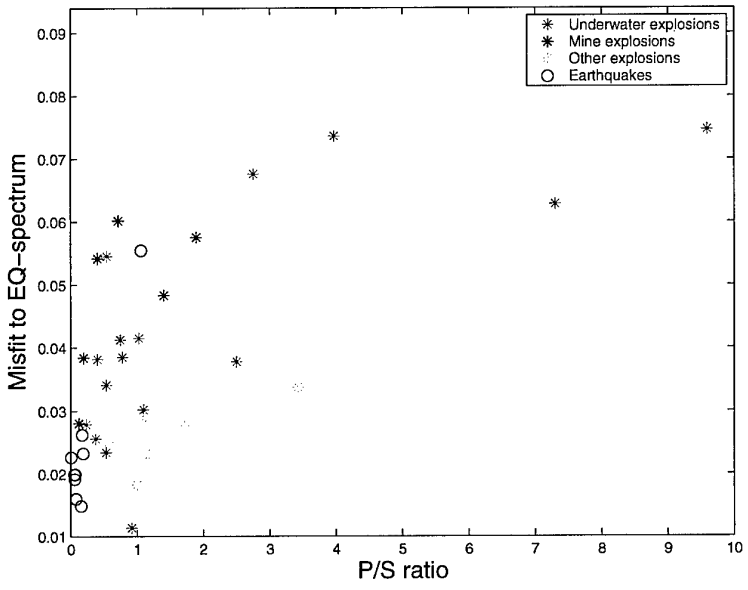

Fig. 6.4.3. Distribution of the P/S ratio and spectral misfit to earthquake for the dataset given in Table 6.4.1. The events where P/S could not be calculated are not represented in the figure.

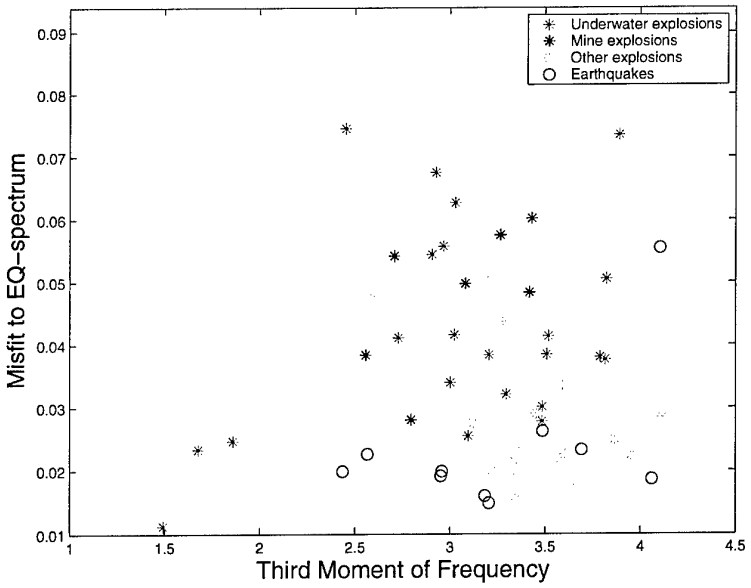

Fig. 6.4.4. Distribution of the TMF and spectral misfit to earthquake for the dataset given in Table 6.4.1.

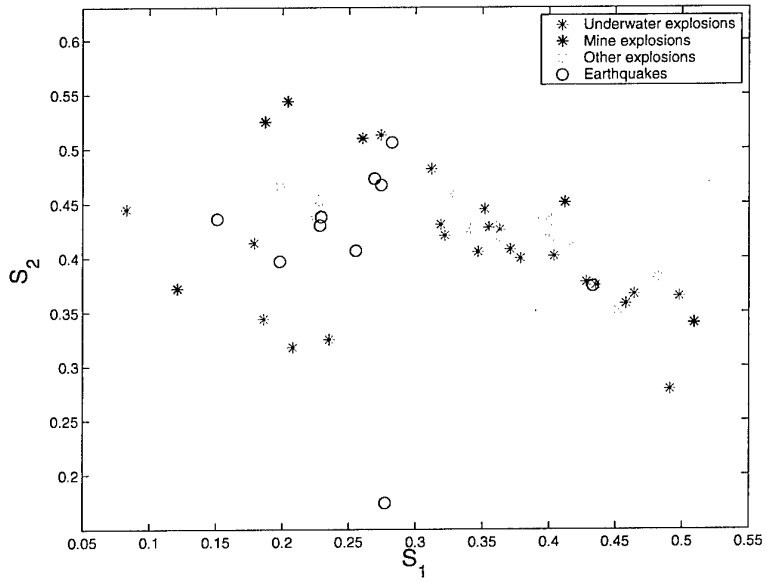

Fig. 6.4.5. Distribution of the two complexity-discriminants for the dataset given in Table 6.4.1.

Four events are studied in more detail, as shown in Fig. 6.4.6 to Fig. 6.4.9. In these figures seismograms are presented, along with the corresponding spectrograms, for 100 seconds of data. Bulletin information, which also specifies the identified phases, is presented in the upper part of the panels. The phases are also marked in the seismograms. Cepstra and spectra of the first P-phases (with spectral fit to earthquake) appear to the right in the panels. Finally the P/S ratios are presented above the seismograms ('NaN'=Not a number (see Fig. 6.4.9), means that P/S could not be calculated, because of missing information about S_n- and S_g-phases).

The four events are the Kursk accident (Fig. 6.4.6), a mining explosion in Sweden (Fig. 6.4.7), an earthquake in Sweden (Fig. 6.4.8), and an ammunition destruction explosion in Sweden (Fig. 6.4.9). The two first show strong spectral modulation, while the two latter do not have this feature. The spectral fit to earthquake is also poor for the first two events, while the last two show better fit. The earthquake has a low P/S value, while the explosions have high values (for the ammunition destruction explosion this value could not be computed).

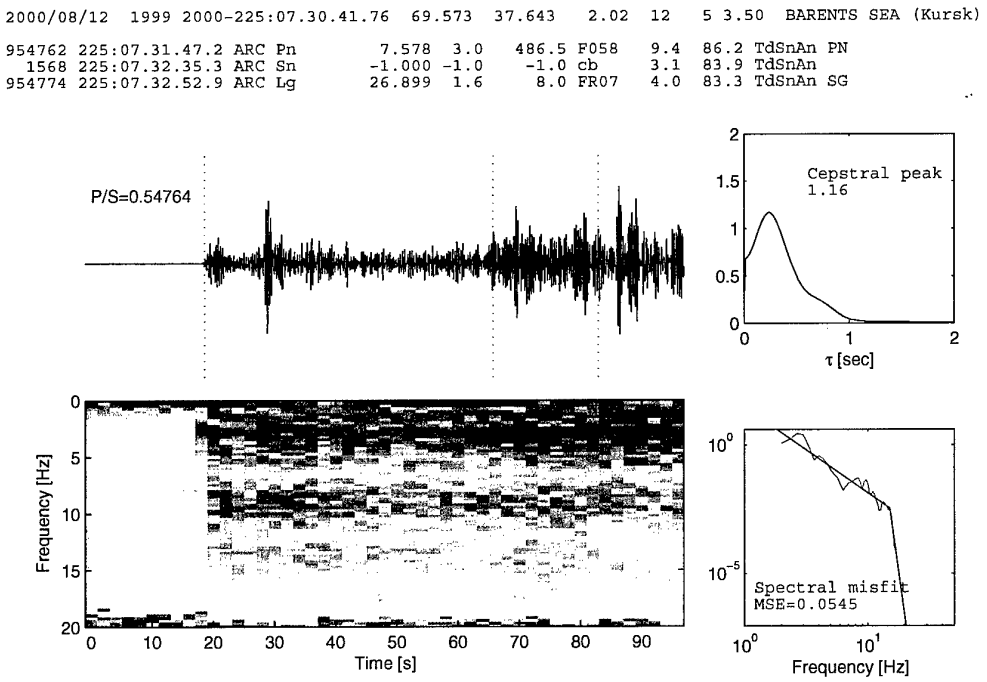

Fig. 6.4.6. Spectrogram, Cepstrum and spectral misfit for the event from the Kursk accident, Barents Sea

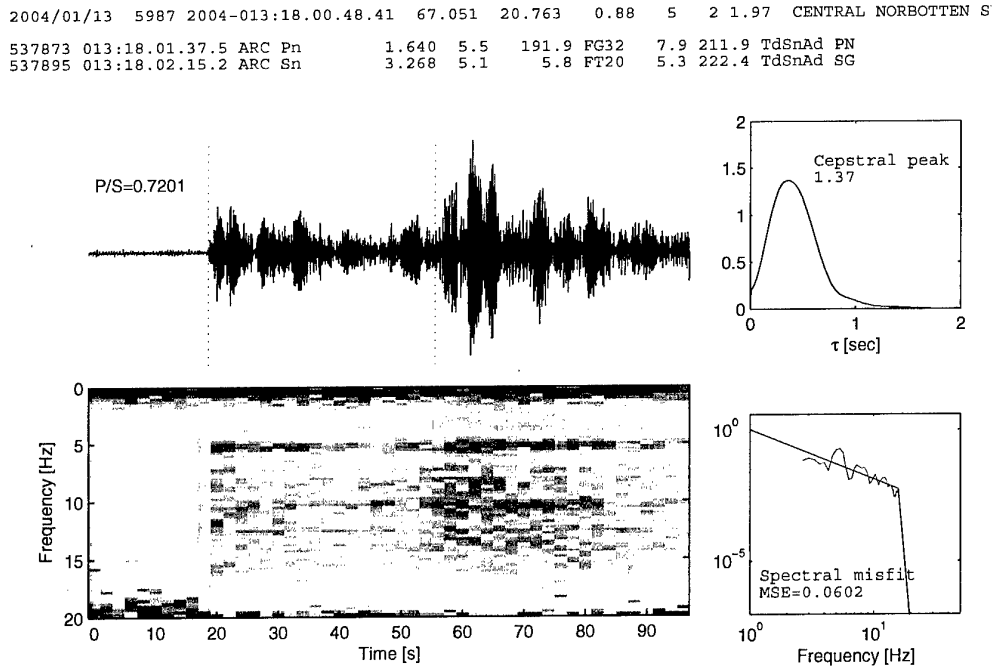

Fig. 6.4.7. Spectrogram, Cepstrum and spectral misfit from a mining explosion in Malmberget, Sweden.

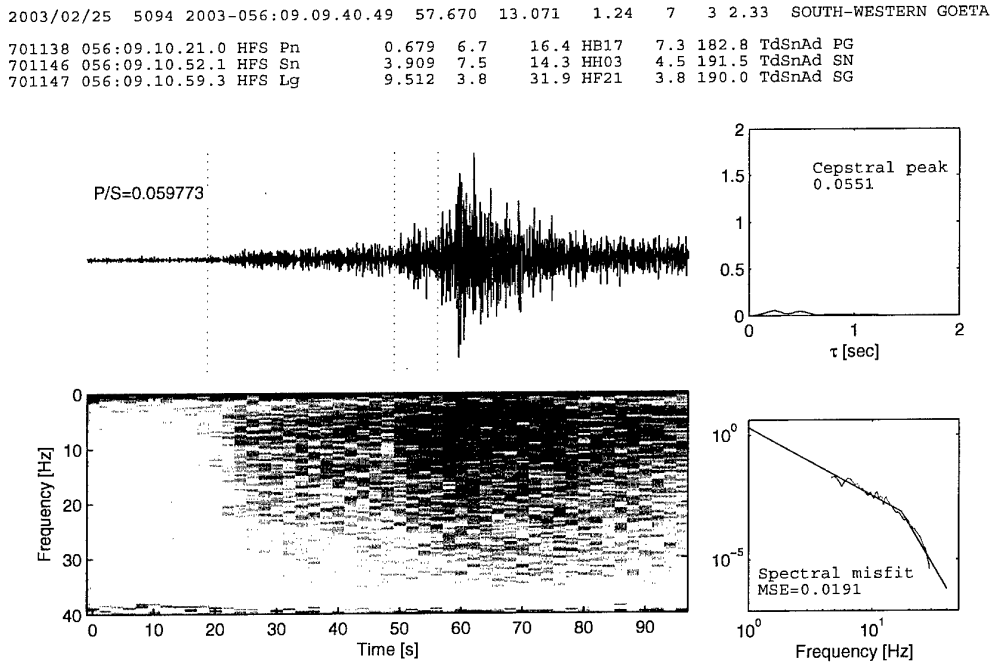

Fig. 6.4.8. Spectrogram, Cepstrum and spectral misfit from an earthquake in south west Sweden.

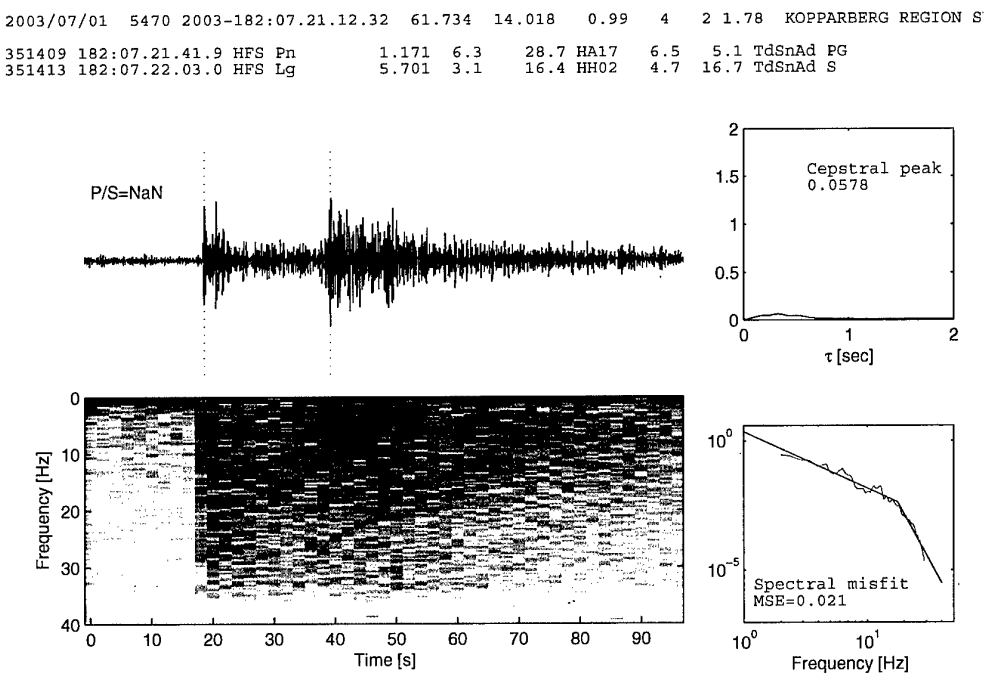

Fig. 6.4.9. Spectrogram, Cepstrum and spectral misfit from an ammunition destruction explosion in Mossibränden, Sweden.

6.4.5 Discussion

One of the earthquakes is definitely an outlier in terms misfit to an earthquake spectrum and also for the P/S ratio. This is the 2001-294 event which was reported felt in Denmark. This earthquake had, however, a cepstral peak that was consistent with the other earthquakes. Since this is the only earthquake that does not fall within the earthquake clusters of Figures 2 and 3, it would be interesting to study it further in greater detail. We would also like to further investigate the algorithm for calculation of the spectral misfit to an earthquake spectrum, in particular for cases when the cut-off frequency is close to the Nyquist frequency of the data (e.g., see Fig. 6.4.7).

The sampling rate of the data is quite high (80 Hz for HFS, and there exists a 100 Hz three-component instrument at ARCES), so that it is possible to consider significantly higher frequencies for the P/S ratio and third moment of frequency. This is particularly interesting since frequencies as high as 40-50 Hz have not previously been studied in detail for discrimination of regional events.

The database used in this study comprises 57 seismic events which is a relatively small database taking into account the large size of the region. A natural extension to this study will be to expand the database considerably. In this connection we note that there are many regions for which comprehensive ground-truth data is available. In particular, this applies to the mining regions of the Kola Peninsula, but such data are also being accumulated for mines in Sweden and Finland. The earthquake population can likewise be expanded considerably, and, in particular the Finnish regional bulletin could be useful for this purpose. Many additional events can

be classified with high certainty as underwater explosions, especially in the Baltic Sea and offshore Norway. Although ground-truth information is not available for these presumed explosions, they can nevertheless be valuable data in these type of studies.

By expanding the dataset as outlined, it would be possible to regionalize the study of the discriminants. It would be of particular interest to study subsets of approximately co-located events of various source types. This would be expected to contribute to a reduction in the scatter for the discriminants, and would thereby enhance their effectiveness in practical operation. A larger database would also make it possible to assess the statistical properties of the discriminants.

Finally, the methods described in this paper lend themselves to automatic or semi-automatic computation on a routine basis, and a script has been developed to facilitate such regular analysis.

Acknowledgements

The 2-month research term of Dan Öberg at NORSAR in 2004 was funded through the EC programme Access to Research Infrastructure (Contract HPRI-CT-2002-00189).

Dan Öberg, FOI, Department of Naval Sensor Systems, Stockholm, Sweden
Tormod Kværna
Frode Ringdal

References

Dahlman, O. and H. Israelsson (1977). Monitoring underground nuclear explosions, Elsevier, Amsterdam.

E.R. Kanasewich (1981). Time sequence analysis in geophysics, 3rd ed., University of Alberta Press, Edmonton.

Gibbons, S., C Lindholm, T. Kværna and F. Ringdal (2002). Analysis of cavity-decoupled chemical explosions. In: NORSAR Semiannual Tech. Summ. 1 January - 30 June 2002, NORSAR Sci. Rep. No. 2-2002, Kjeller, Norway, pp. 78-89

Hedlin M (1998). A global test of a time-frequency small-event discriminant, Bull. Seism. Soc Am. 88, pp. 973-988, August 1998.

Lay, T. and T.C. Wallace (1995). Modern global seismology, Academic Press, San Diego.

Ringdal, F., T. Kværna and B. Paulsen (2000). Seismic events in the Barents Sea at and near the site of the Kursk submarine accident on 12 August 2000. In: NORSAR Semiannual Tech. Summ. 1 April - 30 September 2000, NORSAR Sci. Rep. No. 1-2000/2001, Kjeller, Norway, pp. 77-88

Savage, B. and D.V. Helmberger (2001). Kursk Explosion, Bull. Seism. Soc Am., 91, pp. 753-759.

Schweitzer, J. (2002). Some results derived from the seismic signals of the accident of the Russian submarine Kursk. In: NORSAR Semiannual Tech. Summ. 1 July - 31 December 2001, NORSAR Sci. Rep. No. 1-2002, Kjeller, Norway, pp. 115-121.

6.5 Comparison of the Love-Rayleigh discrepancy in central Europe (GRSN) and southern Scandinavia (NORSAR)

6.5.1 Introduction

The lower crust and mantle are known to be laterally heterogeneous. Furthermore, they are supposed to be anisotropic. However, anisotropy in the upper mantle and the lower crust is a matter of debate, in particular in continental regions and in subduction zones. This question might be investigated by shear-wave splitting studies, but the depth resolution of this method is limited. Investigation of anisotropy by inversion of surface wave observations shows the advantage of a good resolution in depth.

Love-Rayleigh discrepancy denotes the observation that dispersion curves of fundamental Love and Rayleigh modes cannot be explained by the same isotropic one-dimensional model (McEvilly, 1964). It was repeatedly detected in oceanic regions, e.g. in the Pacific (Ekström and Dziewonski, 1998), while for continental regions the amount of the Love-Rayleigh discrepancy was discussed controversially (e.g., Montagner and Tanimoto, 1991). The Love-Rayleigh discrepancy might be explained by radial anisotropy, that means by different velocities for the horizontally polarized SH- and the vertically polarized SV-wave velocities. The fundamental Rayleigh mode is mainly sensitive to the velocity of transversal particle motion in vertical direction, as SV, whereas Love waves are sensitive for velocities in horizontal direction as SH. However, similar effects might be caused by thin isotropic layers of alternating high and low velocities, or by the different influence of lateral heterogeneity or higher modes on the measurements of the phase velocities of Love and Rayleigh waves (Levshin and Ratnikova, 1984; Maupin, 2002). Azimuthal variations in the Love-Rayleigh discrepancy point to azimuthal anisotropy (Maupin, 1985).

Here, we present examples of the investigation of the Love-Rayleigh discrepancy in two tectonically different continental regions: for the Phanerozoic asthenosphere and lithosphere in central Europe and at the border of the Precambrian Baltic Shield.

6.5.2 Method and Measurements

Dispersion curves of the fundamental modes were measured by a two-station method (Meier et al., 2004). One event is recorded at two stations. The cross correlation of the seismograms leads to phase differences and with the known distance between the stations the phase velocities can be calculated. This procedure is repeated for many events. Then, the inversion of averaged phase velocity curves of fundamental surface wave modes yields one-dimensional models of the *S*-wave velocity structure. These are interpreted as a average models describing the structure beneath the paths.

6.5.3 GRSN

Phase velocities of the fundamental Love and Rayleigh modes were determined for two paths between stations of the German Regional Seismic Network (GRSN). This network consists of 16 permanent broadband stations (STS-2) and was installed in the early 1990s. Here, dispersion curves for the two paths BUG-WET and BFO-CLZ were measured (Fig. 6.5.1). The angle between the two paths is about 90 degrees. The lengths of the paths are 473 and 417 km, respectively. For a minimum event magnitude Ms 5.0 and the given geometry and 36 and 72

events were found, respectively. Phase velocity curves for these events were averaged for each path. The maximum azimuthal deviation of the great-circle paths of wave propagation from the great-circle between the stations was limited to 7°.

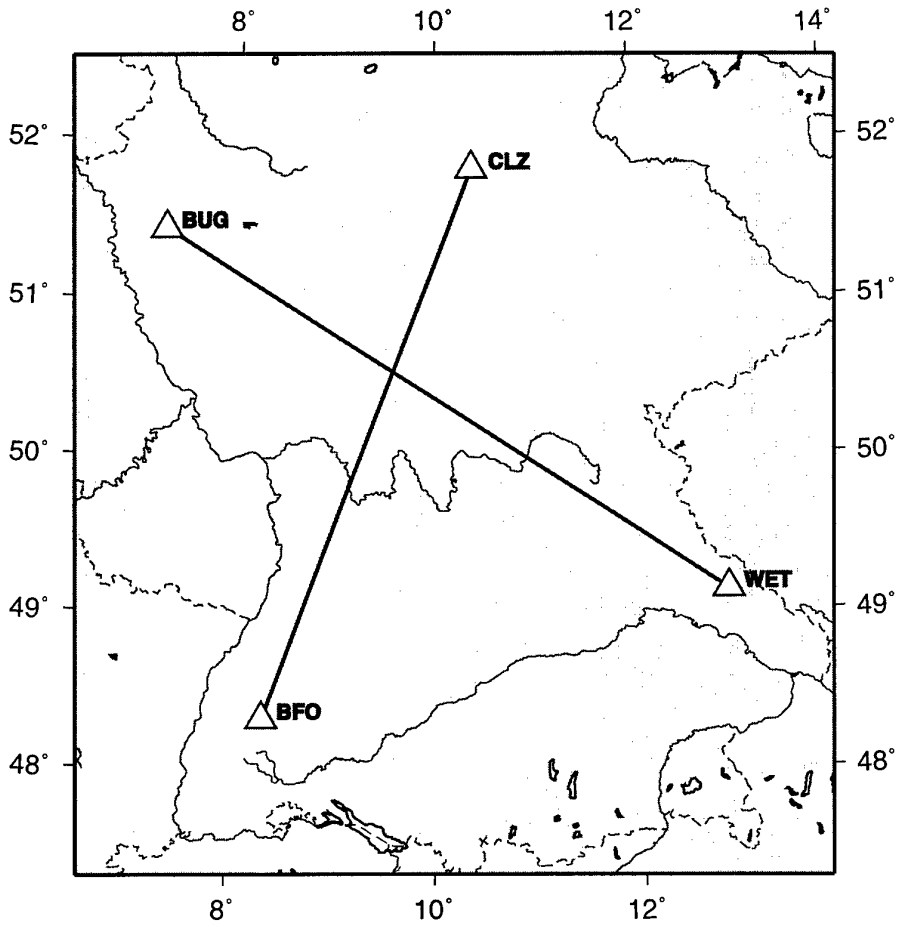

Fig. 6.5.1. Love and Rayleigh phase velocities are measured for the paths BUG-WET and BFO-CLZ using a two-station method (Meier et al., 2004). The inversion of the phase velocities yields 1D-models of the S-wave velocity structure that are interpreted as a average models of the paths. The angle between the two paths is about 90 degrees. The lengths of the paths are 473 and 417 km, respectively.

Phase velocities were determined between 5 and 100 mHz (Fig. 6.5.2, left). The 1D-*S*-wave velocity model that results from the inversion of the Rayleigh wave phase velocity shows an asthenosphere between 80 and 250 km depth. However, it does not show up in the inversion result of Love wave velocity curves (Fig. 6.5.2, right). For both models the theoretical Rayleigh wave phase velocities were calculated and compared to the observed curves (Fig. 6.5.2, left). Both paths show a Love-Rayleigh discrepancy in the frequency band between 5 and 30 mHz. This corresponds to depths between 80 and 250 km. This found discrepancy points to radial anisotropy in the asthenosphere and confirms results by Wielandt et al. (1988) and Friederich and Huang (1996). Remarkably, the amount of this Love-Rayleigh discrepancy

in the asthenosphere is comparable to that of the Pacific around Hawaii (Ekström and Dziewonski, 1998).

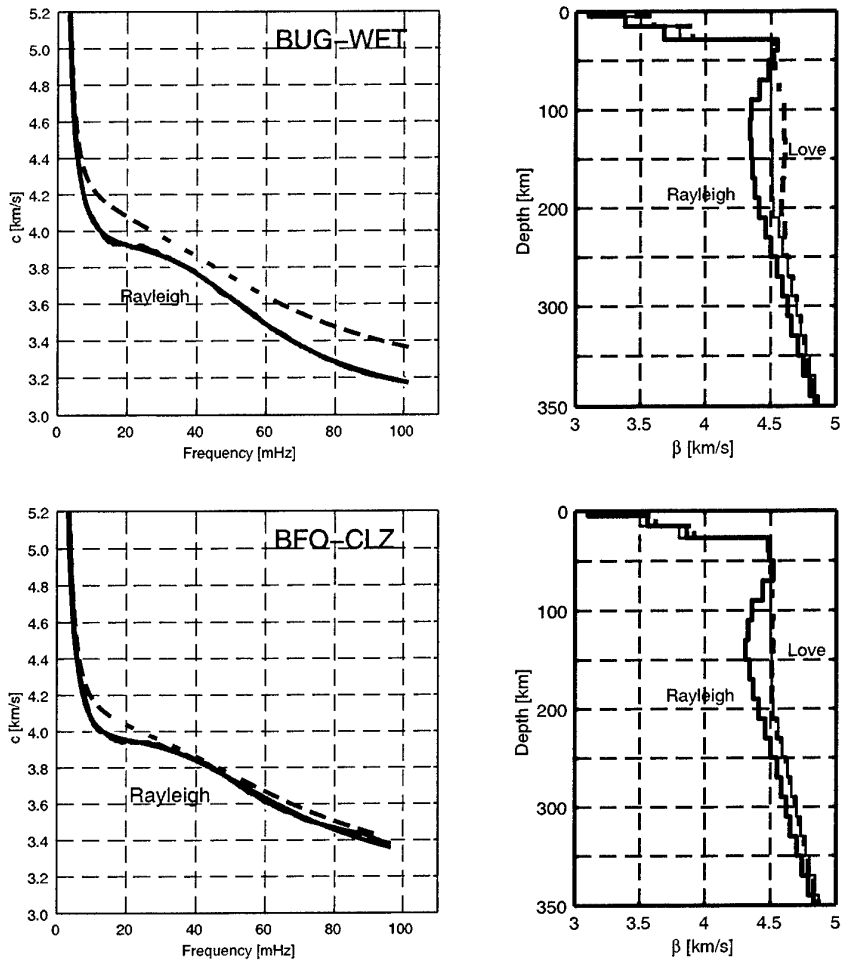

Fig. 6.5.2. The 1D-S-wave velocity model that results from the inversion of the Rayleigh wave phase velocity shows an asthenosphere between about 80 km and 250 km depth. It does not show up in the inversion result of the Love wave velocity curve (right). Theoretical Rayleigh wave phase velocities for both models are depicted on the left (dashed lines). The solid lines show the observed data and the grey area indicates the corresponding standard deviations. Both paths show a Love-Rayleigh discrepancy between 5 and 30 mHz. In addition, a Love-Rayleigh discrepancy is found between about 50 and 100 mHz.

In addition, a Love-Rayleigh discrepancy between 50 and 100 mHz is detected (Fig. 6.5.3). The Love-Rayleigh discrepancy in this frequency range corresponds to lower crustal levels and it differs for the two paths. The Rayleigh-wave phase velocity curves are different above 50 mHz pointing to azimuthal anisotropy in the crust with a fast axis oriented approximately in NE-SW direction. Studies of Pn-anisotropy yield similar results (e.g., Bamford, 1987; Song et al., 2004). Surprisingly, the dispersion curves of the Love waves are similar for both paths. It remains an open question if the behavior of the Love waves is due to finite-frequency effects or due to anisotropy of the lower crust. Finite-frequency effects of wave propagation result from

lateral heterogeneity and are expected to be stronger for Love than for Rayleigh waves. On the other hand this new observation can be explained by models of an anisotropic lower crust.

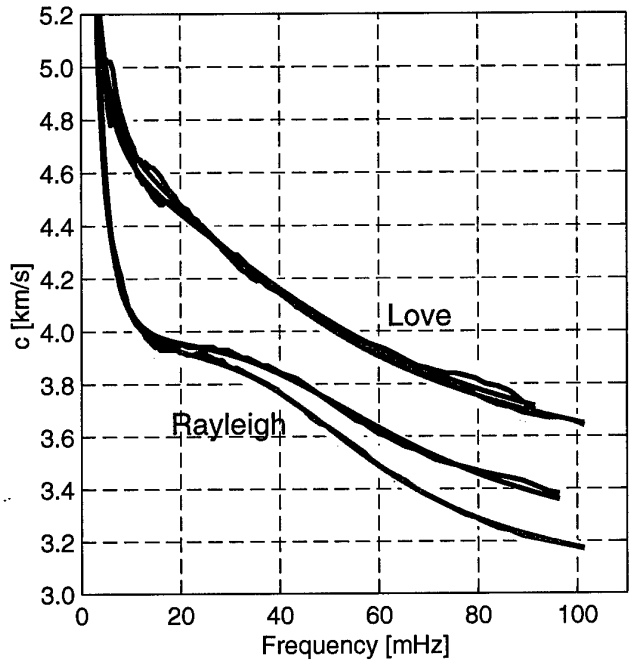

Fig. 6.5.3. Phase velocity curves for the paths BFO-CLZ (blue) and BUG-WET (green); the gray shaded area indicates the uncertainty range of the observations. The dispersion curves of the Love waves are similar for both paths. However, the Rayleigh wave phase velocity curves are different above 50 mHz. The azimuthal variation in the Love-Rayleigh discrepancy might be explained by azimuthal anisotropy in the crust with a NE-SW oriented fast polarization axis. Studies of Pn-anisotropy yield similar results (e.g., Bamford, 1987; Song et al., 2004).

6.5.4 NORSAR

Phase velocities of fundamental Love and Rayleigh modes were determined for 8 paths between six NORSAR broad-band stations (Fig. 6.5.4). The seventh broad-band station in the center of the array could not be used because the inter station distances will then become too short. The distances between the used stations vary between 48 and 72 km. Surface wave observations from altogether 227 events were investigated for the time period January 1996 to July 2003. The number of events evaluated for a single path varies for Rayleigh waves from 17 to 58. A total of 206 events were used for the determination of Love-wave phase velocities. Due to the smaller distances between the stations phase velocities could only be analyzed between about 20 and 100 mHz (Fig. 6.5.5, left).

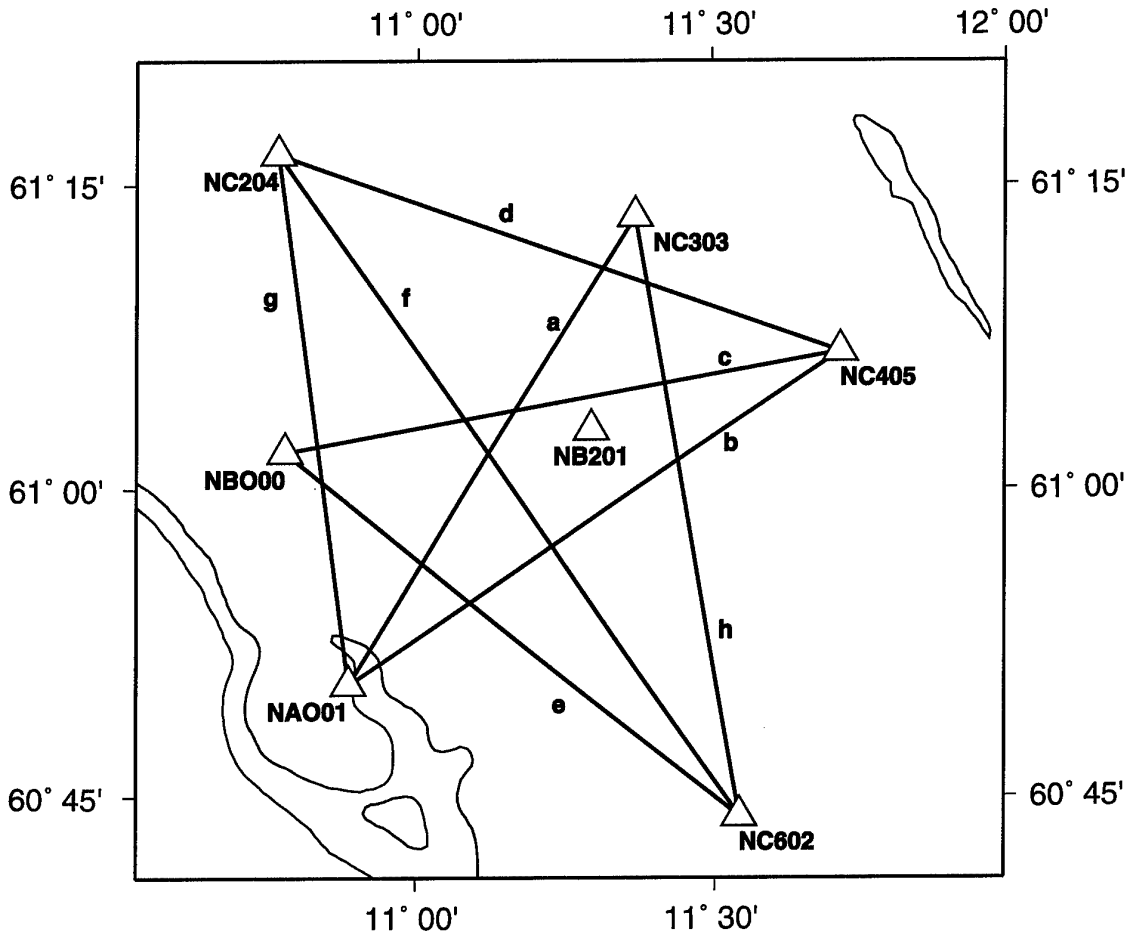

Fig. 6.5.4. Illustration of the eight different paths between six broad-band stations of the NORSAR array used in this study.

The Rayleigh-wave phase velocities of all paths were averaged and inverted to an average model of the structure beneath the NORSAR-array. The resulting 1D *S*-velocity model (Fig. 6.5.5, right) reaches only down to 100 km because of the limited frequency range. The *S*-wave velocity in the mantle lithosphere is lower than expected for stable cratonic regions. The mean depth to the Mohorovicic discontinuity is about 35 km.

Theoretical Love and Rayleigh phase velocity curves were calculated for this model (Fig. 6.5.5, left, red lines). Comparison with the averaged observed curves and their standard deviation shows no significant Love-Rayleigh discrepancy. This might be due to the large standard deviation (gray shaded areas) of the phase velocity curves mainly caused by the small distances between the stations.

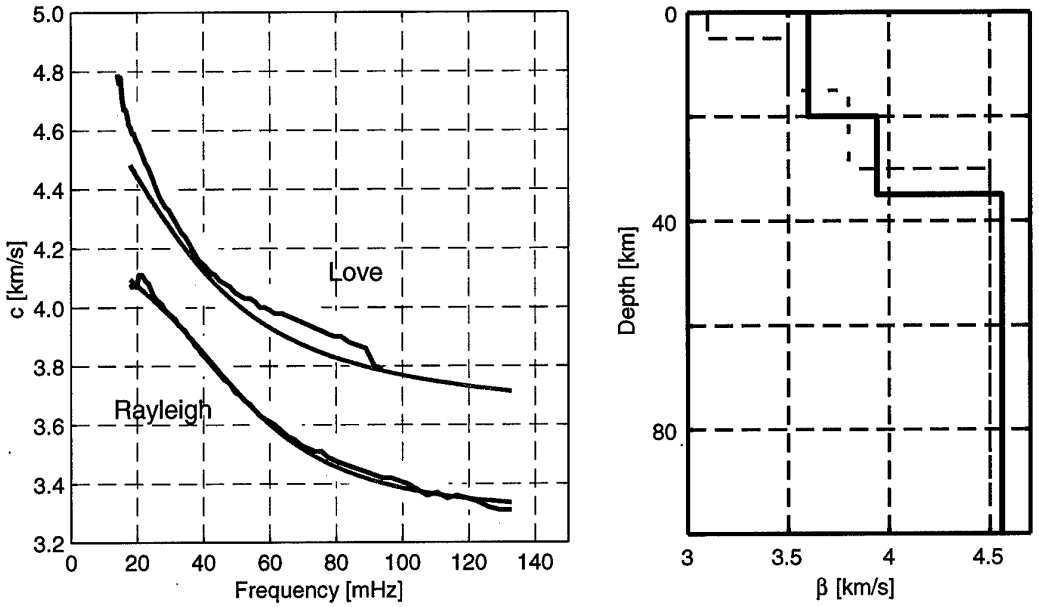

Fig. 6.5.5. Average Love and Rayleigh dispersion curves (left, blue). The inversion of the Rayleigh-wave phase velocity curves yields a 1D-model of the S-wave velocity (right, solid curve; the broken line shows the starting model). Theoretical Love and Rayleigh phase velocity curves for the models are shown on the left (red). Comparison with the averaged observed curves and their standard deviation (gray shaded areas) shows no significant Love-Rayleigh discrepancy.

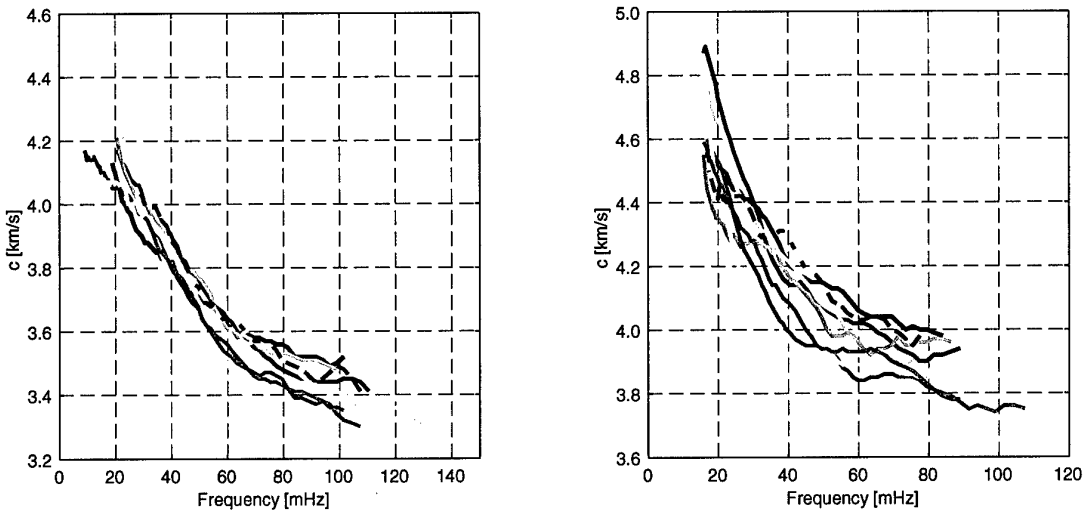

Fig. 6.5.6. Rayleigh (left) and Love wave (right) dispersion curves for the different raypaths crossing the NORSAR array (for path identification see text). Strong differences in the phase velocities are present above 50 mHz for Rayleigh waves and above 20 mHz for Love waves. The variations in phase velocities are similar for Love and Rayleigh waves: Paths with slow Rayleigh wave phase velocities show slow Love wave phase velocities as well. This observation can be explained by lateral heterogeneity in the crust but not by azimuthal anisotropy.

Comparing the phase velocities of the eight paths shows that strong differences are present above 50 mHz for Rayleigh waves and above 20 mHz for Love waves (Fig. 6.5.6). The different paths as labelled in Fig. 6.5.4 correspond with following colors used in Fig. 6.5.6: a (black), b (blue), c (cyan). d (green), e (blue, broken line), f (magenta), g (yellow), and h (red). The structure in a certain depth affects Love wave dispersion curves at lower frequencies than Rayleigh wave dispersion curves. Variations in phase velocities are similar for Love and Rayleigh waves: Paths with slow Rayleigh wave phase velocities show slow Love wave phase velocities as well. This observation can be explained by lateral heterogeneity in the crust.

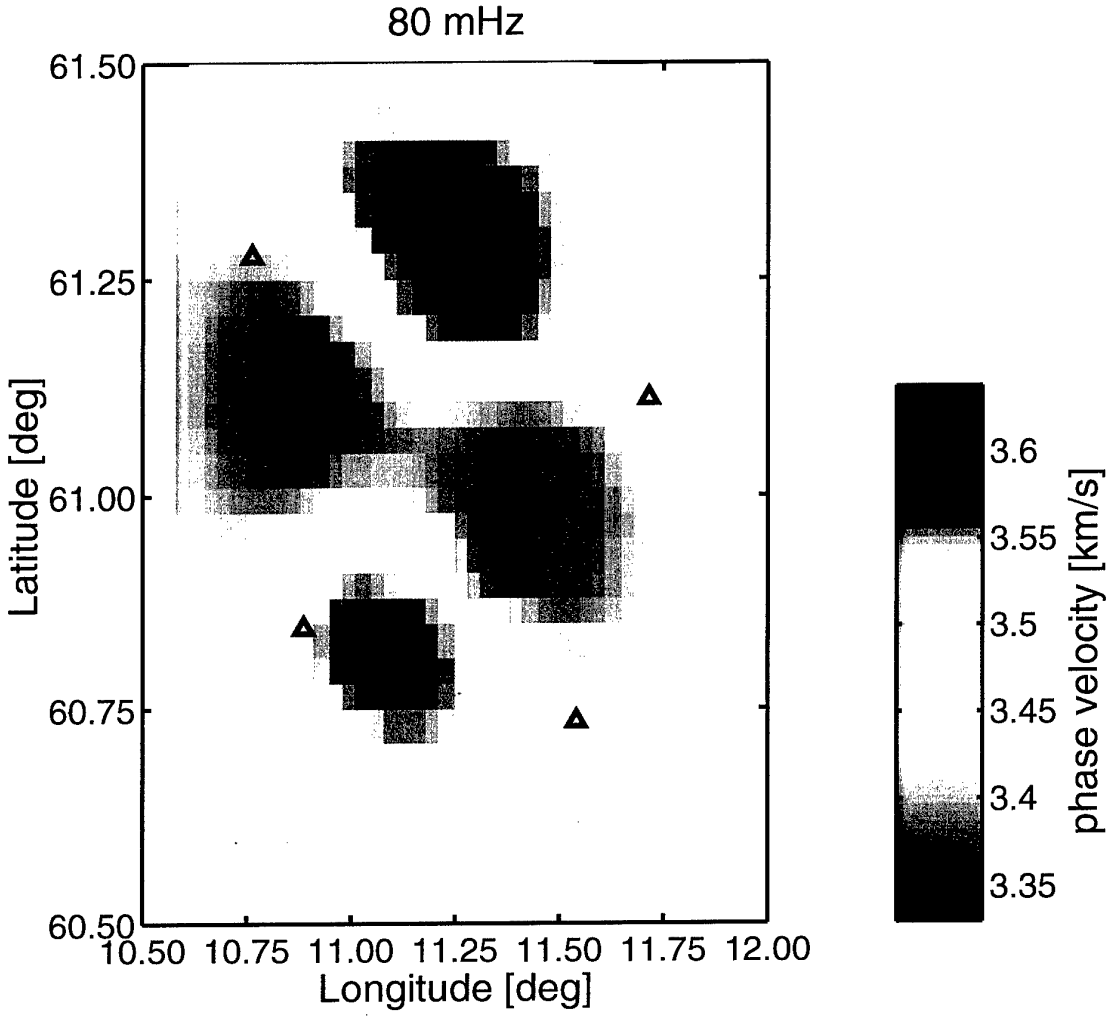

Fig. 6.5.7. Phase velocity map of the fundamental Rayleigh mode at 80 mHz. The strike of the low velocity anomaly in the crust is about NW-SE. It is similar to the strike of the Precambrian structures at the surface. A comparable result was obtained by the classical ACH-study using relative P-wave residuals observed at the NORSAR array (Aki et al., 1977).

To locate such lateral heterogeneities a phase velocity map of the fundamental Rayleigh mode at 80 mHz was calculated (Fig. 6.5.7). Rayleigh waves of about 80 mHz are mostly sensible for the middle crust at a depth range between 15 and 25 km. The strike of the low velocity anomaly in the crust is about NW-SE. It is similar to the strike of the Precambrian structures at the surface. For the crust, a comparable result was obtained by the classical ACH-tomography study using teleseismic P-phase observations at the single NORSAR sites (Aki et al., 1977).

6.5.5 Conclusions

GRSN

In Central Europe the asthenosphere is found between 80 km and 250 km depth. The Love-Rayleigh discrepancy in the asthenosphere amounts to about 5%. This is comparable to the degree of Love-Rayleigh discrepancy in the Pacific.

Azimuthal variations of the Rayleigh phase velocity point to azimuthal anisotropy in the lower crust. The orientation of the fast axis is approximately NE-SW.

In contrast to the Rayleigh wave phase velocities, Love waves do not show dependence on azimuth. Further studies should reveal if this discrepancy is caused by finite-frequency effects, or contamination of the Love-wave phase velocities by higher modes, or if this discrepancy might yield constraints on models of the anisotropy in the lower crust.

NORSAR

The *S*-wave velocity in the mantle lithosphere is lower than expected for stable cratonic regions. However, the NORSAR array is located at the border of the Precambrian Baltic Shield and this region was influenced by several tectonic processes. The depth of the Moho is about 35 km.

Variations in the phase velocity between the paths point to lateral heterogeneities with S velocity variations of up to +/- 3.5%. The strike of the observed velocity anomaly in the crust is NW-SE. It is similar to the strike of the Precambrian structures at the surface.

The amount of the Love-Rayleigh discrepancy in the lower crust is not significant, which might be partly due to the large standard deviation of the phase velocities.

Acknowledgements

The 2-months research term of MB at NORSAR in 2003 was funded through the EC programme Access to Research Infrastructure (Contract HPRI-CT-2002-00189).

Monika Bischoff, Ruhr-University Bochum
Johannes Schweitzer
Thomas Meier, Ruhr-University Bochum

References

Aki, K., A. Christofferson and E. Husebye, E.S. (1977). Determination of the three-dimensional seismic structure of the lithosphere. J. Geophys. Res. **82**, 277-296.

Bamford, D. (1987). Pn velocity anisotropy in a continental upper mantle. Geophys. J. R. astr. Soc. **49**, 29-48.

Ekström, G. and A.M. Dziewonski (1998). The unique anisotropy of the Pacific upper mantle. Nature **394**, 168-172.

Friederich, W. and Z.X. Huang (1996). Evidence for upper mantle anisotropy beneath southern Germany from Love and Rayleigh wave dispersion. Geophys. Res. Lett. **23**, 1135-1138.

Levshin, A.L. and L. Ratnikova (1984). Apparent anisotropy in inhomogeneous media. Geophys. J. R. astr. Soc. **76**, 65-70.

Maupin, V. (1985). Partial derivatives of surface wave phase velocities for flat anisotropic models. Geophys. J. R. astr. Soc. **83**, 379-398.

Maupin, V. (2002). The amplitude of the Love-Rayleigh discrepancy created by small-scale heterogeneities. Geophys. J. Int. **150**, 58-64.

Meier, T., K. Dietrich, B. Stoeckhert and H.-P. Harjes (2004). One-dimensional models of shear wave velocity for the eastern Mediterranean obtained from the inversion of Rayleigh wave phase velocities and tectonic implications. Geophys. J. Int. **156**, 45-58.

Montagner, J.-P. and T. Tanimoto (1991). Global upper mantle tomography of seismic velocities and anisotropies. J. Geophys. Res. **96**, 20337-20351.

McEvilly, T. V. (1964). Central US crust-upper mantle structure from Love and Rayleigh wave phase velocity inversion. Bull. Seis. Soc. Am. **54**, 1997-2015.

Song, L.-P., M. Koch, K. Koch and J. Schlittenhardt (2004). 2-D anisotropic Pn-velocity tomography underneath Germany using regional traveltimes. Geophys. J. Int. **157**, 645-663.

Wielandt, E., A. Plesinger, A. Sigg and J. Horálek, J. (1988). Deep structure of the Bohemian Massif from phase velocities of Rayleigh and Love waves. Phys. Earth planet. Int. **51**, 155-156.